Continuous Casting Consortium

Multiphase Flow, Inclusion Nucleation, Growth, Removal and Entrapment – in Molten Steel and Continuous Casting

Lifeng Zhang, Brian G. Thomas

Department of Mechanical &. Industrial Engineering
University of Illinois at Urbana-Champaign
May 10, 2004

Acknowledgements

- Continuous Casting Consortium
- Fluent Inc.
- National Science Foundation
- National Center for Supercomputing Applications

Outline

1. Introduction: Inclusions and Defects in steel
2. Inclusion Nucleation, Growth and Removal in Steel
   - Fundamentals
   - Interaction between Inclusion and Bubble
3. Fluid Flow and Inclusion Motion, Removal in Steel

   3.1 In ladles

   3.2 In continuous casting tundish

   3.3 In the SEN

   3.4 In the Mold

   3.5 Effect of argon gas on fluid flow in the mold

1. Introduction: Inclusions and Defects in Steel

Inclusions in Steel

Origin of Inclusions:

- Deoxidation (in ladles)
- Reoxidation by air or slag (transfer process)
- Slag entrainment, lining erosion

Growth Inclusions:

- Microscale phenomena
  - Nucleation
  - Growth by diffusion, Brownian collision and turbulent collision
  - Attaching to bubble surface

Inclusion Motion and Removal:

- Fluid flow transport
- Ladle, Tundish, Nozzles, Mold

Nucleation, Growth and Removal of Inclusions

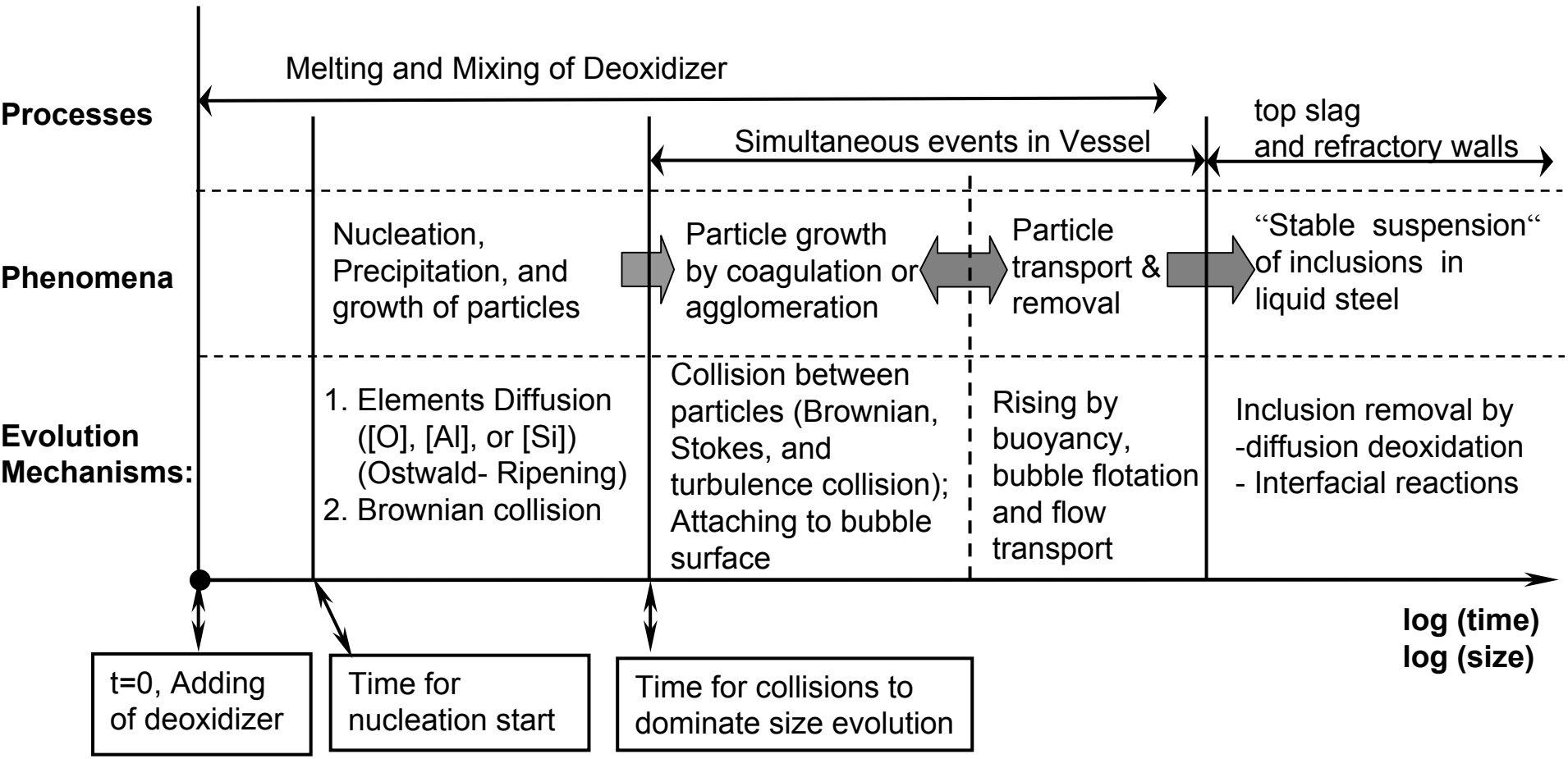

Indigenous Inclusions (Alumina Clusters)

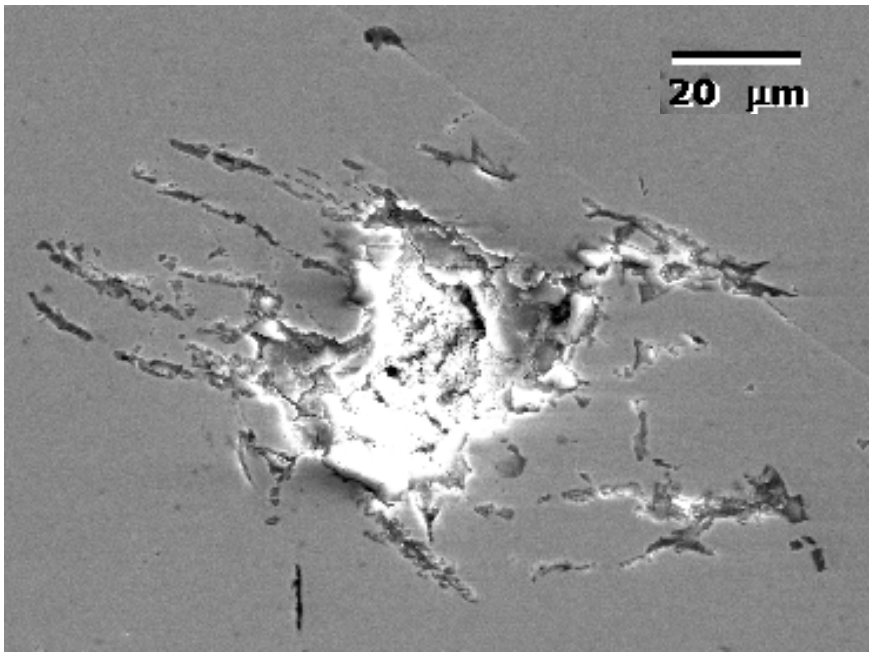

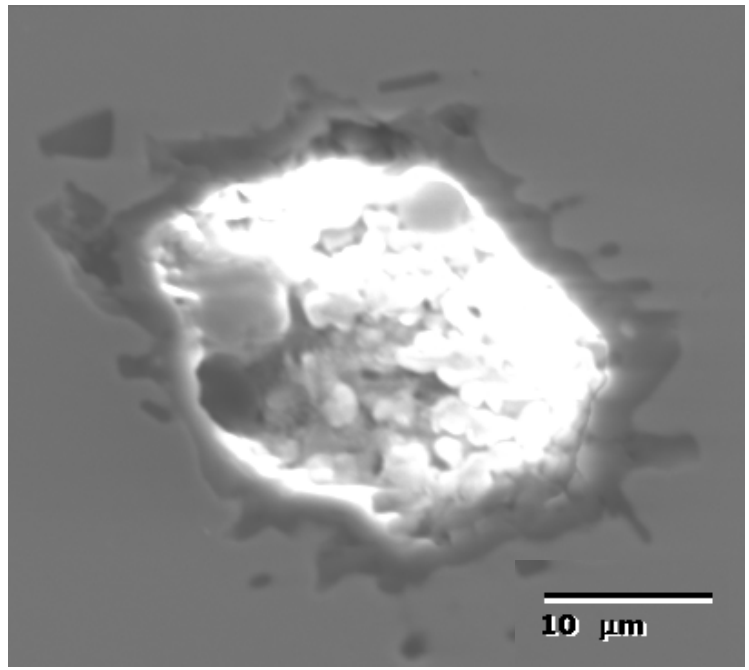

Lifeng Zhang, Brian G. Thomas, Bret Rietow. Investigation of Ingot Inclusions Using Microscope and SEM . Univ. of Illinois at Urbana-Champaign. IMF project report. May. 04, 2004

Inclusion Morphologies

Dendritic alumina

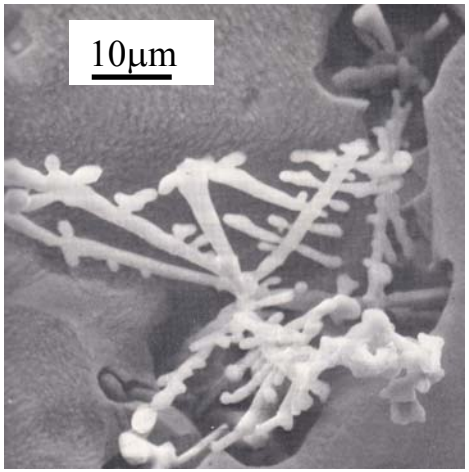

Alumina cluster

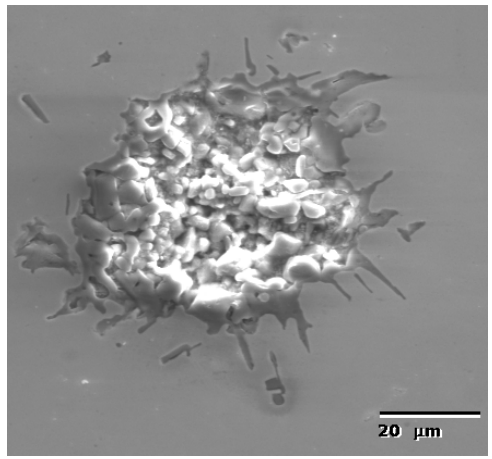

Flower-like plate alumina

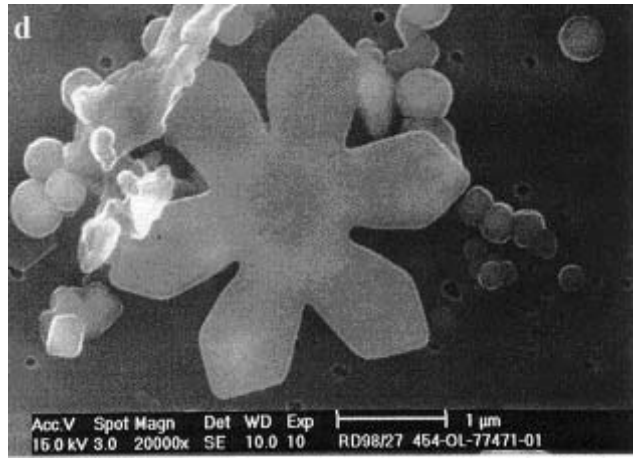

Inclusions from mold flux

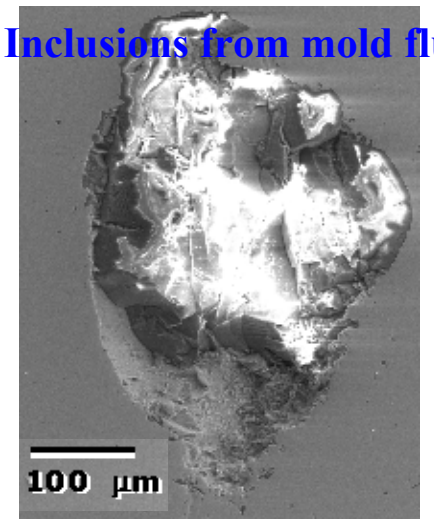

Slag inclusions

Refs:

1. L. Zhang, B. Thomas. ISIJ 2003, No.3, pp271-291
2. L. Zhang, B. Thomas, B. Rietow. Investigation of Ingot Inclusions Using Microscope and SEM . Univ. of Illinois at Urbana-Champaign. IMF project report. May. 04, 2004
3. R. Dekkers, B. Blanpain and P. Wollants: *Metall. mater. trans.*, (2003), **34B**, 161.

Typical Defects in Steel Caster

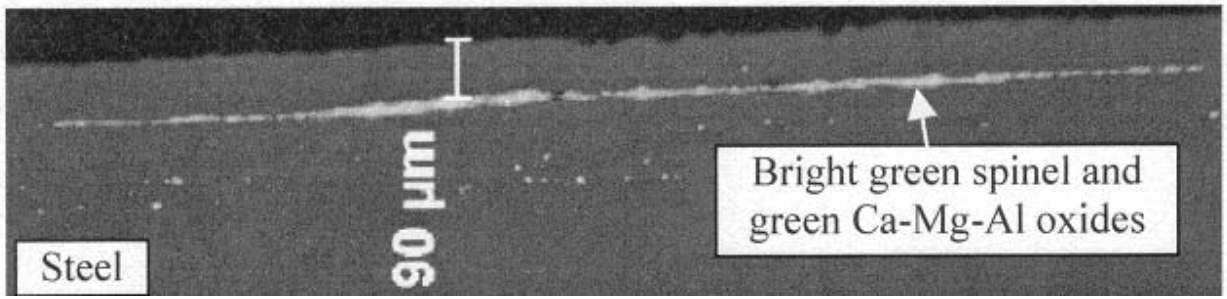

Inclusion sliver in the longitudinal section of a sheet product

H. Yin and H. T. Tsai, in ISSTech2003 Conference Proceedings, eds., ISS, Warrandale, PA, (2003), 217-226.

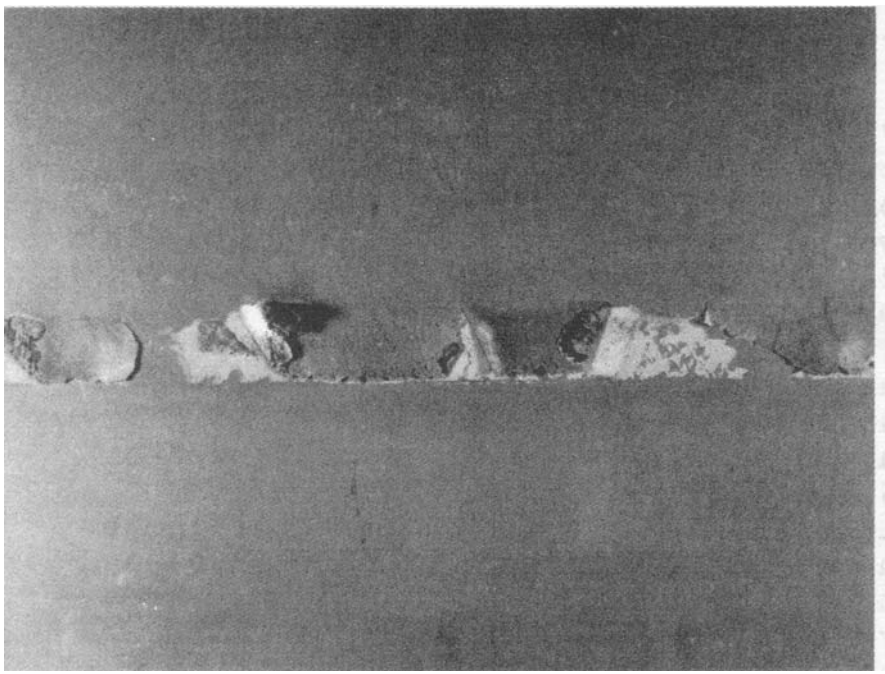

Very serious sliver defects stainless steel (first slab) sheet

A. R. Obman, W. T. Germanoski and R. C. Sussman, in 64th Steelmaking Conference Proc, **64**, eds., ISS, Warrendale, PA, (1981), 254-258.

Steps of Inclusion Nucleation and Growth during Deoxidation

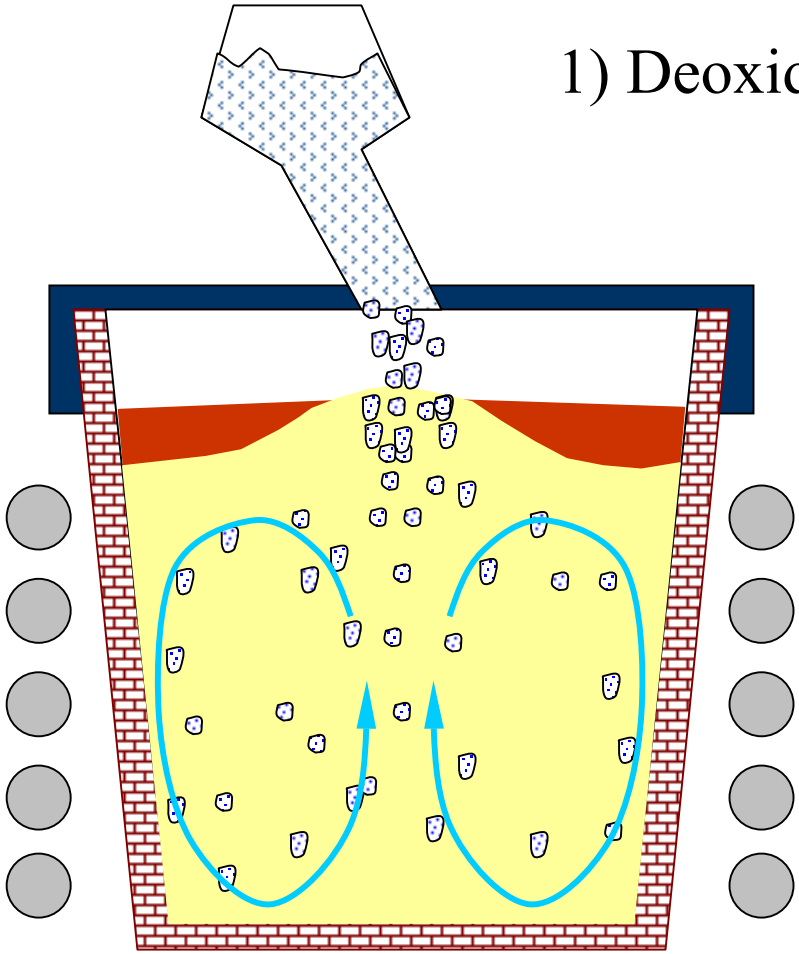

Liquid steel

Top slag

Deoxidizer alloy

Steps of Inclusion Nucleation and Growth during Deoxidation

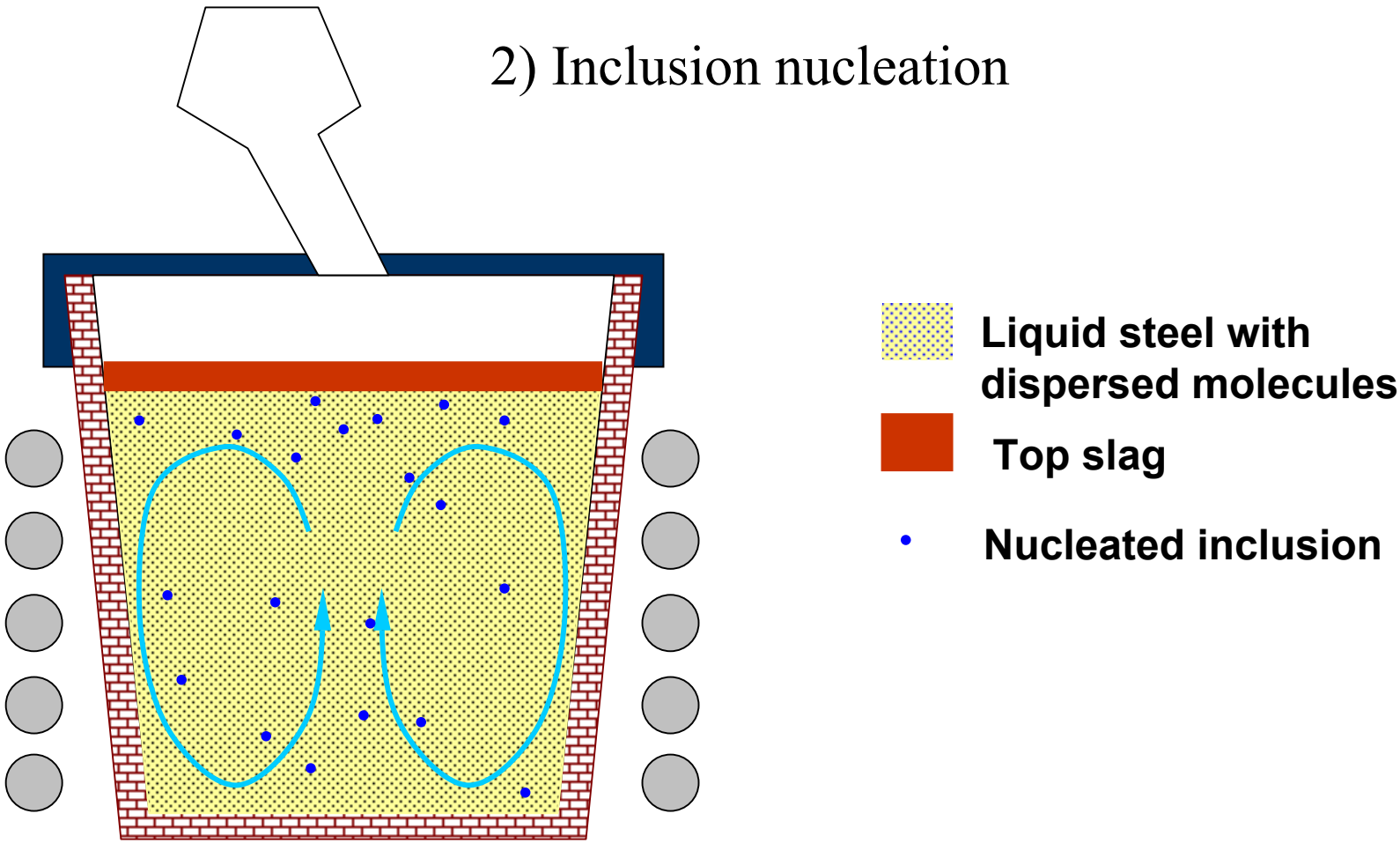

Steps of Inclusion Nucleation and Growth during Deoxidation

3) Inclusion growth and collision

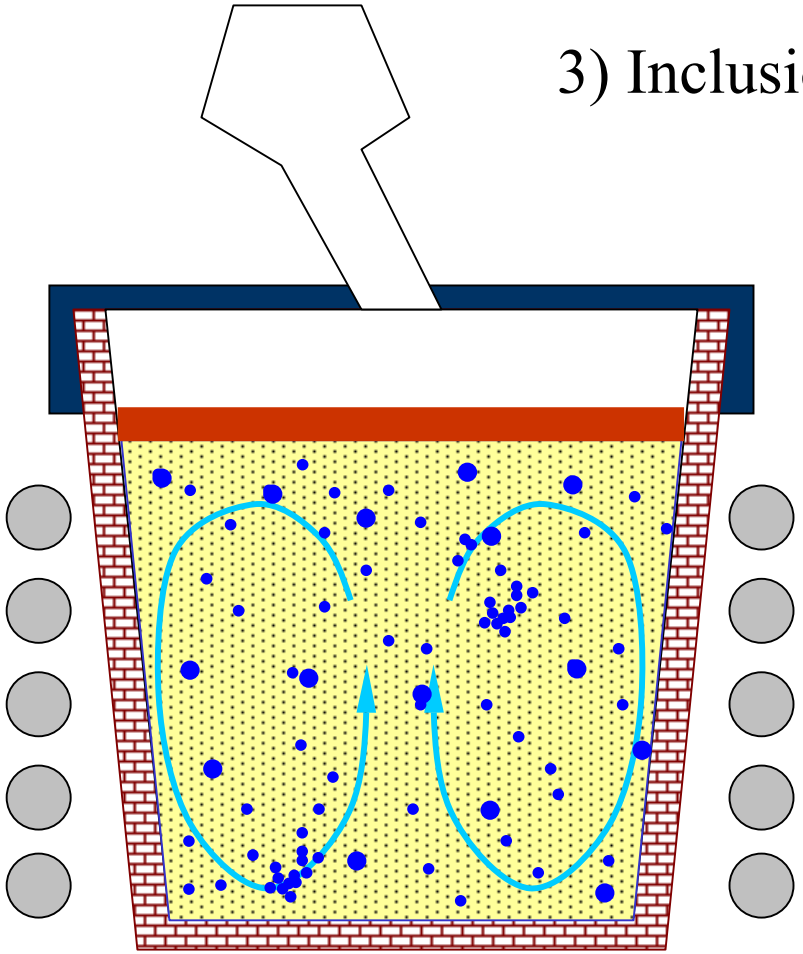

Liquid steel with dispersed molecules

Top slag

Nucleated inclusion

Dendritic inclusion

Inclusion Cluster

Steps of Inclusion Nucleation and Growth during Deoxidation

4) Inclusion transport & removal

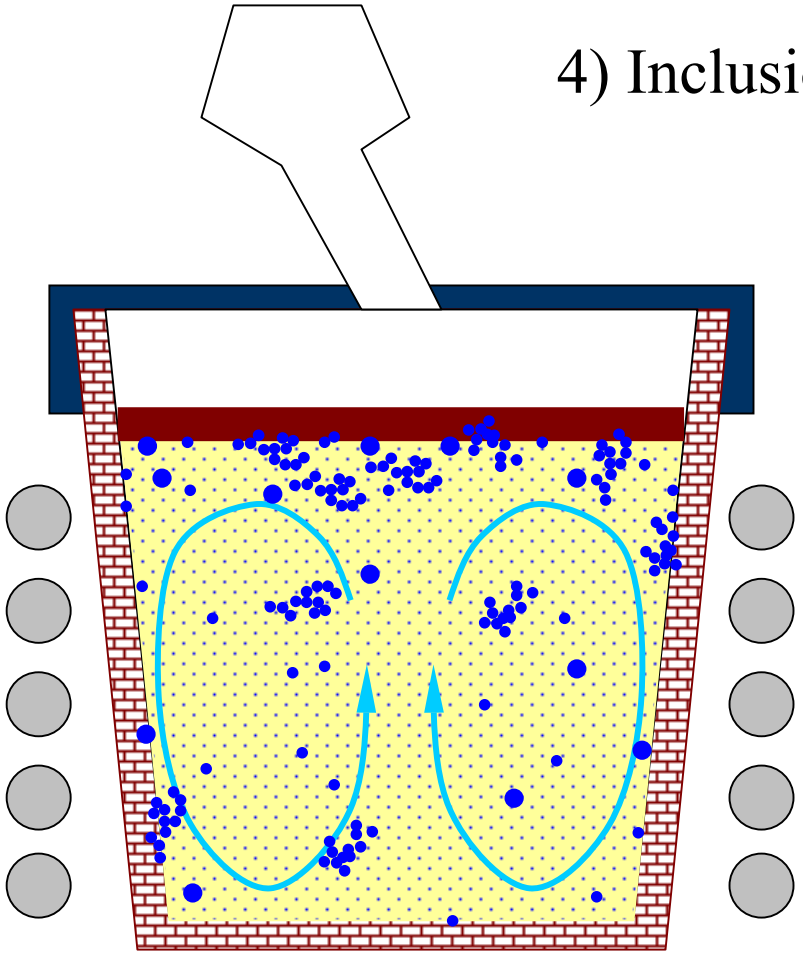

Liquid steel with dispersed molecules

Top slag

Nucleated inclusion

Dendritic inclusion

Inclusion Cluster

2. Inclusion Nucleation and Growth and Removal in Molten Steel Systems

Mechanisms of Inclusion Evolution

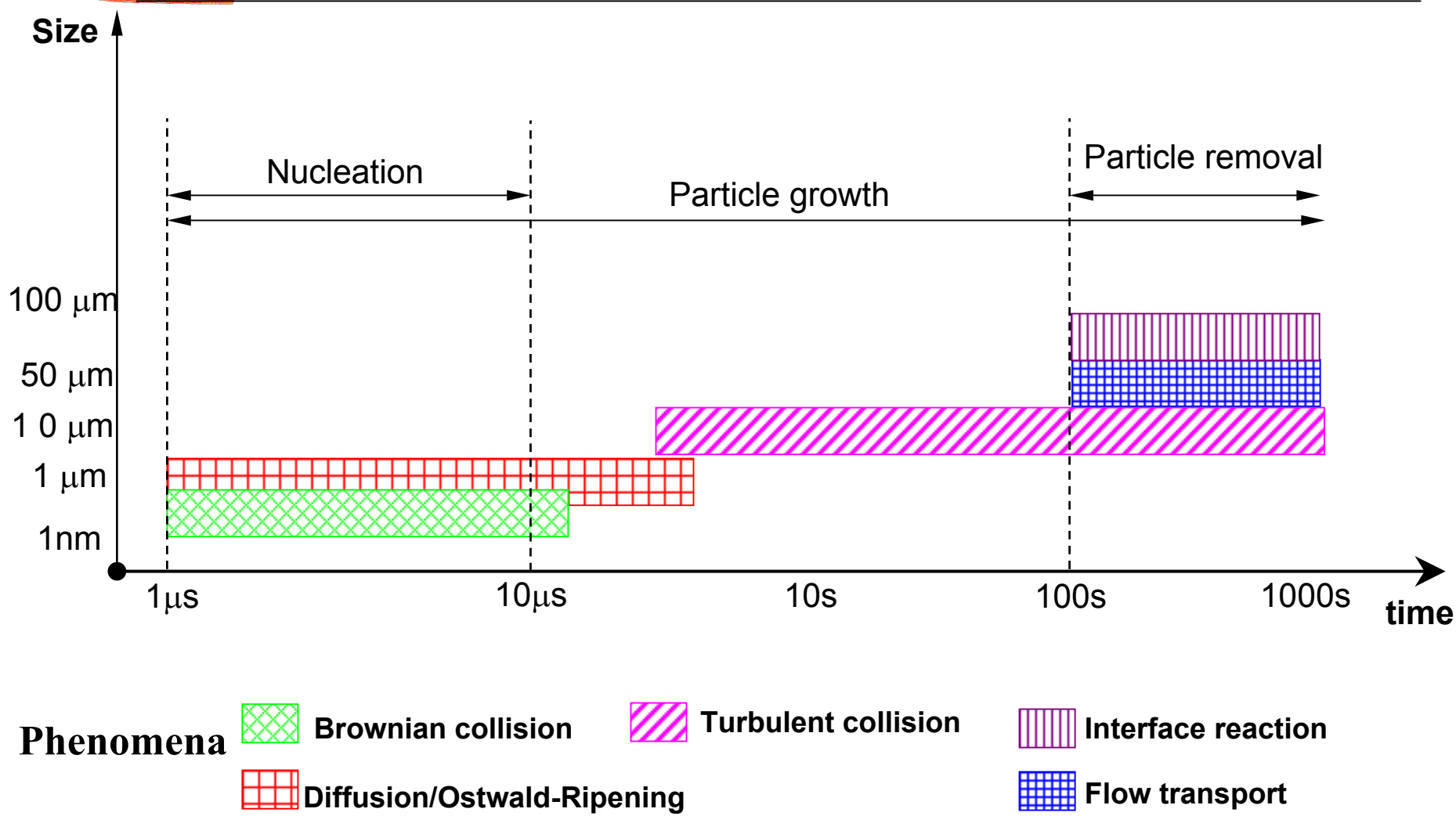

2.1 Fundamentals of Nucleation and Growth of Inclusions

Diffusion (Growth if Stable)

$$\beta_{D,i} = 4\pi D_1 r_i$$

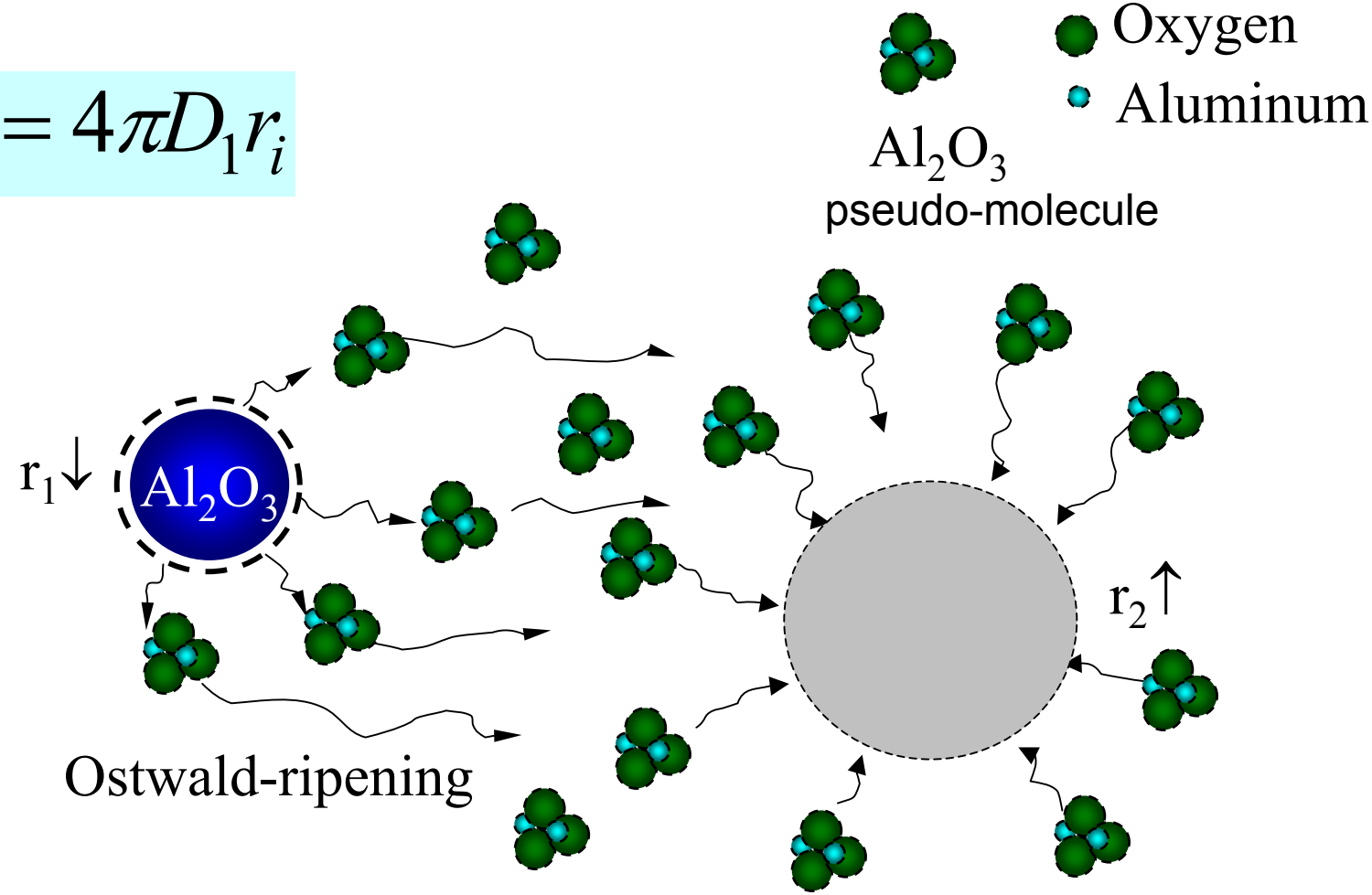

1. E.T. Turkdogan, JISI, 1966, 914-919.
2. W. Ostwald, Z. Phys. Chem., Vol. 34, 1900, 495.

Homogeneous Nucleation Criterion

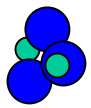

Al_2O_3
pseudo-molecule

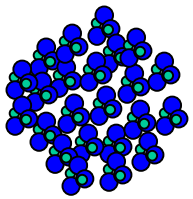

Random group of
pseudo-molecules

$$r_C = r_1 i_c^{1/3} = \frac{2\sigma V_m}{RT \ln \Pi}$$

1) If a random group of "pseudo-molecules" is larger than this critical size:
   - nucleation occurs,
   - particle is stable and will grow.

2) Critical nucleus size decreases with:
   - increasing supersaturaion
   - decreasing surface tension.

Simulation results: - 0.83nm radius initial inclusions **at 0.5μs,**
- Containing 42 Al_2O_3 molecules each.

Experimental proof: - Minimum inclusion radius in Al-killed steel: 1- 5nm.
- K. Wasai, et al., ISIJ Inter., Vol. 42 (5), 2002, 459-466.

Brownian Collision

$$\beta_{B,ij} = \frac{2kT}{3\mu}\left(1/r_i + 1/r_j\right)\left(r_i + r_j\right)$$

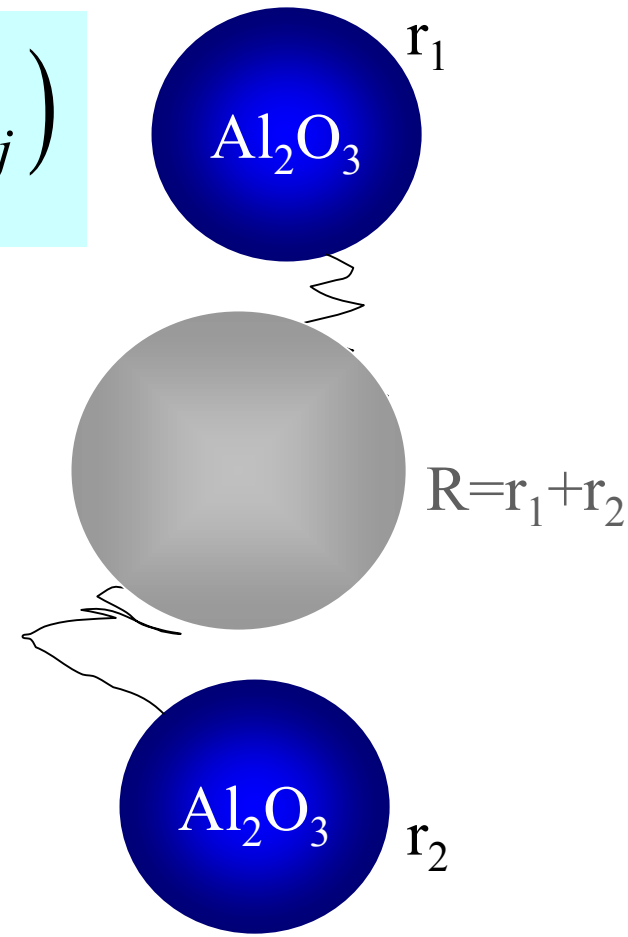

1. A. Einstein, Ann. Phys., Vol. 17 (549), 1905,
2. M.V. Smoluchowski, Zeit. F. Physik. Chemie, Vol. 92, 1917, 129.

Turbulent Collision

$$\beta_{D,ij} = 1.3\left(r_i + r_j\right)^3 \left(\varepsilon/\nu\right)^{1/2}$$

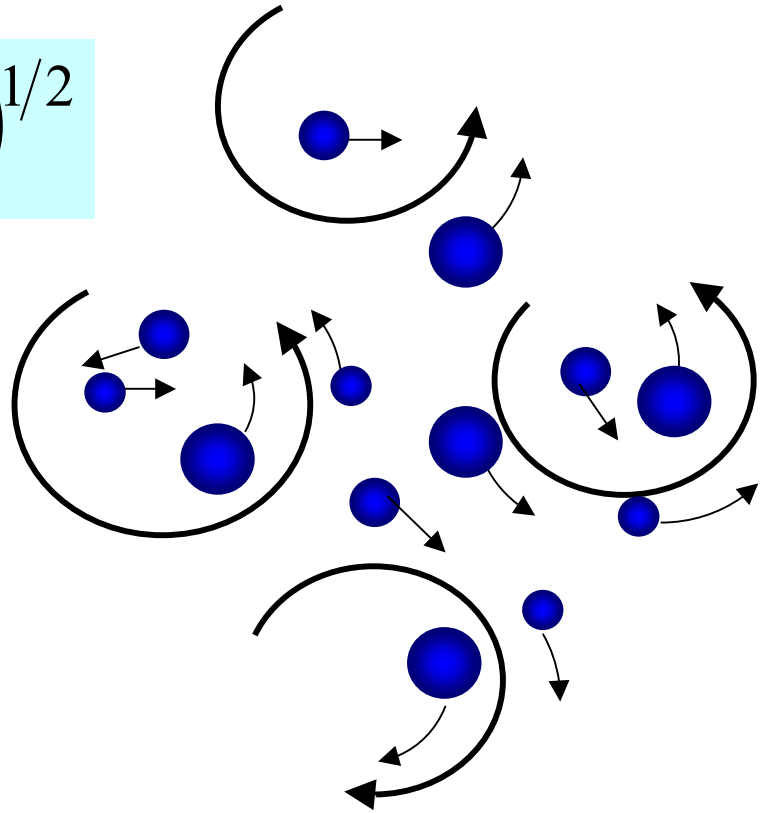

1. P.G. Saffman, et al., J. Fluid Mech., Vol. 1, 1956, 16.
2. H. Knuppel, et al., Stahl und Eisen, Vol. 85 (11), 1965, 675.

Population Balance Equations

$2 \le i < i_C$ **(Before nucleation)**

$$\frac{dN_i}{dt} = \overbrace{-\beta_{D,i} N_1 N_i + \beta_{D,i-1} N_1 N_{i-1}}^{\text{“Molecule” diffusion}} \overbrace{- \alpha_i A_i N_i + \alpha_{i+1} A_{i+1} N_{i+1}}^{\text{“particle” dissolution}}$$

Loss of “particle” *i*

Generation of “particle” *i*

Diffusion

Population Balance Equations

$i_C \le i < 10^{15}$ **(after formation of stable inclusion particles)**

"Molecule" diffusion

"particle" dissolution

$$\frac{dN_i}{dt} = -\beta_{D,i} N_1 N_i + \beta_{D,i-1} N_1 N_{i-1} - \alpha_i A_i N_i + \alpha_{i+1} A_{i+1} N_{i+1}$$

Loss of "particle" *i*

Generation of "particle" *i*

Diffusion

$$-\phi N_i \sum_{j=1}^{\infty} \left(\beta_{B,ij} + \beta_{T,ij}\right) N_j + \frac{1}{2}\phi \sum_{j=1}^{i-1} \left(\beta_{B,j,i-j} + \beta_{T,j,i-j}\right) N_j N_{i-j}$$

Loss of "particle" *i*

Generation of "particle" *i*

Collision

Comparison of Inclusion Growth Constants

Diffusion:

$$\beta_{D,i} = 4\pi D_1 r_i$$

Brownian collision:

$$\beta_{B,ij} = \frac{2kT}{3\mu}\left(1/r_i + 1/r_j\right)\left(r_i + r_j\right)$$

Turbulent collision:

$$\beta_{T,ij} = 1.3\left(r_i + r_j\right)^3\left(\varepsilon/\nu\right)^{1/2}$$

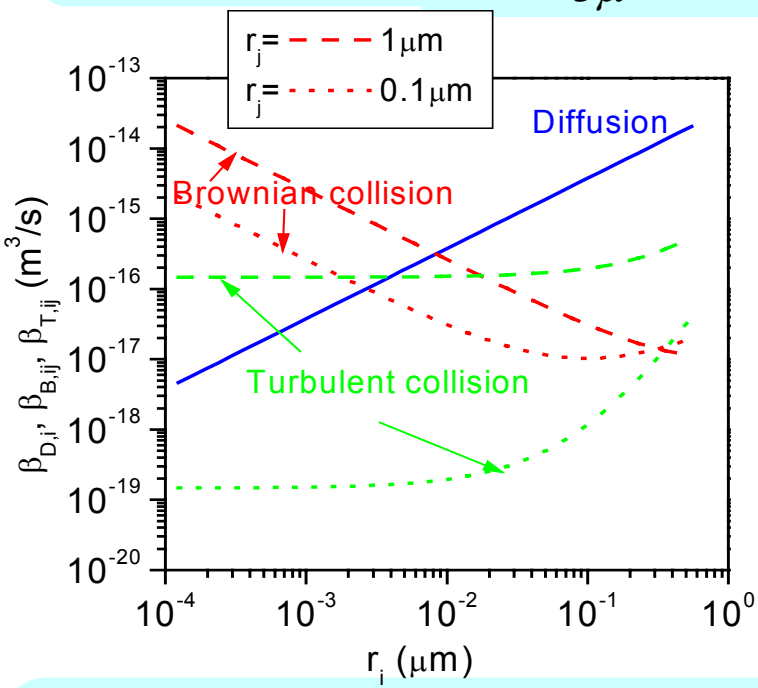

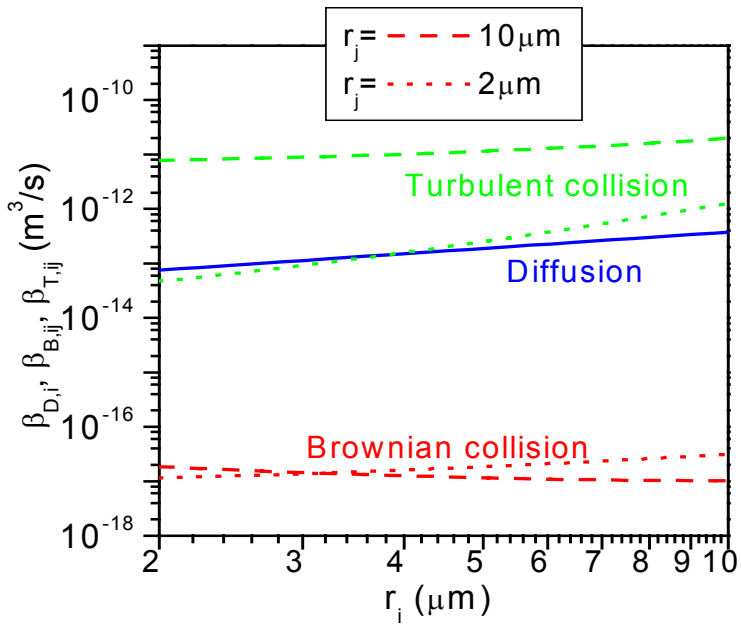

- Brownian scale (L_B<0.01μm)
- Diffusion Scale (L_D=0.01-5 (Particle growth))
- Turbulent scale (L_T>5μm (Particle collisions))

Alumina Cluster from Deoxidation

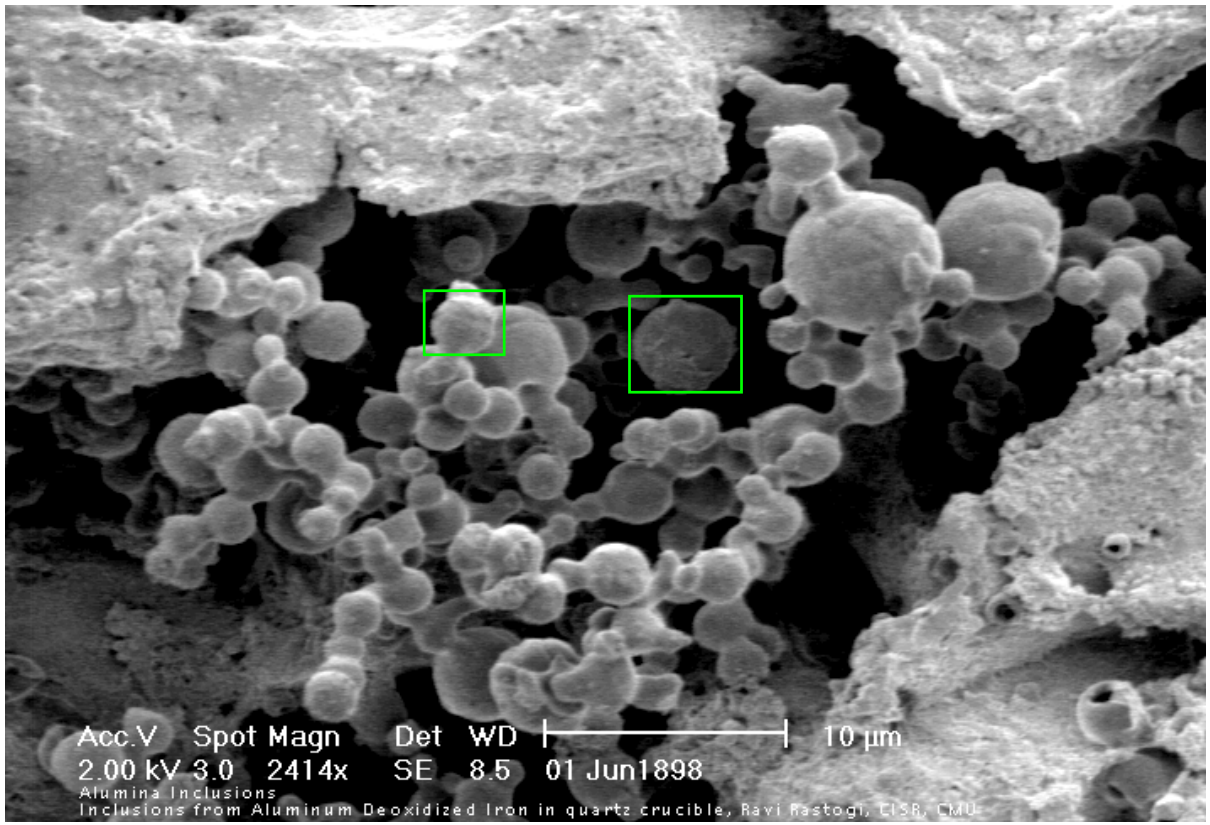

1-6µm

Ref.: Ravi Rastogi and Alan Cramb, Personal communication, 2002,

Characteristic of Inclusion Features

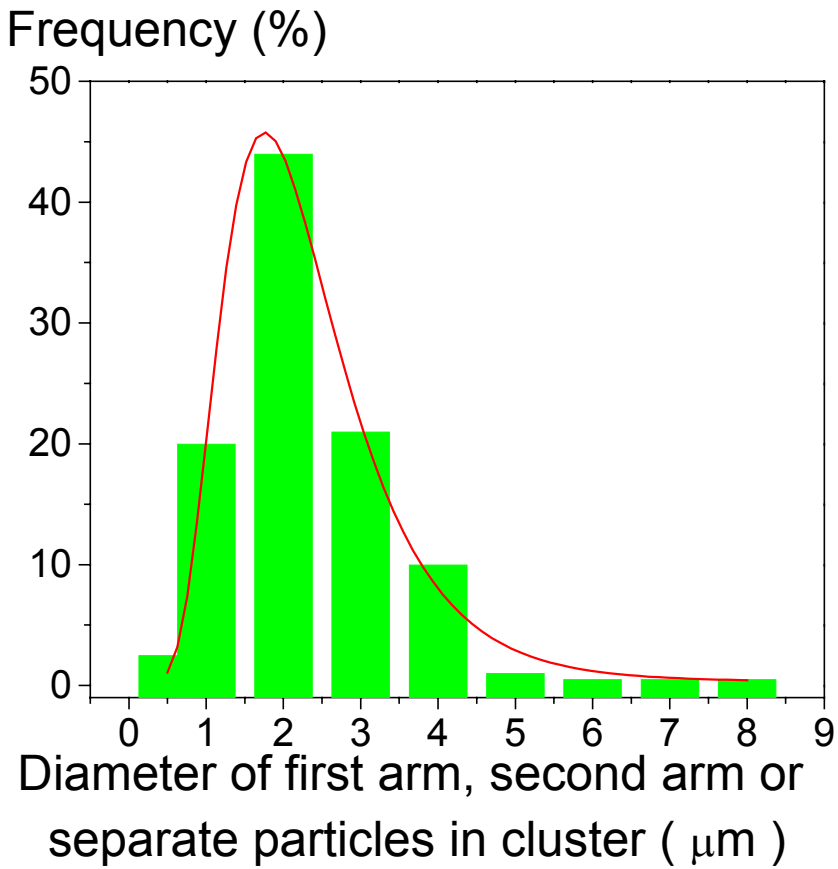

Alumina inclusion features have consistent 1~5 μm size

- Central globules
- Secondary dendrite arms
- Separate spheres in clusters

Measurement of the figures published by some researchers

2.2 Interaction Between Inclusion and Bubble in Liquid Steel

Functions of Gas Injection into Liquid Steel

1) to achieve homogeneity in the temperature and metal composition
2) to assist in the removal of second phases and dissolved impurities (inclusions) from molten steel.

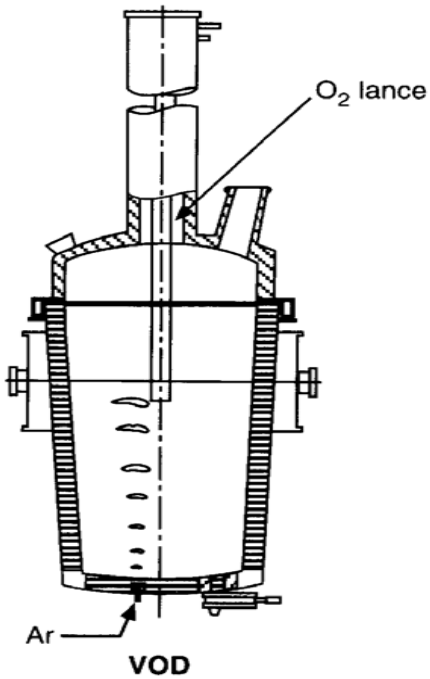

VOD ladle treatment

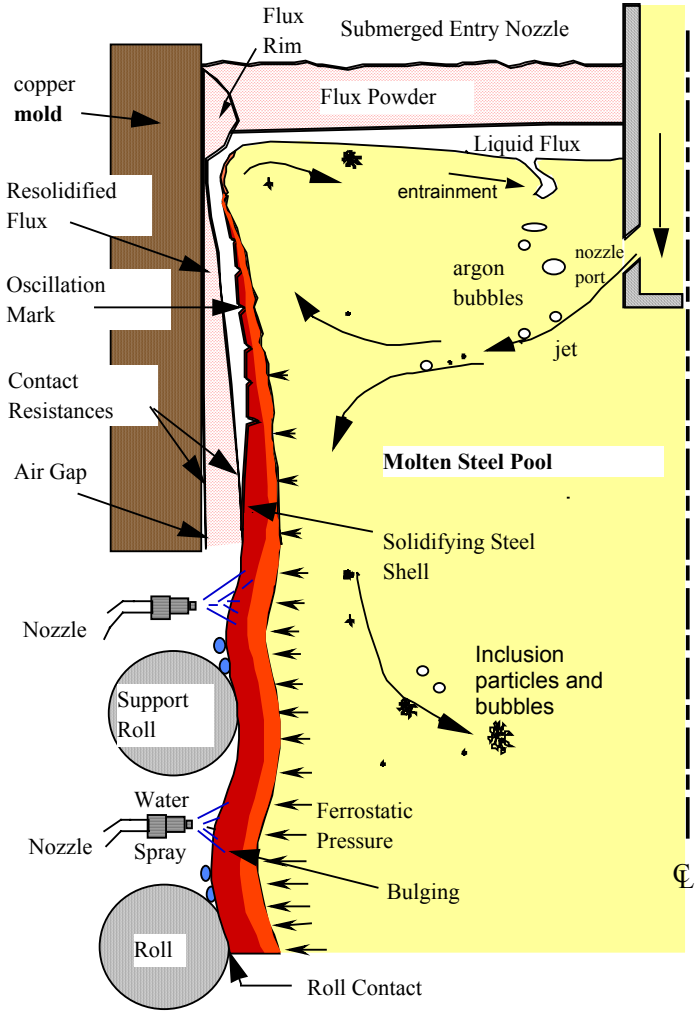

Continuous Casting Mold

Example of Inclusion Capture by Bubbles in Steel

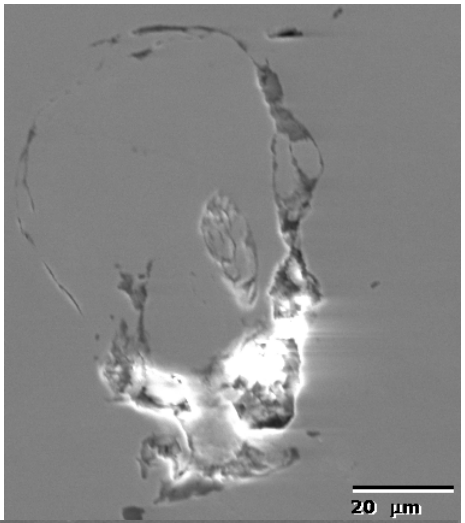

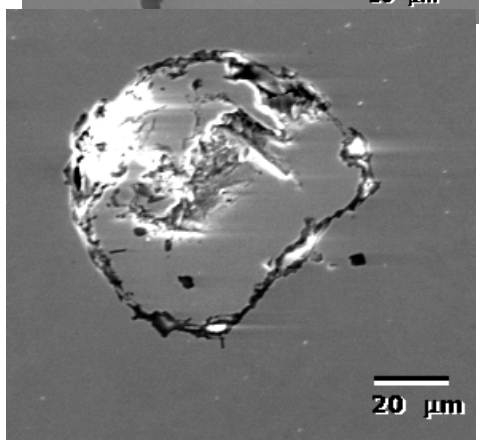

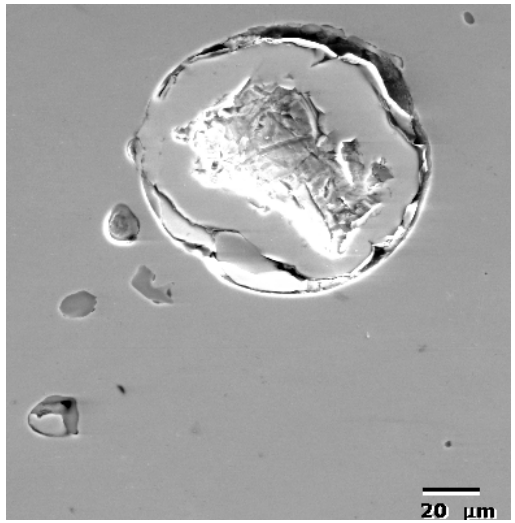

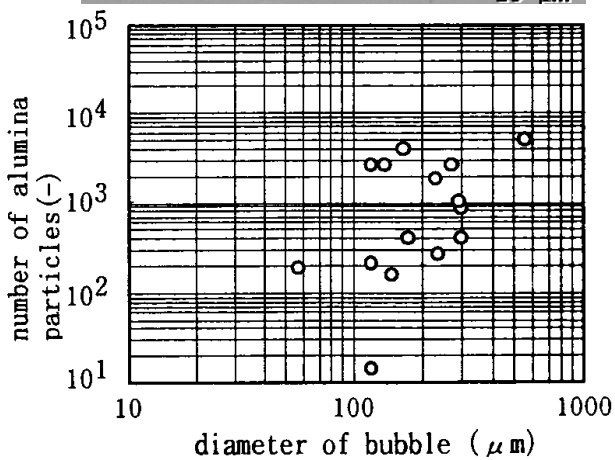

- Good for inclusion removal of bubbles float out;
- Bad for steel cleanliness is bubbles entrapped by the solidifying shell.

1. L. Zhang, B. Thomas, B. Rietow. Investigation of Ingot Inclusions Using Microscope and SEM . Univ. of Illinois at Urbana-Champaign. IMF project report. May. 04, 2004
2. L. Kiriha et al., CAMP-ISIJ, Vol. 13, 2000, 120.

Argon Bubbles and Clusters in the Wake of a Larger Bubble

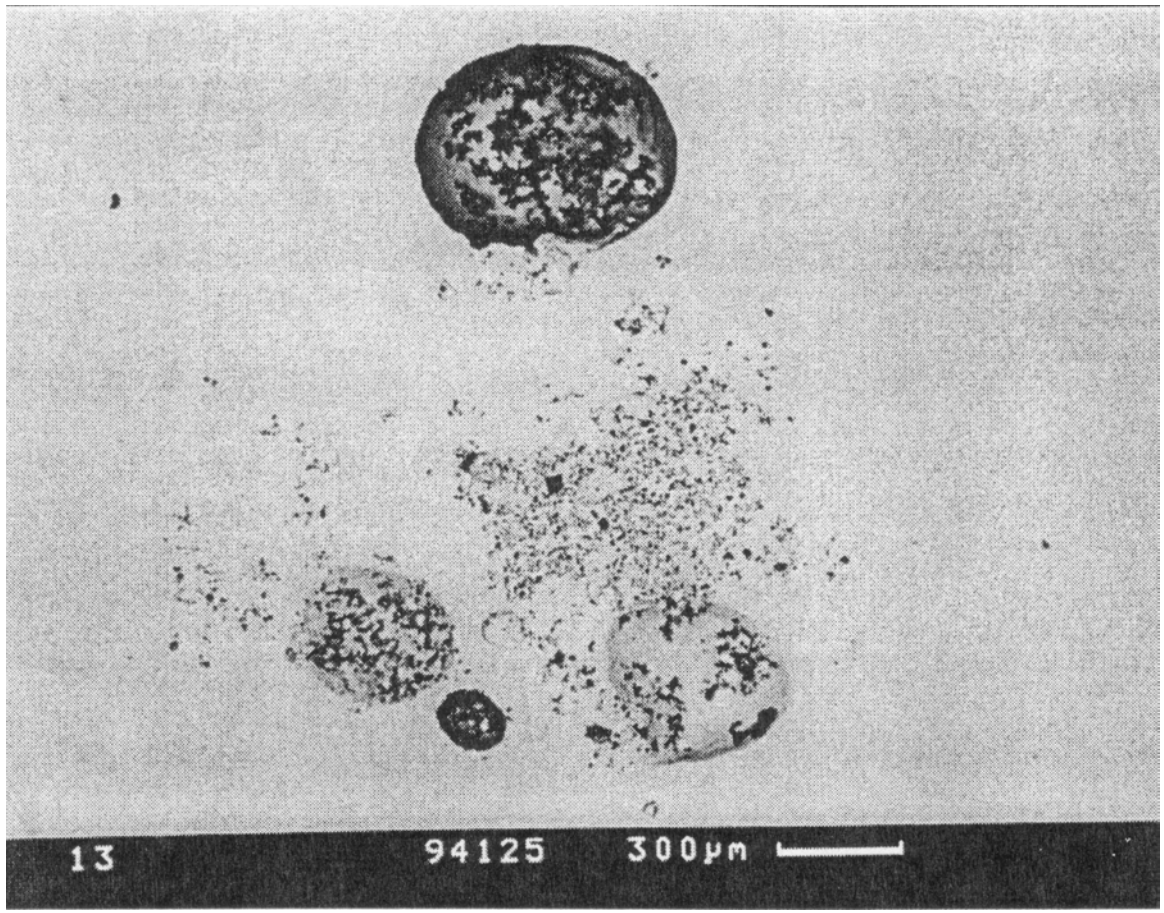

Damen, W., G. Abbel, et al. (1996). "The Influence of the Mould Process on Argon Bubbles in Slabs.".

Abbel, G., W. Damen, et al. (1996). "Argon Bubbles in Slabs." ISIJ **36**: S219-S222.

Bubble Size as Function of Gas Flow Rate and Bulk Stirring Power

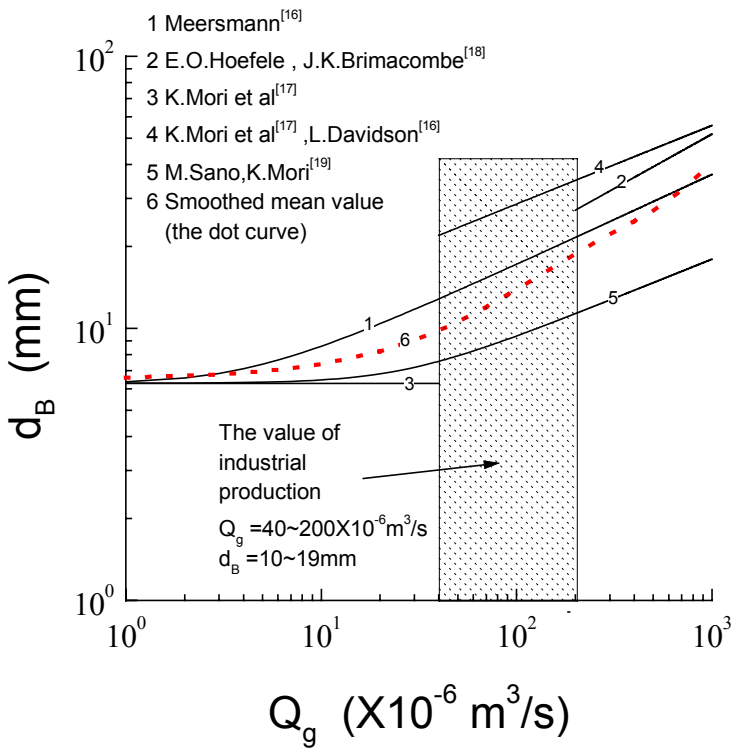

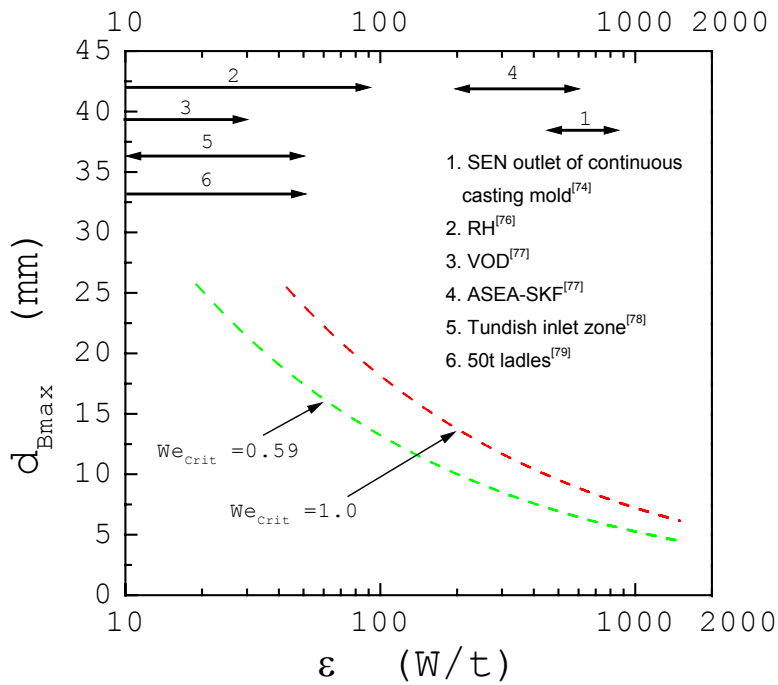

Ar bubble in liquid steel

Bubble Shape and Terminal Velocity

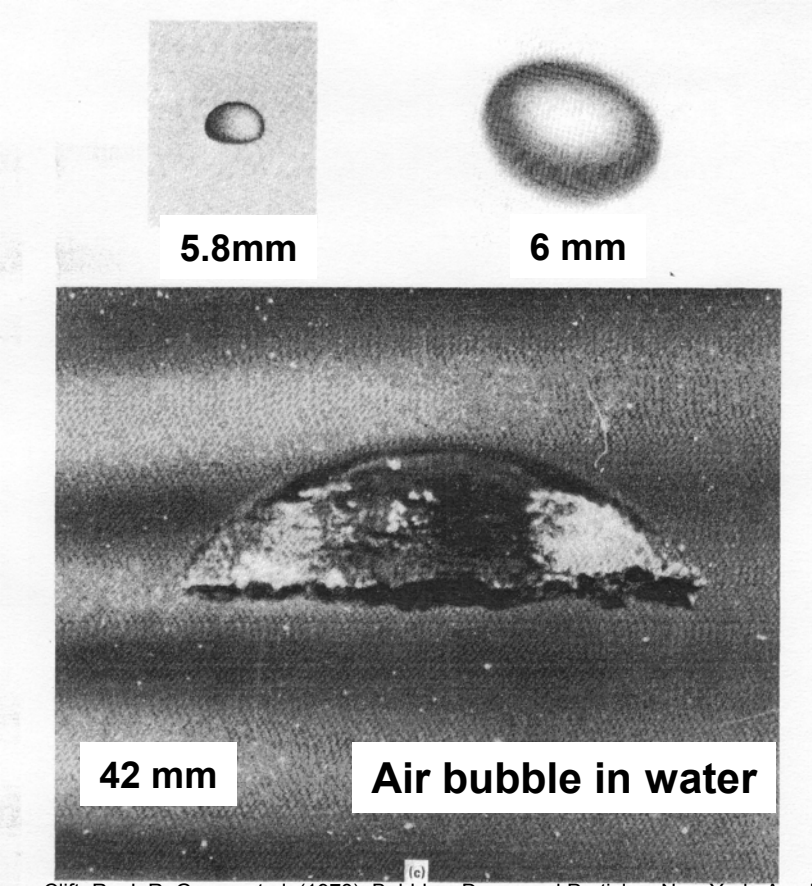

Clift, R., J. R. Grace, et al. (1978). Bubbles, Drops and Particles. New York, Academics Press, INC.

Ar bubble Terminal Velocity in Liquid Steel

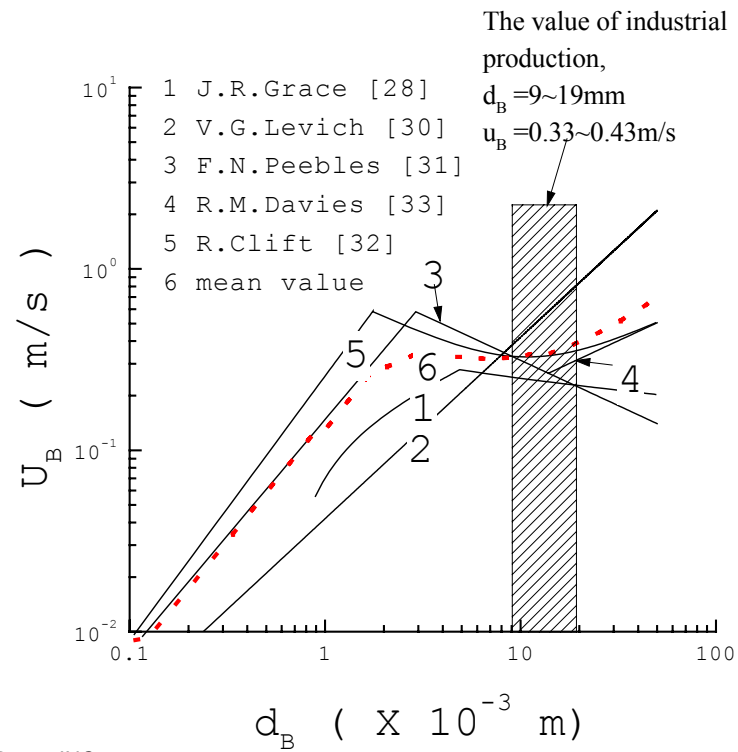

1) A peak of terminal velocity at a bubble diameter of 3 mm exists.
2) The terminal velocity and shape of bubble depend on the bubble size and bubble Reynolds number.

Fluid Flow around a Rigid Sphere (Water)

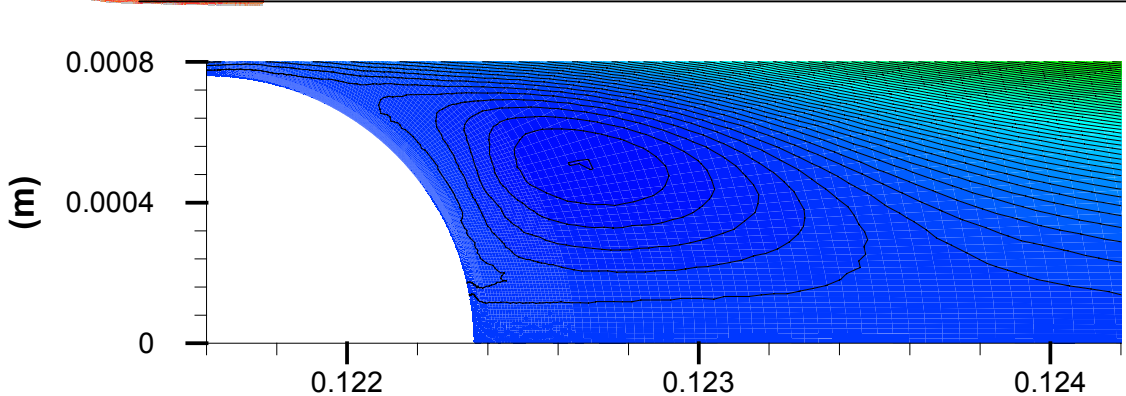

Simulation of fluid flow behind a rigid sphere

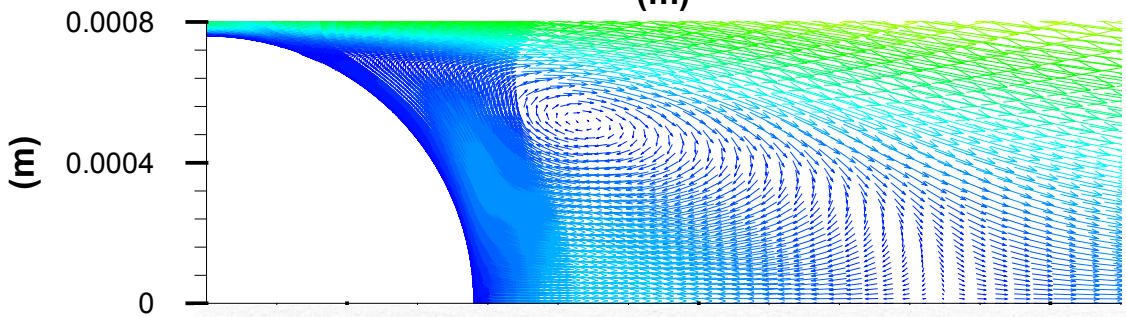

Re=480

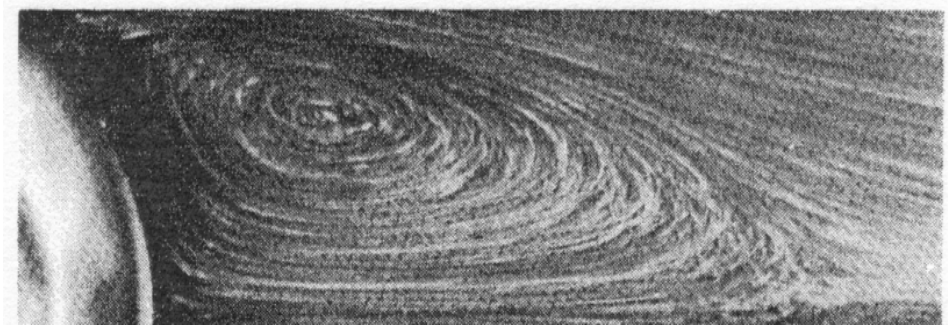

Experiments of fluid flow behind a rigid sphere.

Clift, R., J. R. Grace, et al. (1978). Bubbles, Drops and Particles. New York, Academics Press, INC.

Re=133

Collision Probability by Different Models

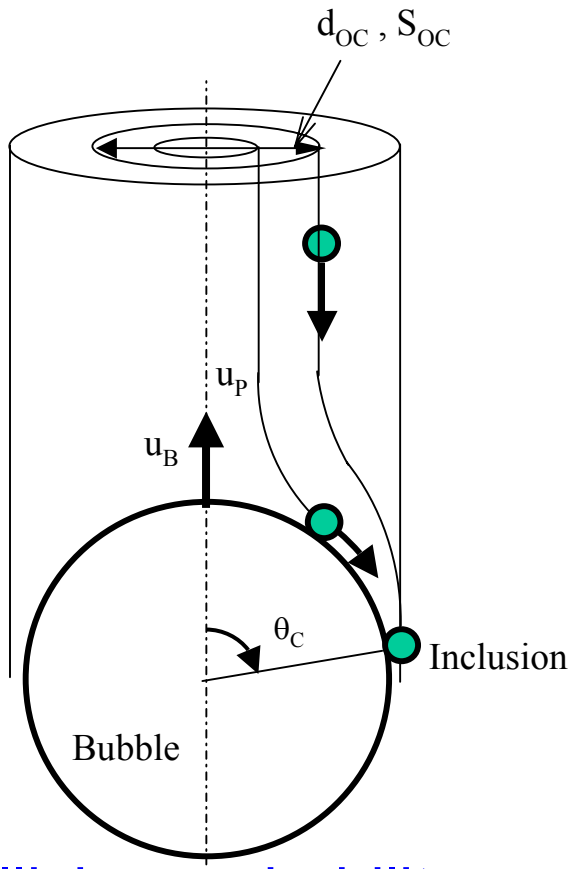

Collision probability, P_C

$$P_C = \left(\frac{d_{oc}}{d_B + d_{oc}} \right)^2$$

SiO_2 particles attachment to a bubble (1.52mm diameter and 0.316m/s rising velocity) in water

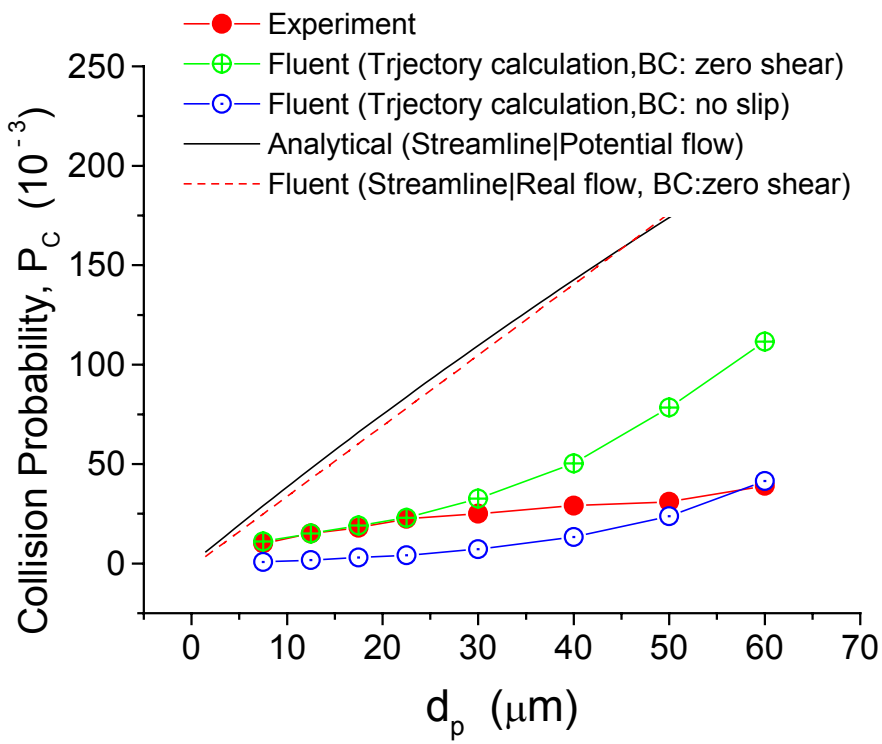

Conclusion: the trajectory model with a bubble boundary condition of zero shear stress has a best agreement with the experiments.

Collision Probability by Trajectory Calculation

Silica inclusions attachment to a bubble in Liquid steel

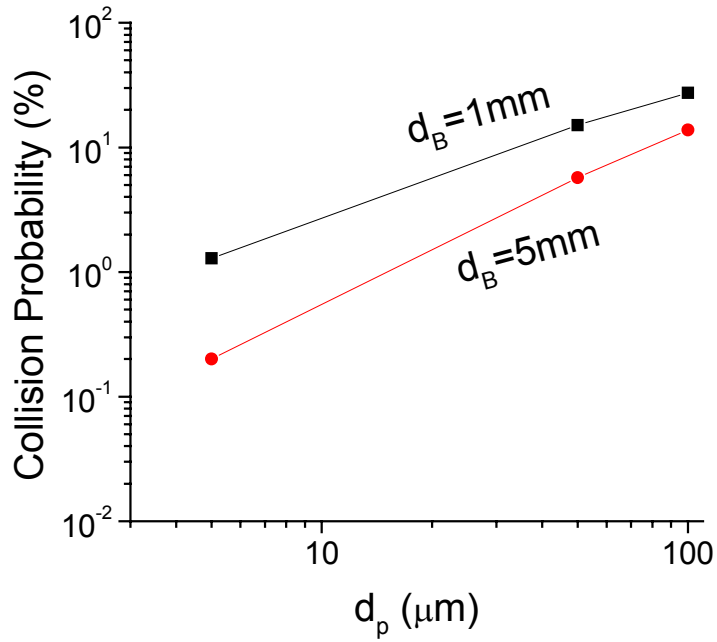

Conclusion: The attachment probabilities between the smaller bubbles and larger inclusions are larger that between larger bubbles and smaller inclusions.

Stream Function and Inclusion Trajectory in Liquid Steel (ρ: 7120 kg/m3)

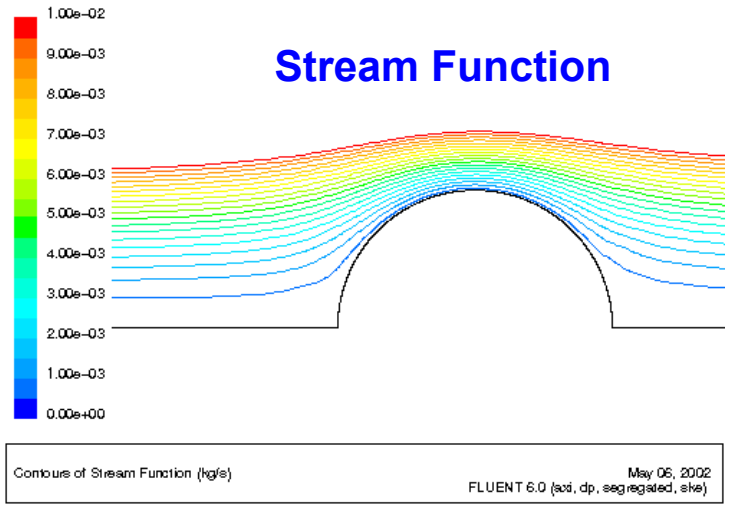

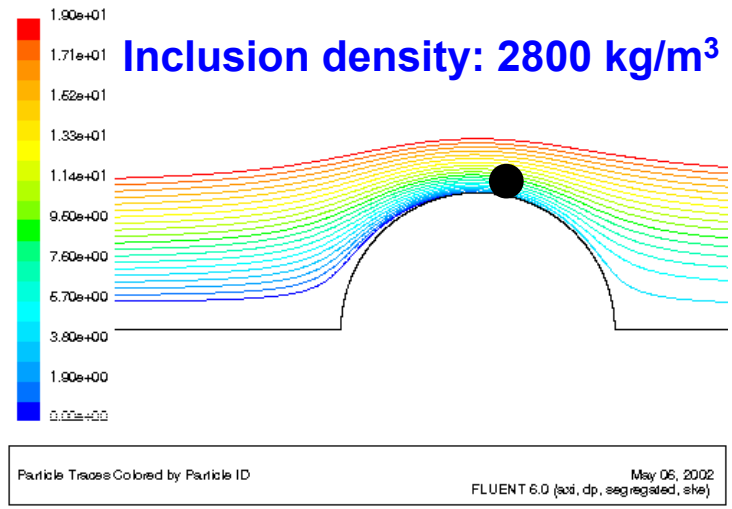

d_p=100μm

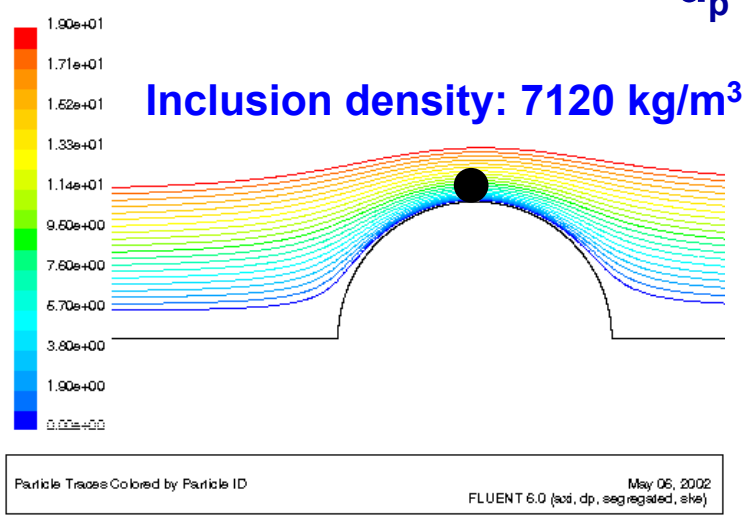

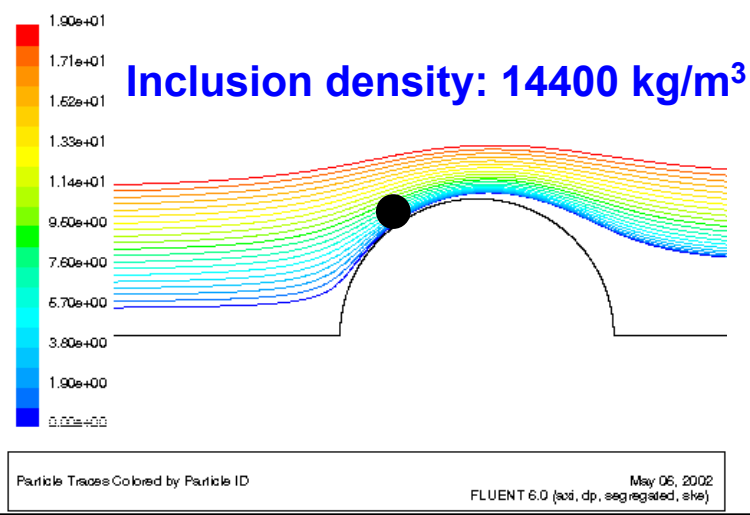

Effect of Turbulence Fluctuations on Inclusion Trajectory

100μm Silica inclusions moving towards a 5mm bubble in Liquid steel

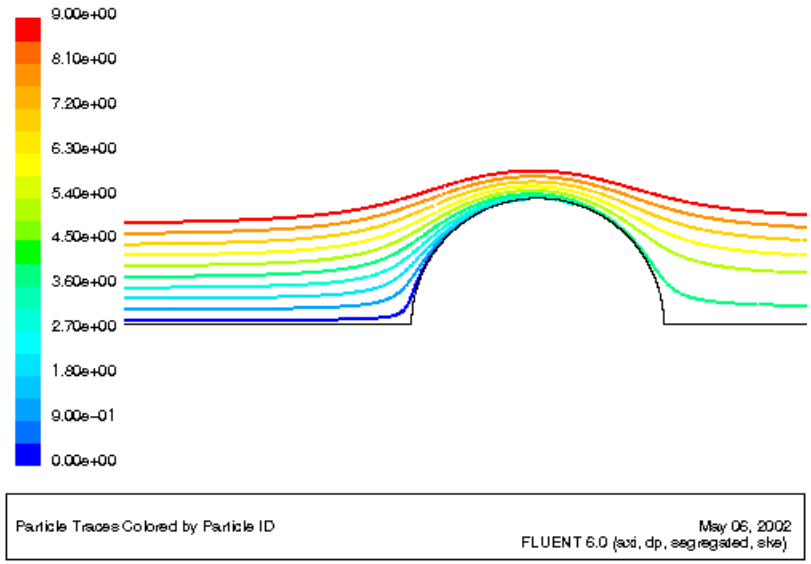

Streamline model

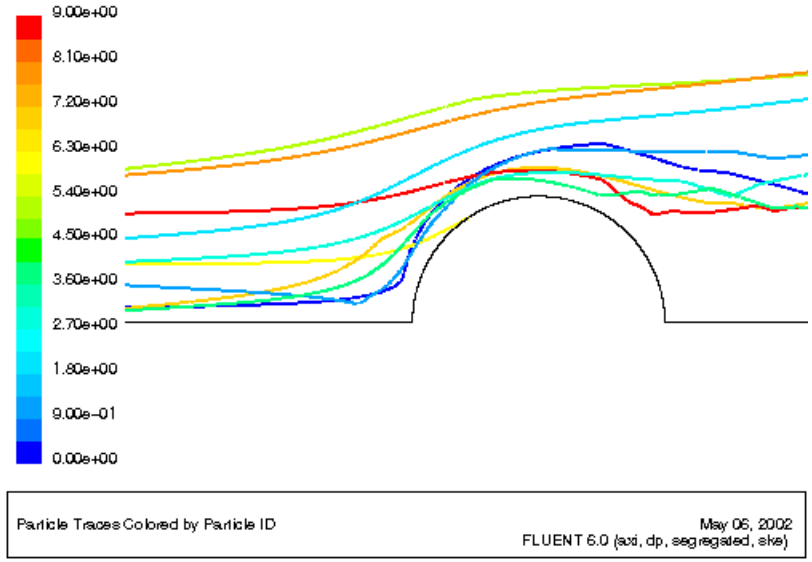

Random-walk model

The Optimum Bubble Size for Inclusion Removal by Bubble Flotation

One important conclusion: Small bubbles favor inclusion removal by bubble flotation compared to the large bubbles with the same gas fraction.

Shortcomings of very small bubbles:

1).Smaller bubbles require longer rising time. In practice, shorter treatment times significantly reduce operational costs.

2).Small bubbles (<1mm) are much more easily trapped in the recirculation zone of the bulk or re-entrained into bulk from the interface between liquid steel and slag and some of then finally are captured in the solidified front.

The optimum bubble size:

High inclusion removal efficiencies, and short refining times → 1~5mm bubbles. The better place to inject bubbles is the shroud between ladle and tundish.

3. Fluid Flow and Inclusion Motion and Removal in Steel

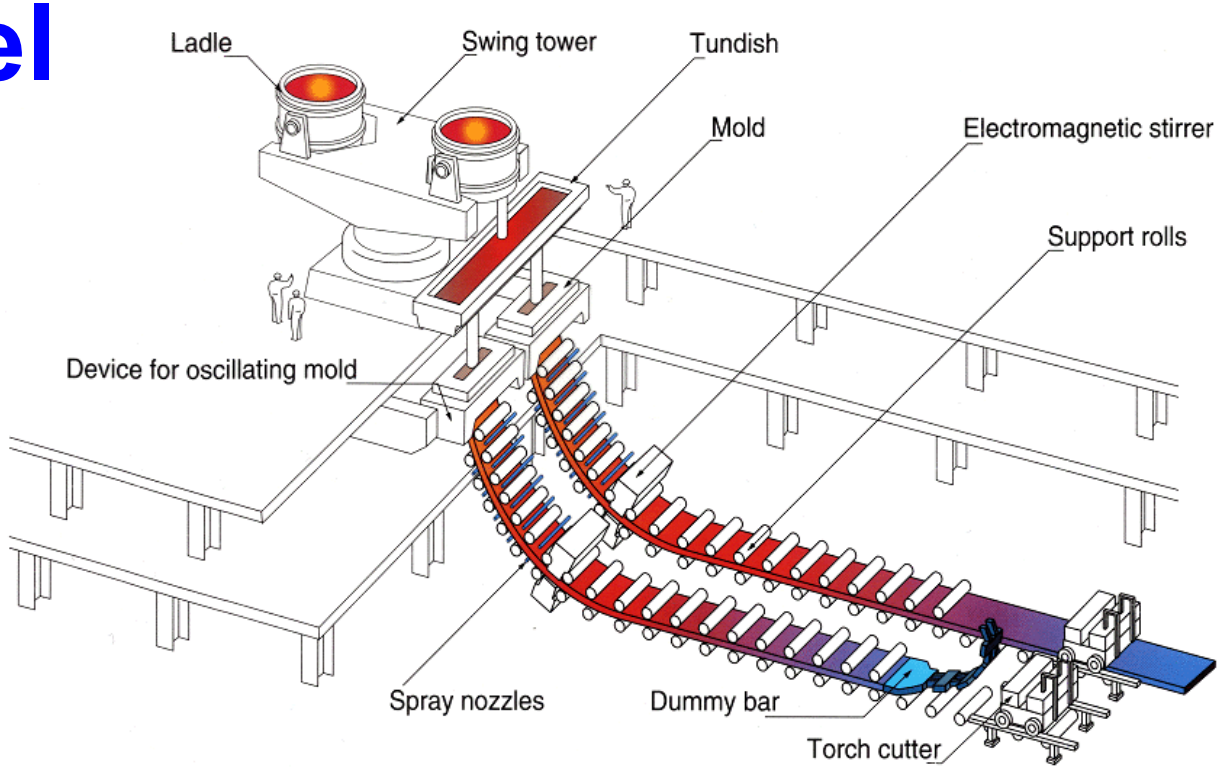

3.1 In Argon-Stirred ladles

Fluid Flow and Inclusion Motion in Argon-Stirred Ladle

Ladle: 300 tonne capacity, 3.2m bottom diameter, 3.8m top diameter, 4.5m height, argon flow rate 0.5 Nm^3/min

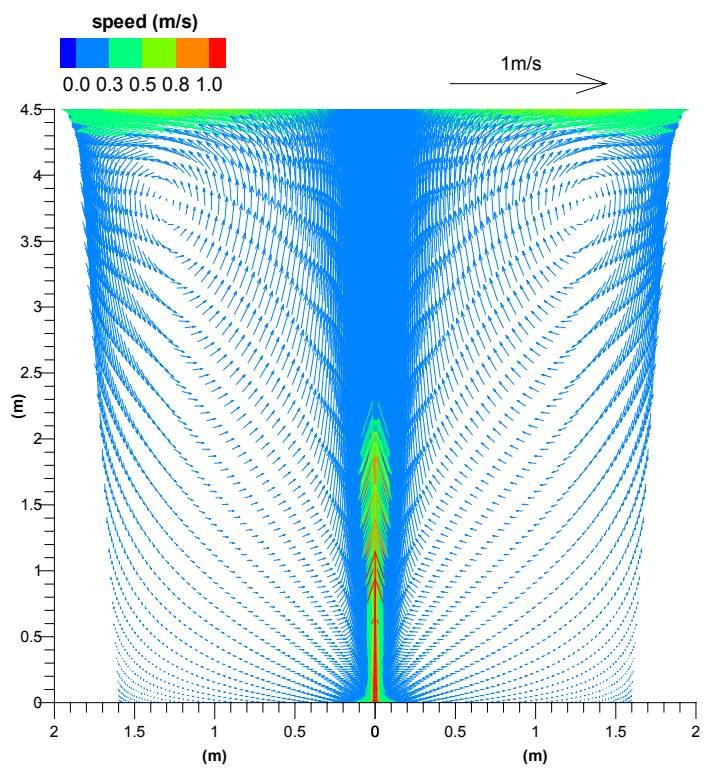

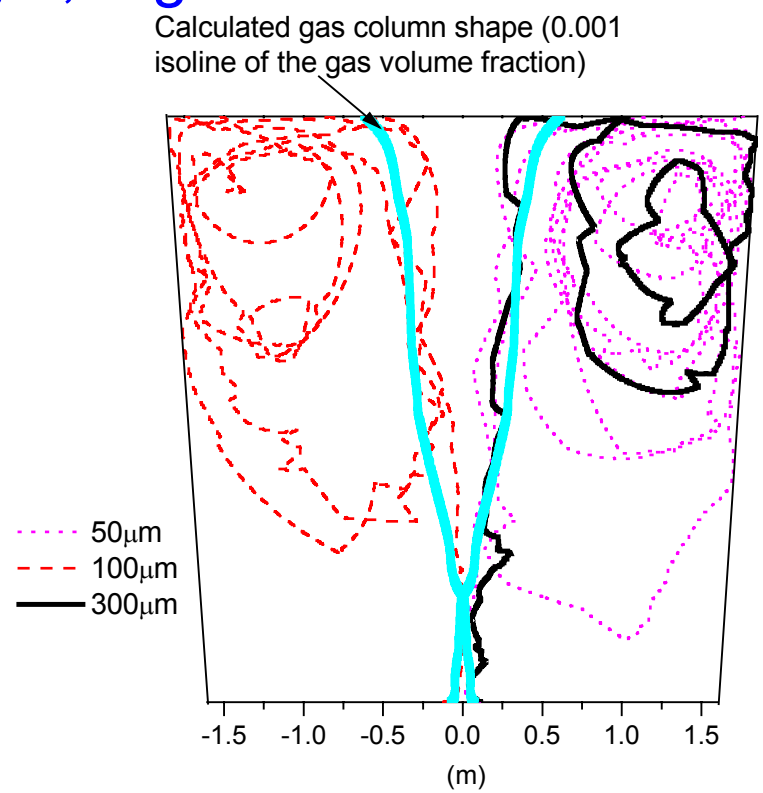

Moving path length before reaching top surface to be removed: 300mm inclusion: 24.0m (147.1s); 33mm bubble: 5.0m (3.9s)

Example Liquid Steel Ladle System

Aluminum deoxidation during ASEA-SKF Steel Refining

Ladle: 50 tonne, 2.3m diameter and 1.7m depth

Turbulent energy dissipation rate 0.01224 m^2/s^3

T.O before deoxidation: 300ppm

Free oxygen at equilibrium: 3ppm

Inclusion Size Distribution Evolution with Time

1) Particle size range is:
   0.1~1μm at 6s,
   0.1~36μm at 100s.
2) With increasing time:
   - smaller inclusions decrease in number concentration
   - larger inclusions increase

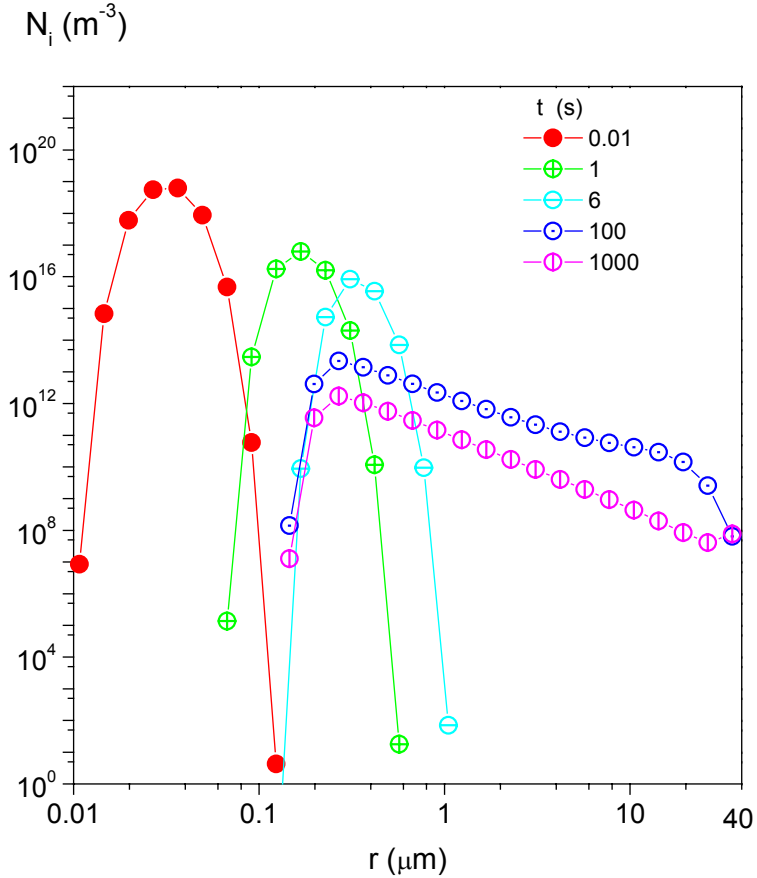

Effect of Stirring Power on Inclusion Size Distribution

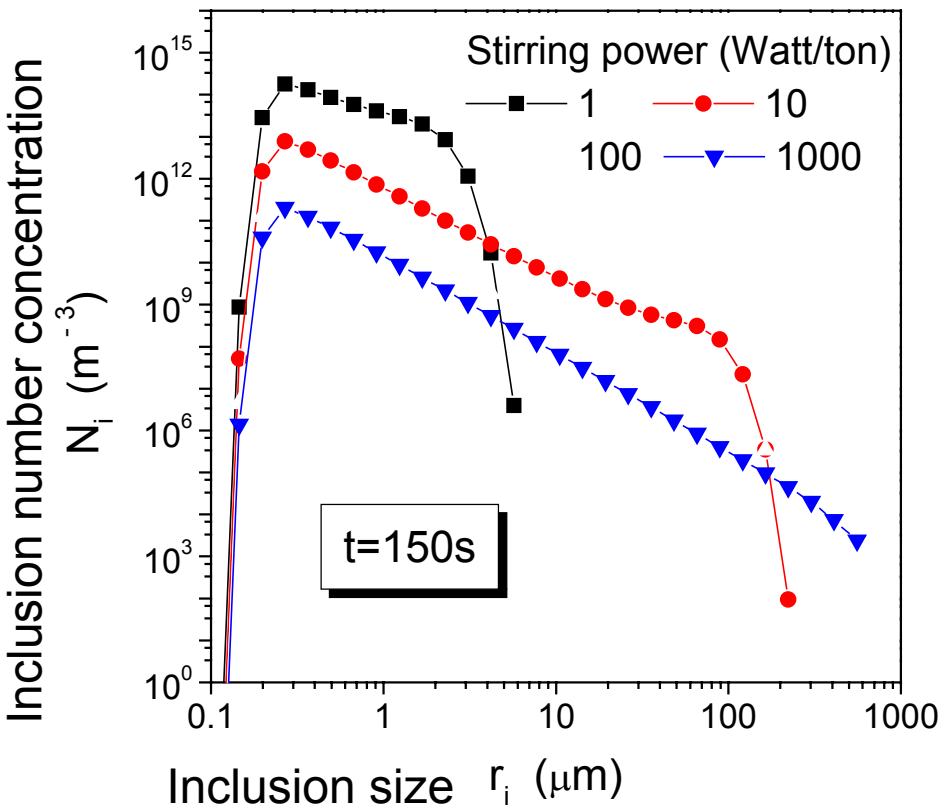

- The inclusion size distribution evolves to form larger inclusions with increasing stirring power.

- Actual steel refining processes have a range of different stirring powers.

Effect of Stirring Power on Steel Cleanliness

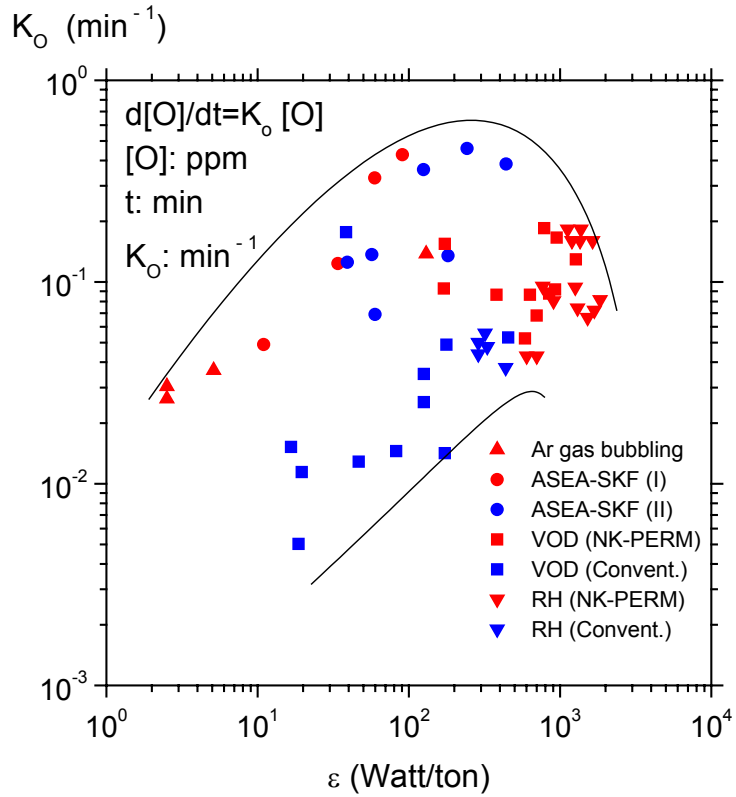

Stirring helps to lower T.O. if

1) Sufficient high stirring power
   - helps collisions
   - helps transport to interfaces

2) Not too vigorous or long
   - avoid reoxidation (eyes)
   - avoid ladle erosion
   - avoid detrimental collisions and formation of large clusters at end of refining

Refs: 1) K. Ogawa, in Nishiyama Memorial Seminar, Vol. 143/144, ISIJ, 1992, 137-166. 2) M. Matsuno et al., I & Smaker, Vol. 20 (7), 1993, 35-38.

Effect of Stirring Power on Steel Cleanliness

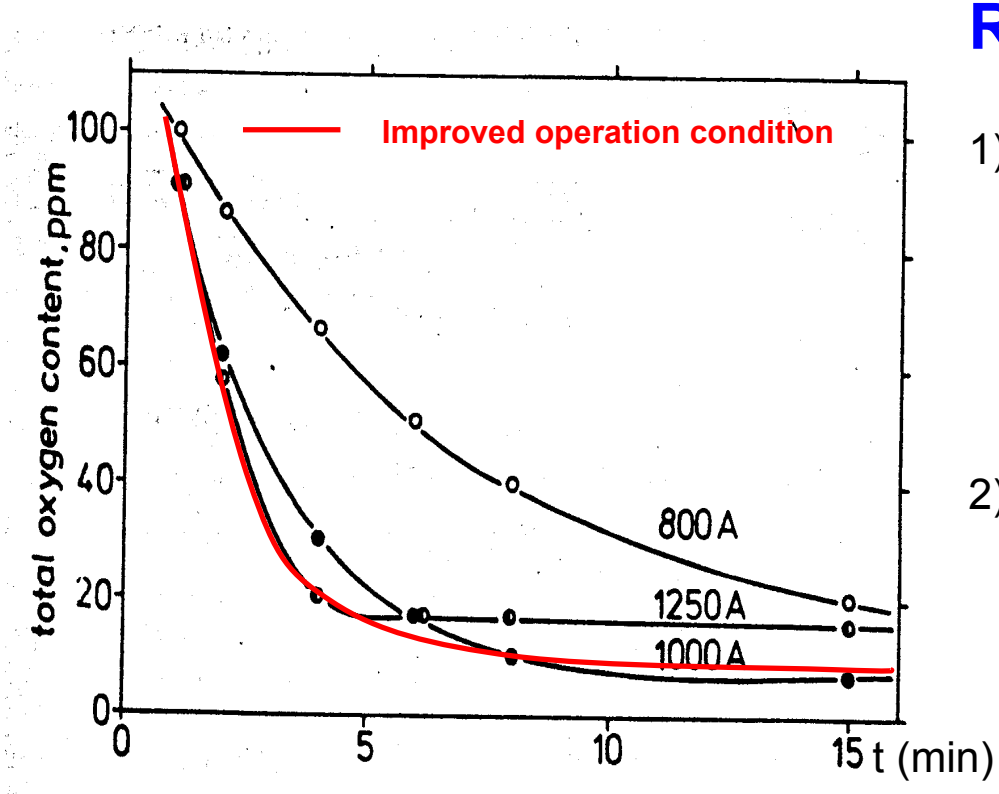

Ref: K. Schwerdtfeger, Arch. Eisenhutten, Vol. 54, 1983, 87-98.

Recommendation:

1) first stir vigorously to encourage the collision of small inclusions into large ones,

2) "final stir" slowly recirculates the steel to facilitate their removal into the slag while minimizing the generation of more large inclusions via collisions.

Conclusions

- Homogeneous nucleation takes 1μs - 10 μs.
- Initial growth via Ostwald ripening and Brownian collision: spherical inclusions < 1μm.
- Inclusions > 2μm grow by turbulent collisions: large clusters, which retain minimum feature sizes of 1~2μm.
- For optimal inclusion removal, a suitable stirring process should be chosen.

3.2 In Continuous Casting Tundish

Geometry of Tundishes

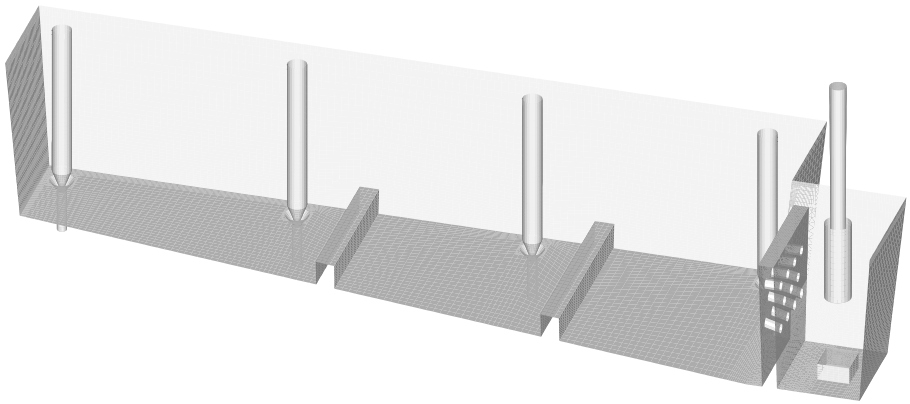

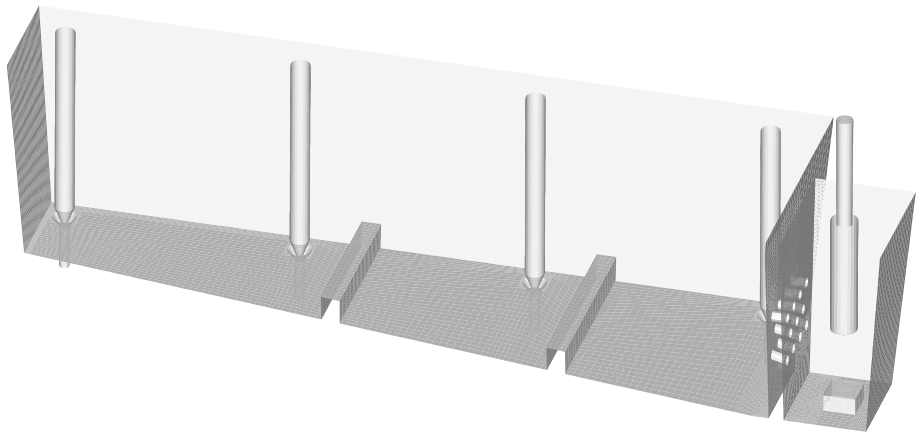

Tundish A:
780mm depth
660mm weir

Tundish B:
1000mm depth
1000mm weir

Iso-surface of $\varepsilon=10^{-5}$ m^2/s^3

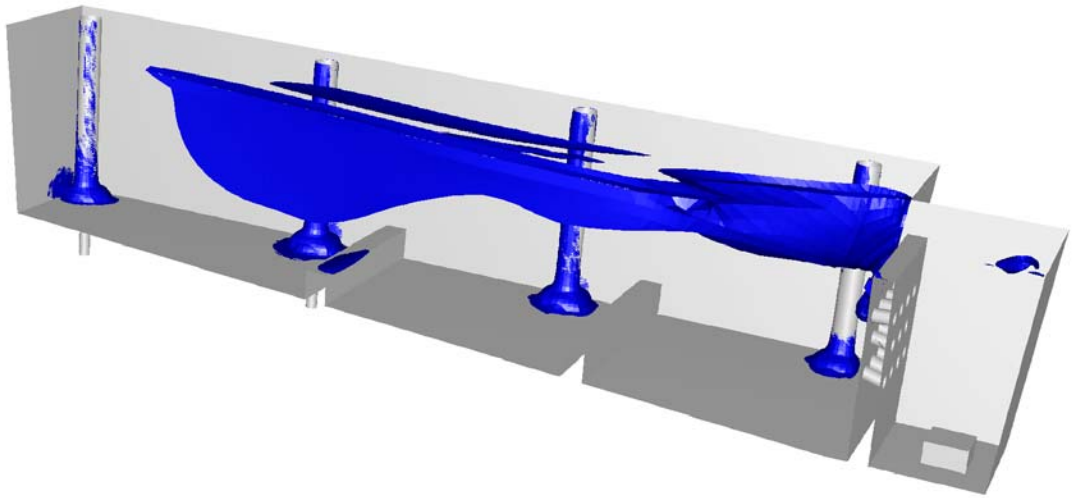

Tundish A

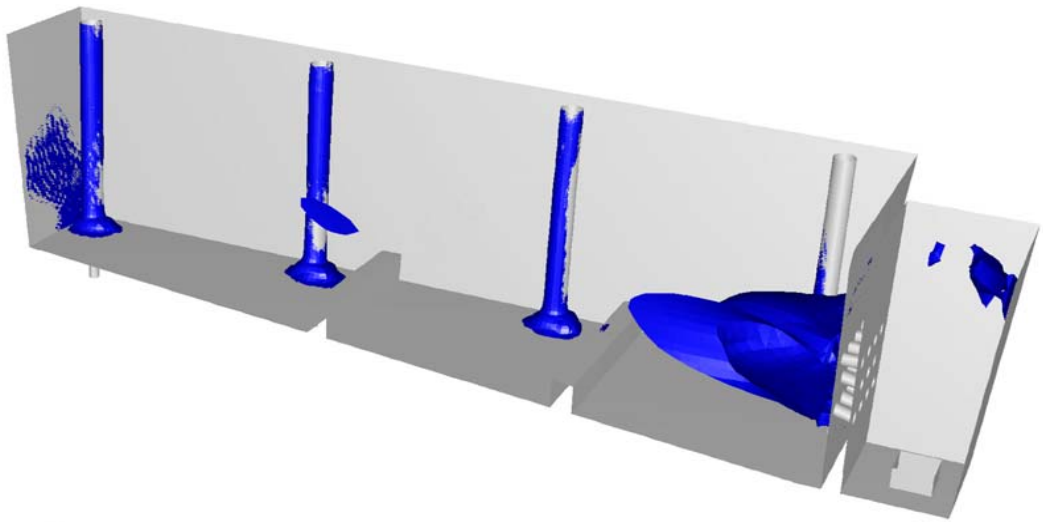

Tundish B

Inclusion Trajectories in the Tundish

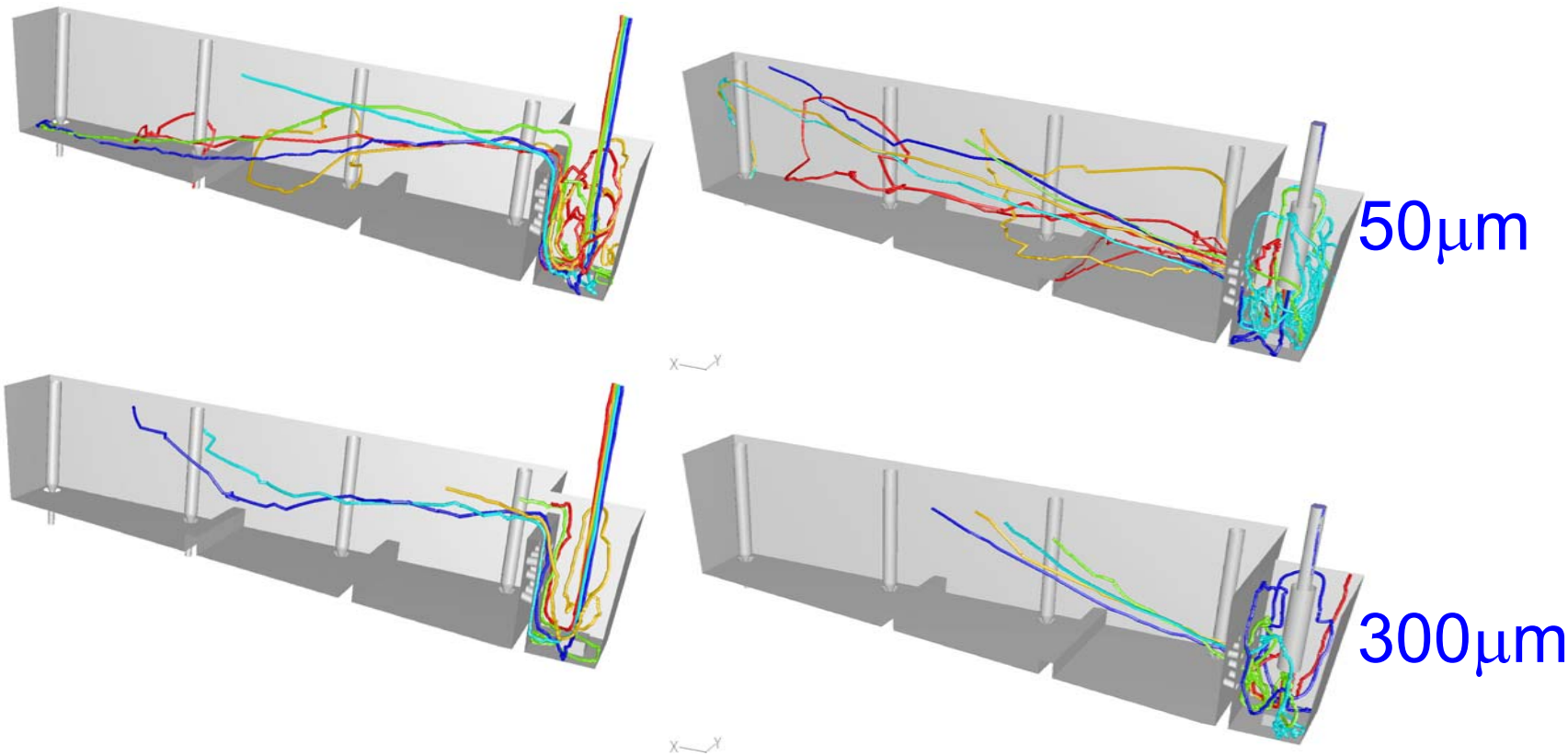

Tundish A

Tundish B

Inclusion Positions in the Tundish

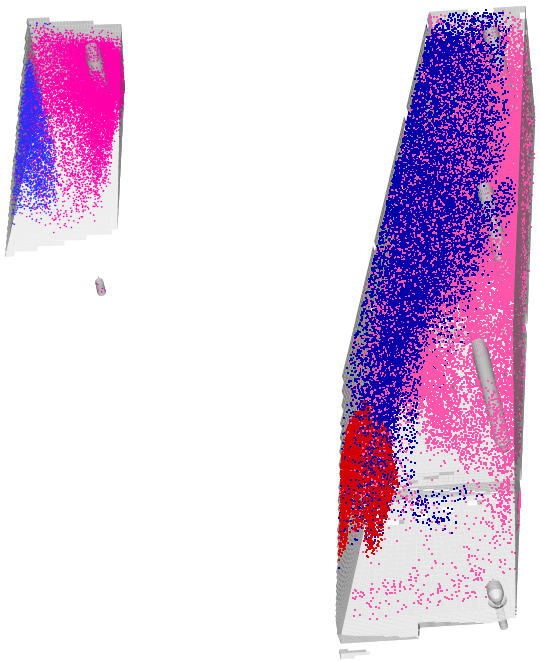

Safe removal fraction:
Tundish A: 13%

Tundish B: 32%

Deeper tundish with a full depth of weir favors inclusions removal.

Red: t=30s, blue: t=130s, pink: t-230s

Tundish A Tundish B

3.3 Fluid Flow and Inclusion Motion in SEN

Parameters for SEN Simulation

Turbulence	k-ε two equation, Fluent
Inclusion motion model	Random-Walk, 0.001s time step, 10000 particles each size

Parameters	Value
SEN bore diameter, length (mm)	80, 1292
SEN submergence depth (mm)	300
Port width× port height (mm × mm)	65 × 80
Port thickness (mm)	30
Port angle	Down 15 deg, up 15 deg, zero deg
Bottom well depth (mm)	10
Liquid steel flow rate (m^3/s)	0.0065
Casting speed (m/min)	1.2
Fluid density (kg/m^3)	7020
Fluid kinetic viscosity (m^2/s)	9.54×10^{-7}
Particle size (diameter) (μm)	49, 225
Particle density (kg/m^3)	5000
Inlet condition	From the simulation of tundish outlet

Dimension and Mesh

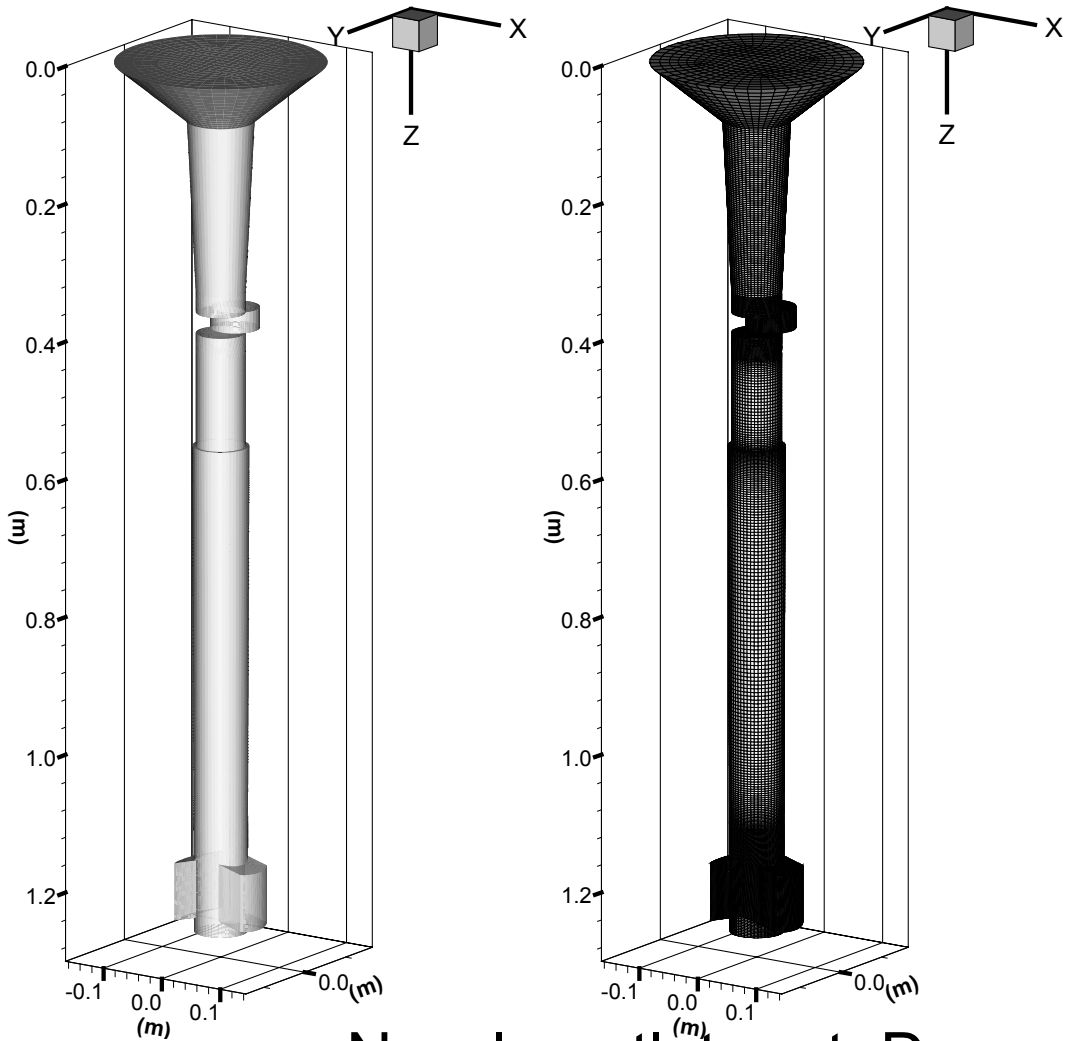

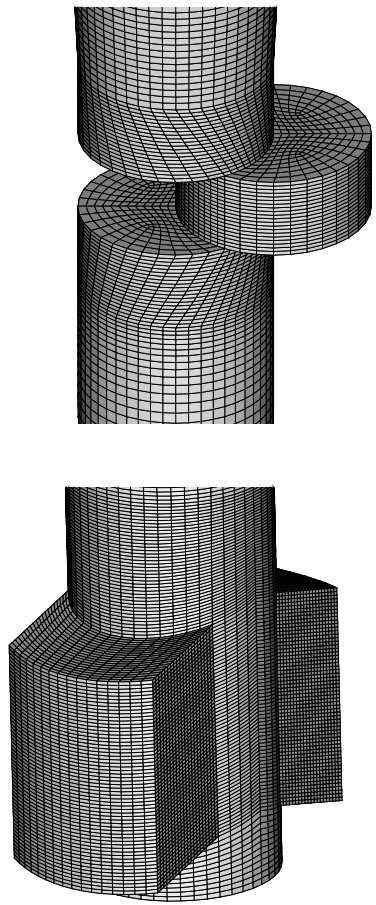

Nozzle outlet port: Down 15°

Comparison between Step Nozzle and Non-Step Nozzle

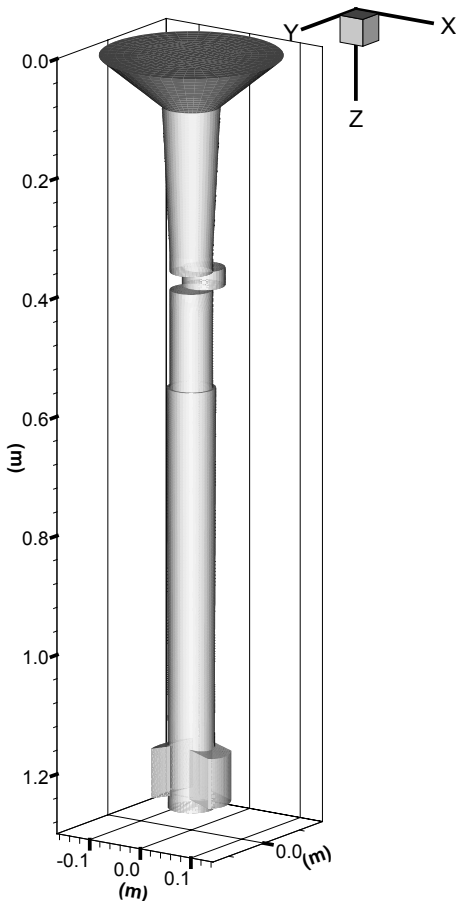

Non-Step Nozzle

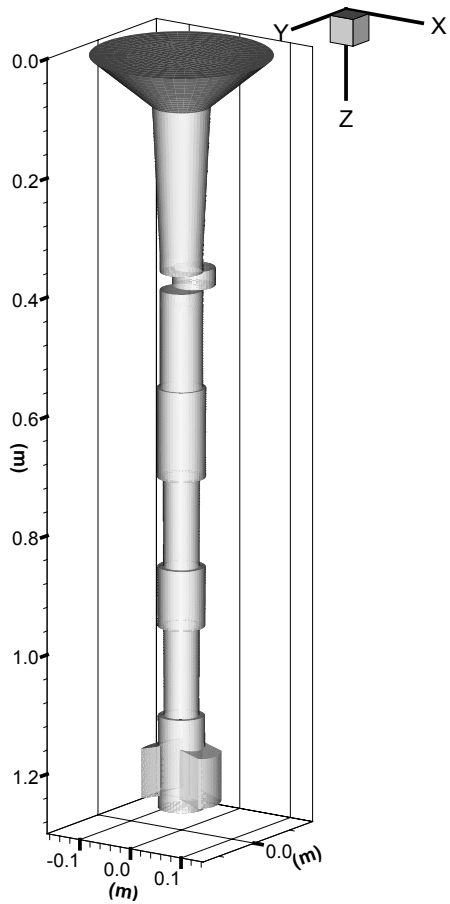

Step Nozzle

Nozzle outlet port: Down 15°

Fluid Flow at SEN Outlet Port

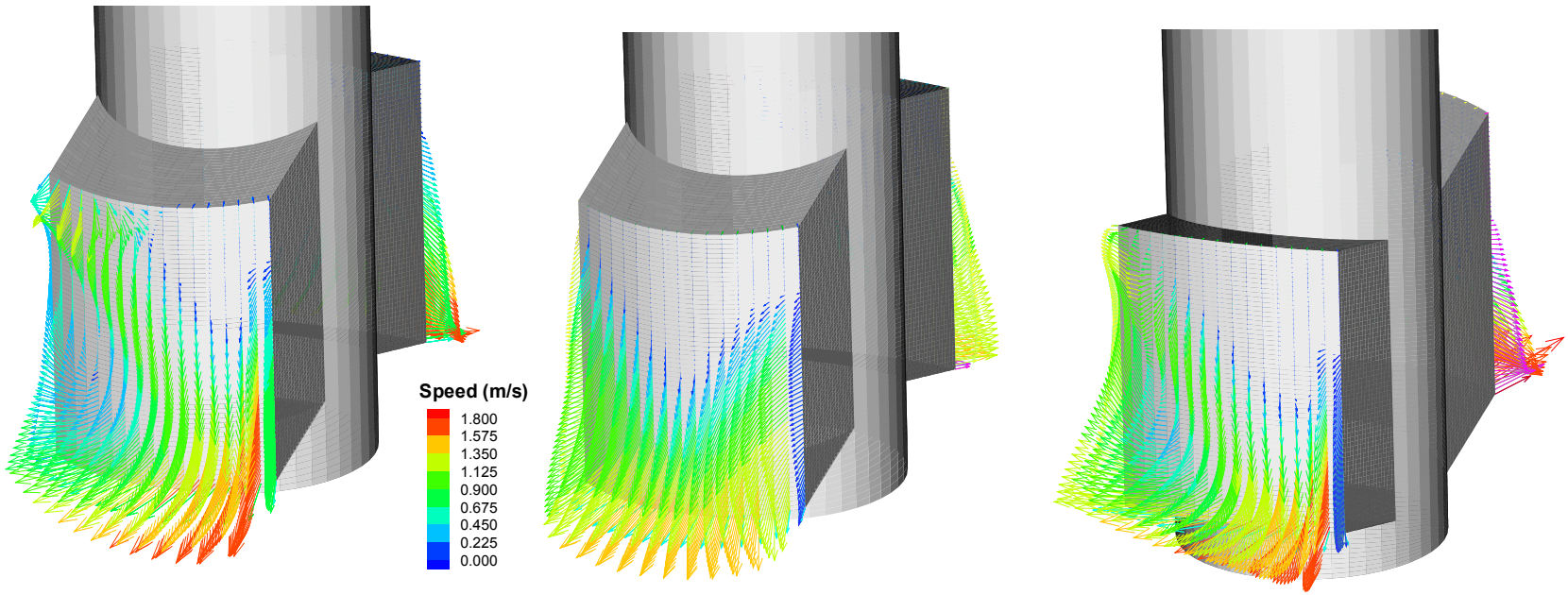

Down 15°
Non-Step

Down 15°
Step

Up 15°
Non-Step

Velocity Distribution and Inclusion Entrapment in SEN

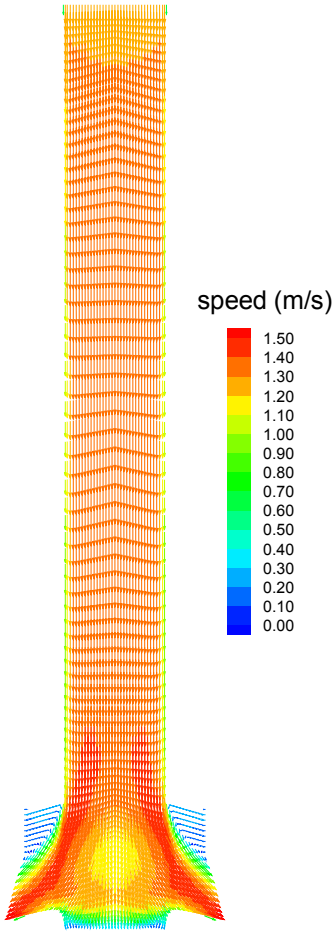

Vertical section

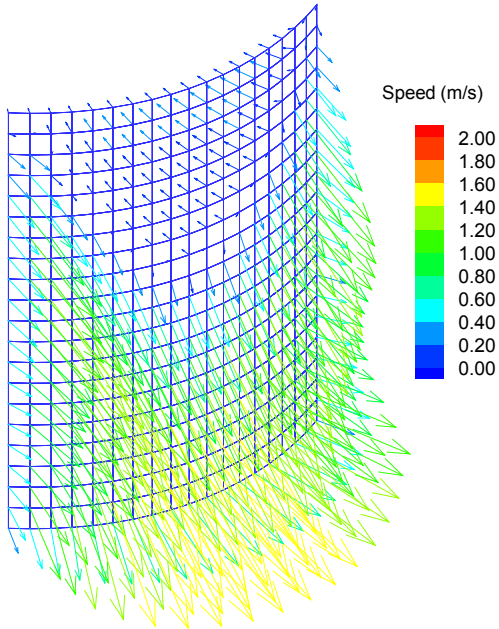

Outlet port

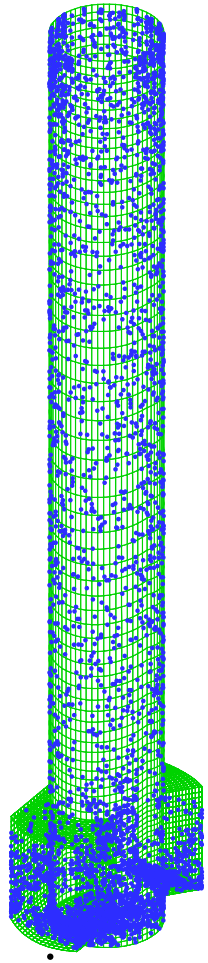

Inclusion position trapped on walls

SEN Jet Characteristics

SEN Outport angle	**Zero**	**Up 15º**	**Down 15º**	**Down 15º**
With steps or not	No	No	No	Two steps
Weight average x velocity (m/s)	0.86	0.87	0.80	0.96
Weight average y velocity (m/s)	-0.0071	0.0018	-0.035	0.012
Weight average z velocity (m/s)	0.28	0.14	0.45	0.32
Weight average turbulent energy (m^2/s^2)	0.31	0.32	0.27	0.20
Weight average turbulent energy dissipation rate (m^2/s^3)	8.88	10.47	6.41	5.27
Vertical jet angle (º)	**17.76**	**9.10**	**29.29**	**18.23**
Horizontal jet angle (º)	-0.47	0.12	-2.52	0.72
Jet speed (m/s)	0.90	0.89	0.92	1.01
Back-flow zone fraction (%)	**20.73**	**26.15**	**15.31**	**29.38**

Fluid Flow at SEN Center Section

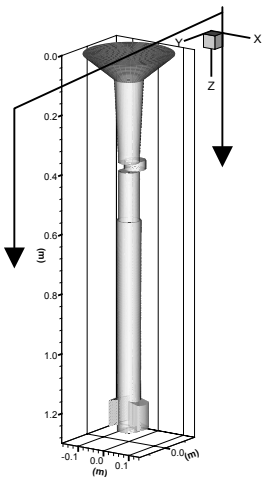

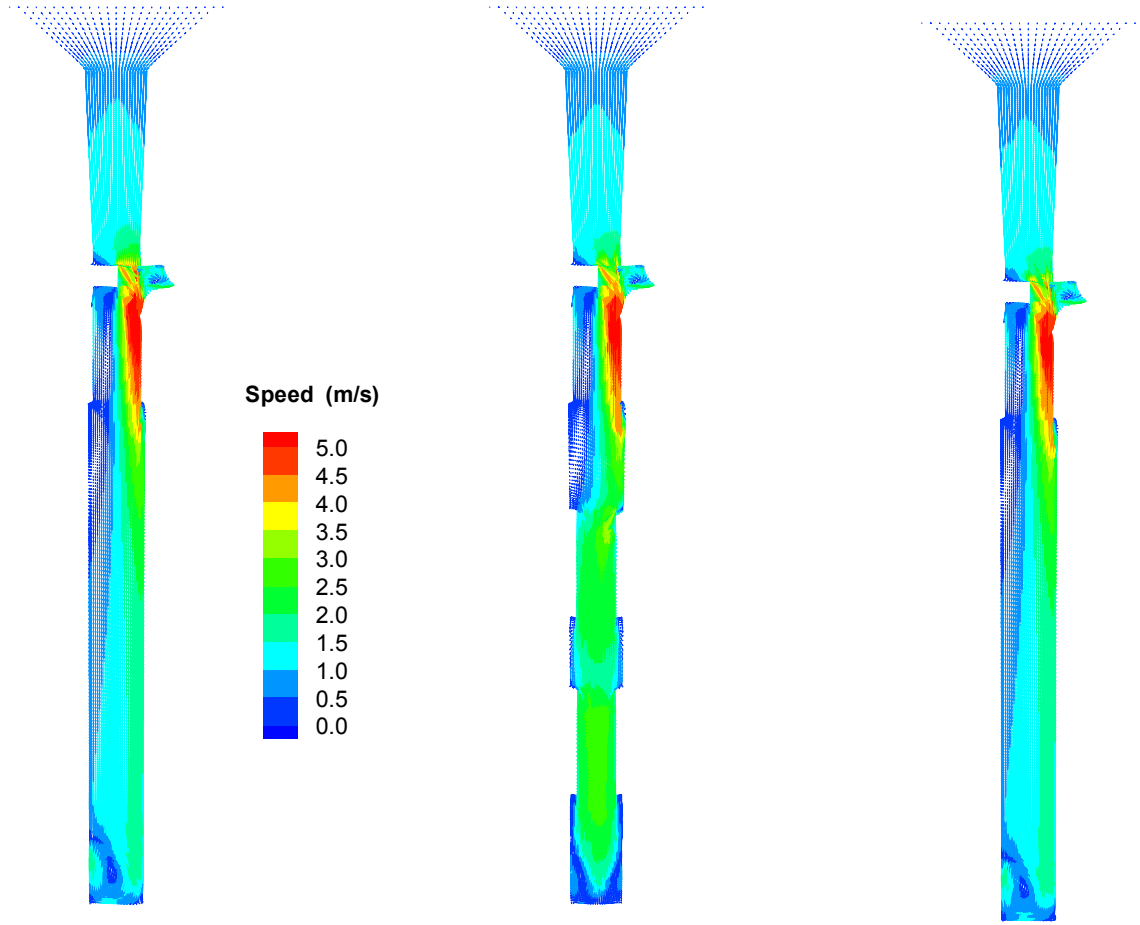

Down 15° Non-Step

Down 15° Step

Up 15° Non-Step

Fluid Flow at SEN Center Section

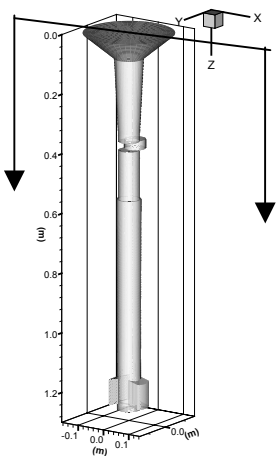

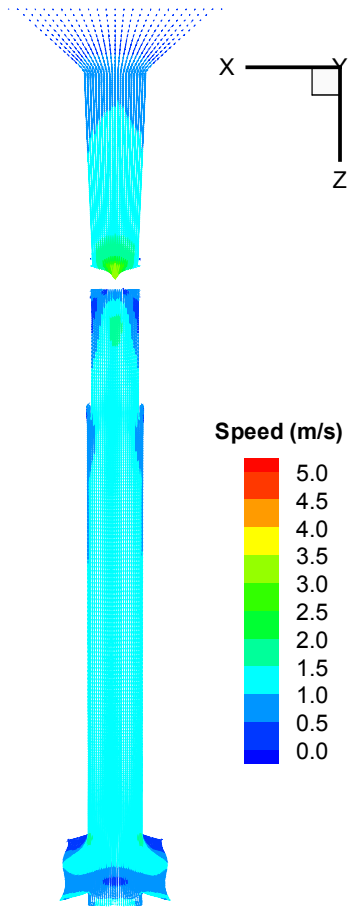

Down 15° Non-Step

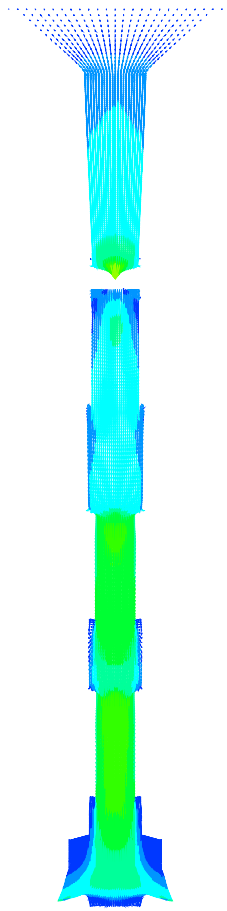

Down 15° Step

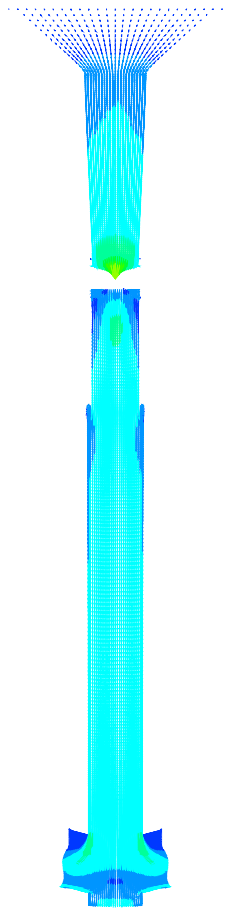

Up 15° Non-Step

Fluid Flow at SEN Outport Section

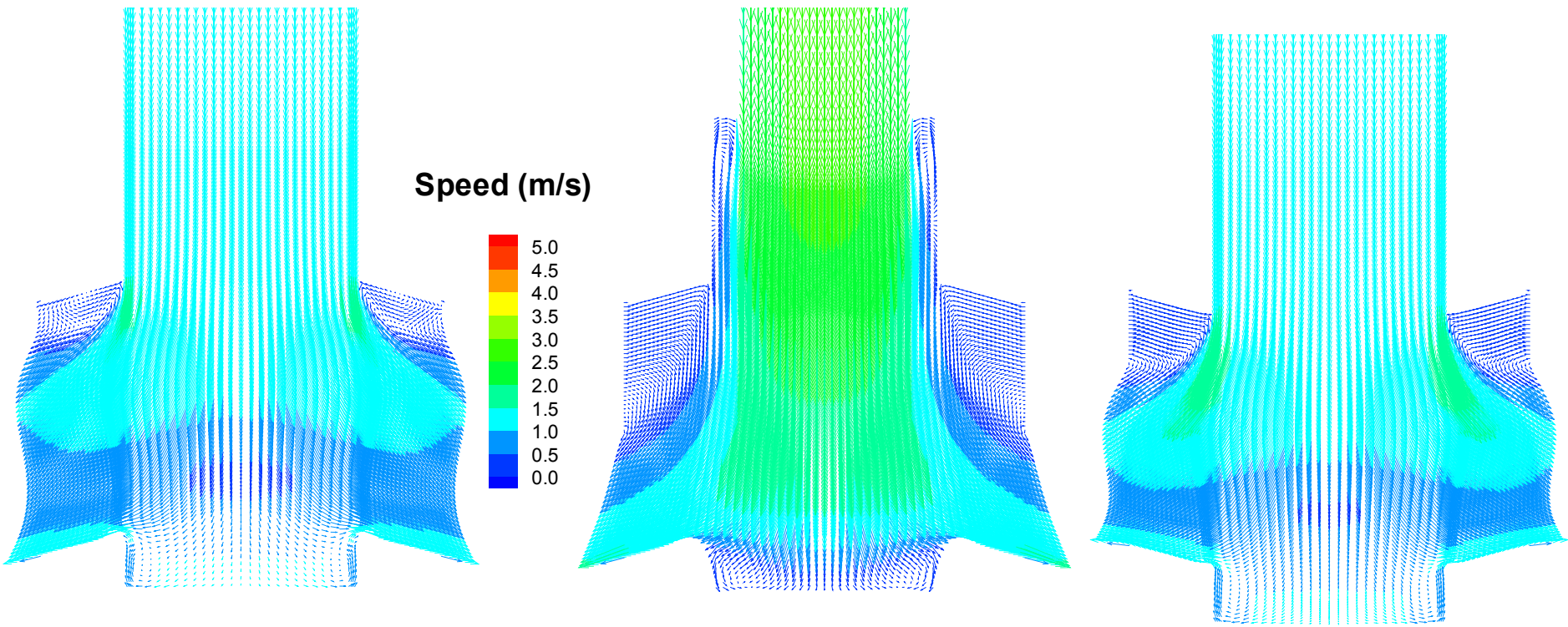

Down 15° Non-Step

Down 15° Step

Up 15° Non-Step

Fluid Flow near SEN Bottom

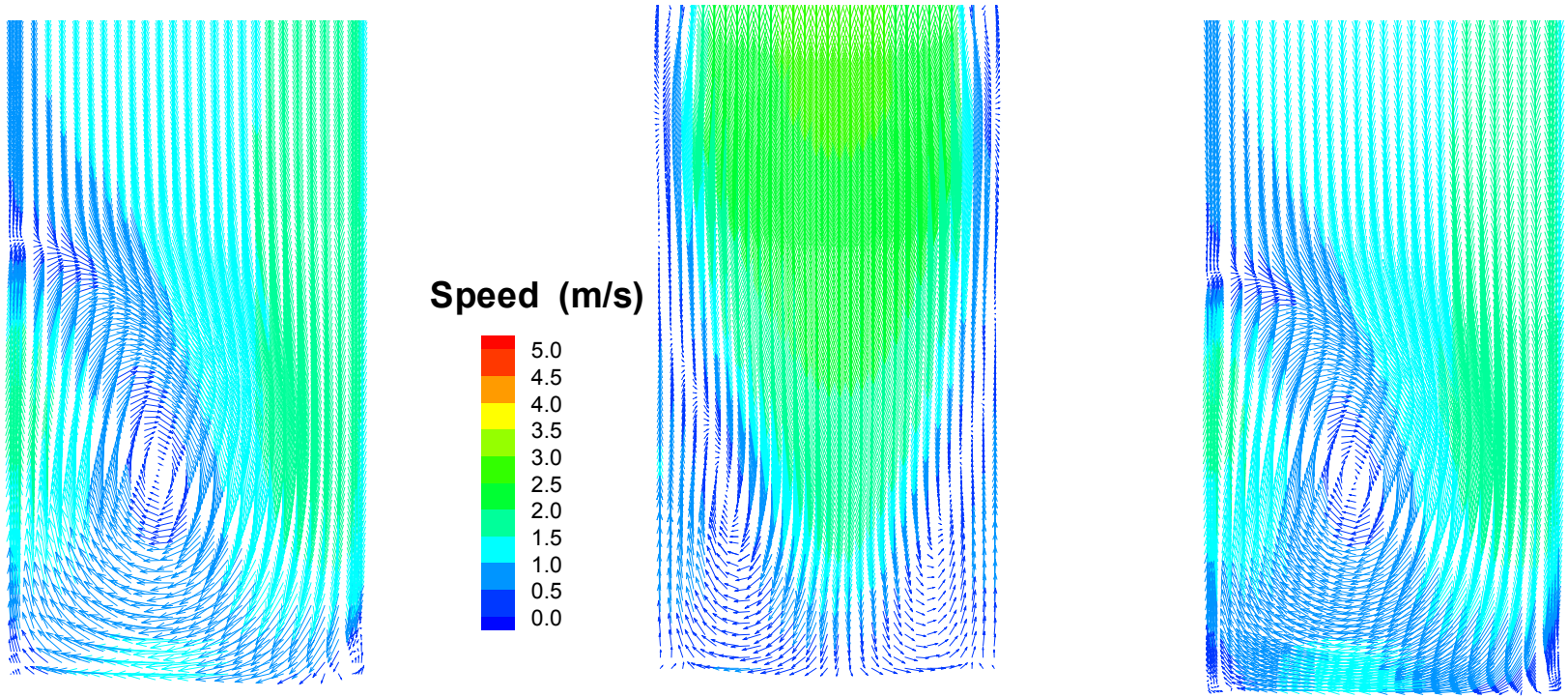

Down 15° Non-Step

Down 15° Step

Up 15° Non-Step

Steps in the SEN eliminate the strong single swirl at the outports.

Inclusion (50μm) Motion in SEN

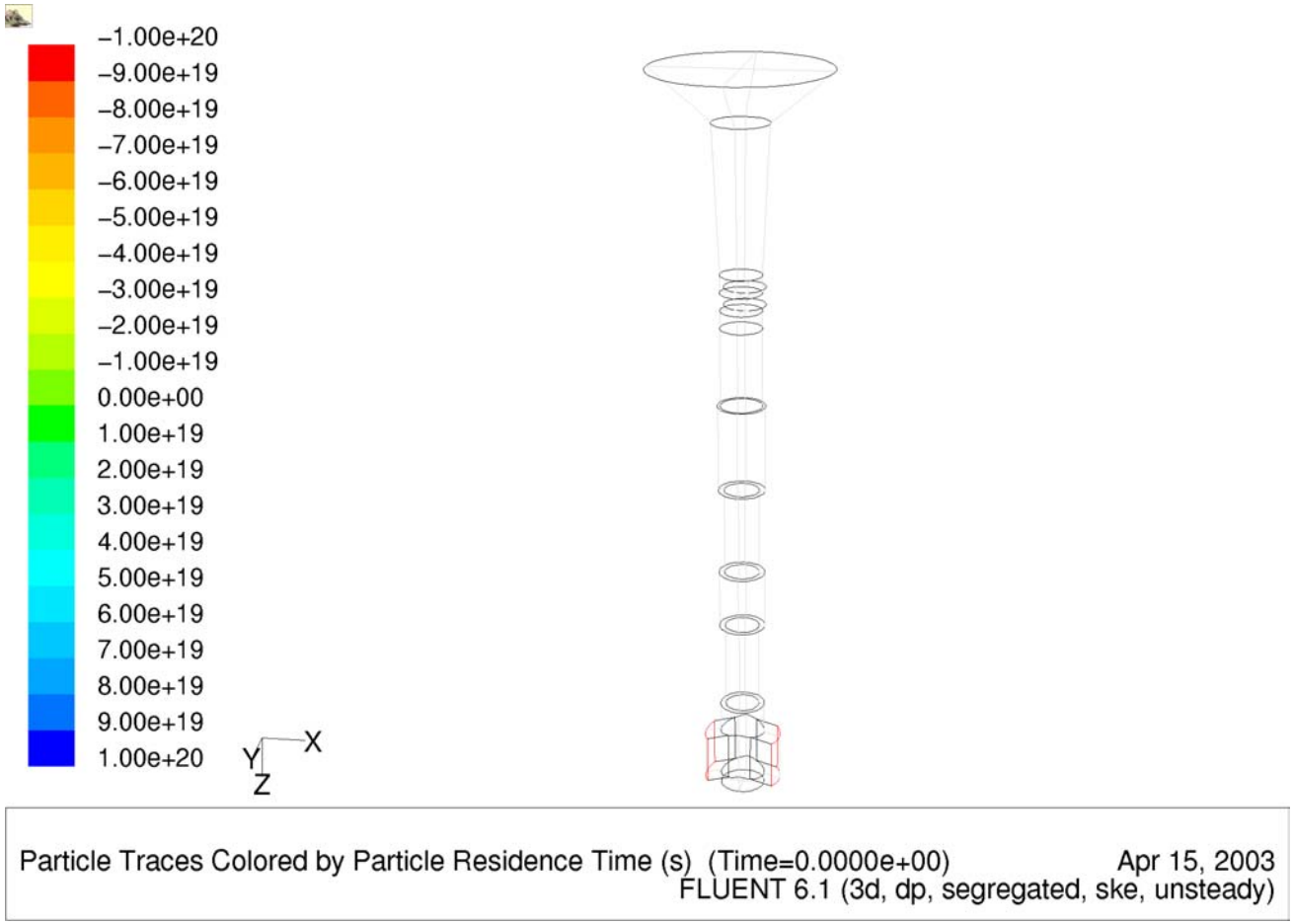

Inclusion (50μm) Motion around Slide Gate Part

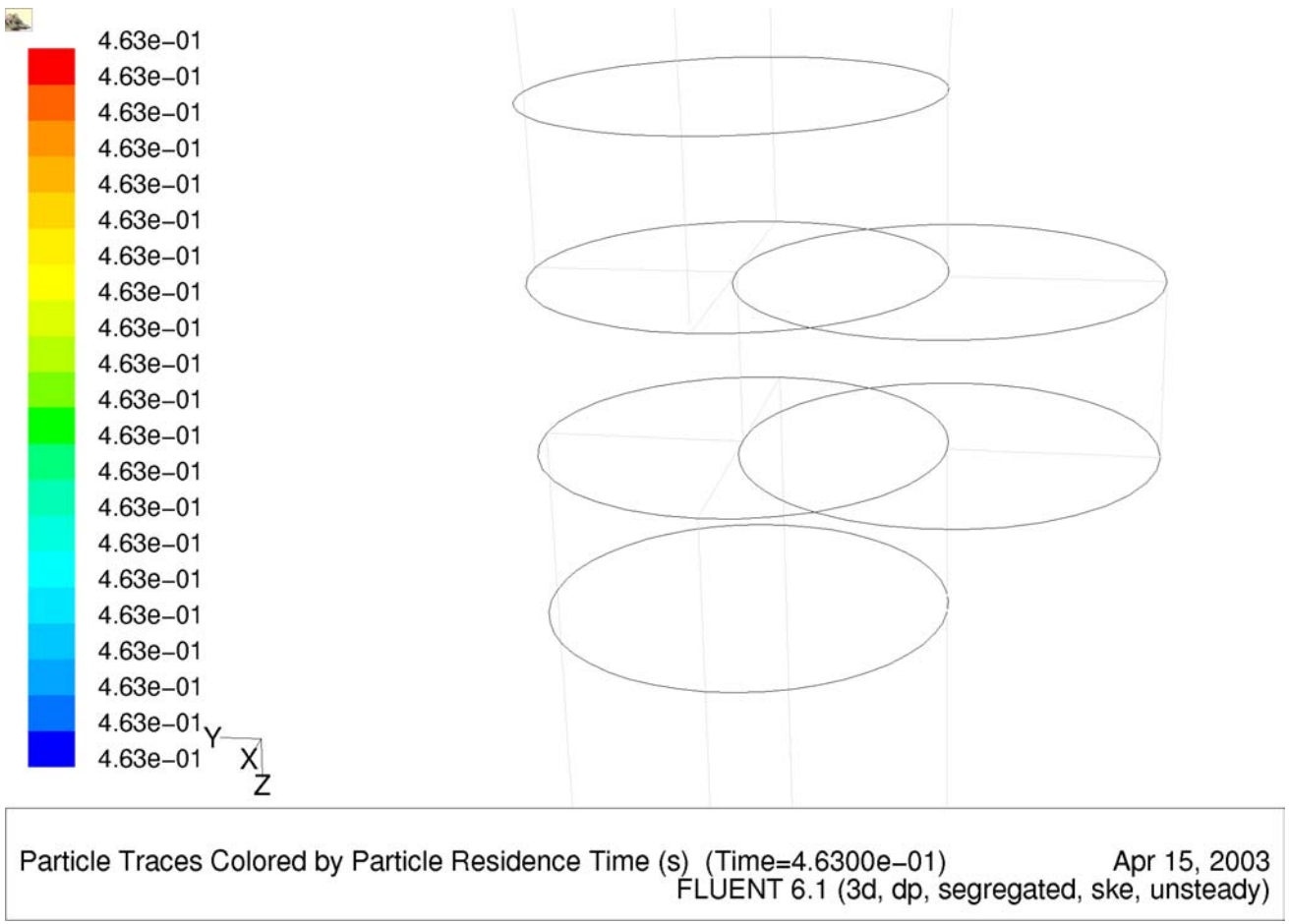

3.4 Fluid Flow and Inclusion Motion in the Mold

Phenomena Related to Inclusions in CC

Continuous Casting Consortium

Inclusion Sources:

- Carrying in through nozzle
  - Deoxidation Products
  - Nozzle clog
  - Entrainment of tundish/ladle slag (reoxidation by SiO_2, FeO, MnO in slag)
- Entrainment of mold slag by excessive top surface level fluctuation
- Reoxidation by air absorption from nozzle leaks
- Argon bubbles
- Precipitation of inclusion in low superheat, such as TiO_2

Inclusion Removal:

- Buoyancy rising
- Fluid flow transport
- Attachment to bubble surface and fast rising (Bubble flotation)
- Inclusion growth by collision and Ostwald-Ripening
- Absorption from steel to slag at interface

Inclusion Destination:

- Top slag layer (safe removal)
- Trapped in solidification shell (defect)

Parameters for Caster Simulation

Turbulence model	k-ε, by Fluent
Inclusion motion model	Random walk model , 0.1s time step ,by Fluent
Boundary condition for inclusions	Escape from top surface and open bottom, trapped at narrow and wide face walls

Inlet port size (width× height) (m × m)	0.065×0.080
Nozzle angle	Down 15°, up 15°, zero
Submergence depth (m)	0.3
Domain height/width/thickness (m)	2.55/1.3/0.25
Average inlet flow rate (half mold) (m^3/s)	0.00325
Casting speed (m/min)	1.2
Fluid density (kg/m^3)	7020
Fluid kinetic viscosity (m^2/s)	0.954×10^{-6}
Particle density (kg/m^3)	5000
Particle diameter (μm)	49, 225
Inlet condition	Nozzle simulation result
Gas flow rate	None

Fluid Flow in the Caster

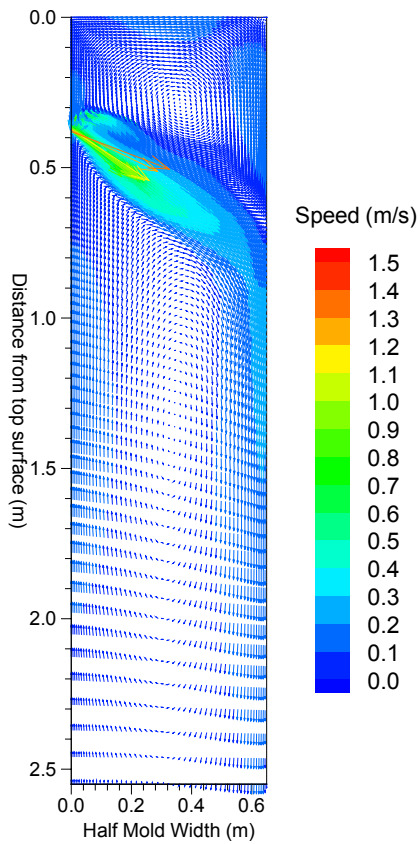

Down 15°,Non-Step

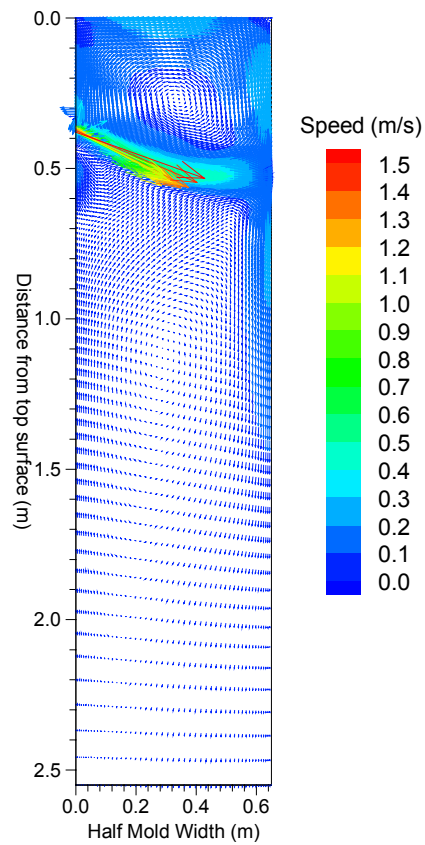

Down 15°, Step

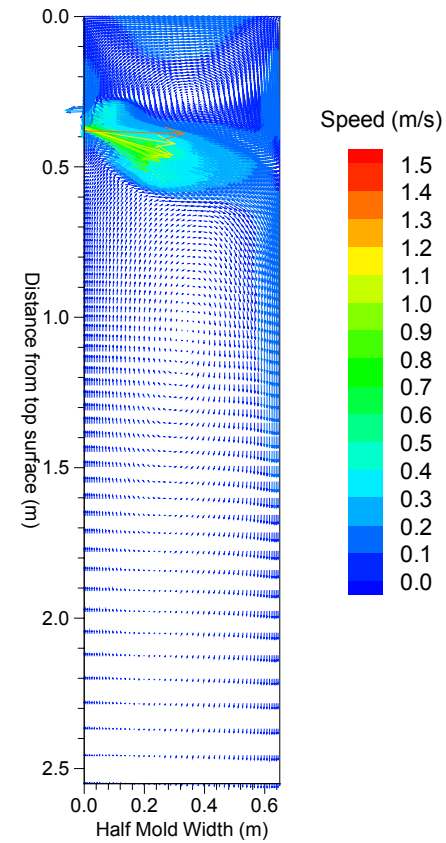

Up 15°, Non-Step

Steps in the SEN decrease the jet impingement depth in the mold.

Fluid Flow in the Caster

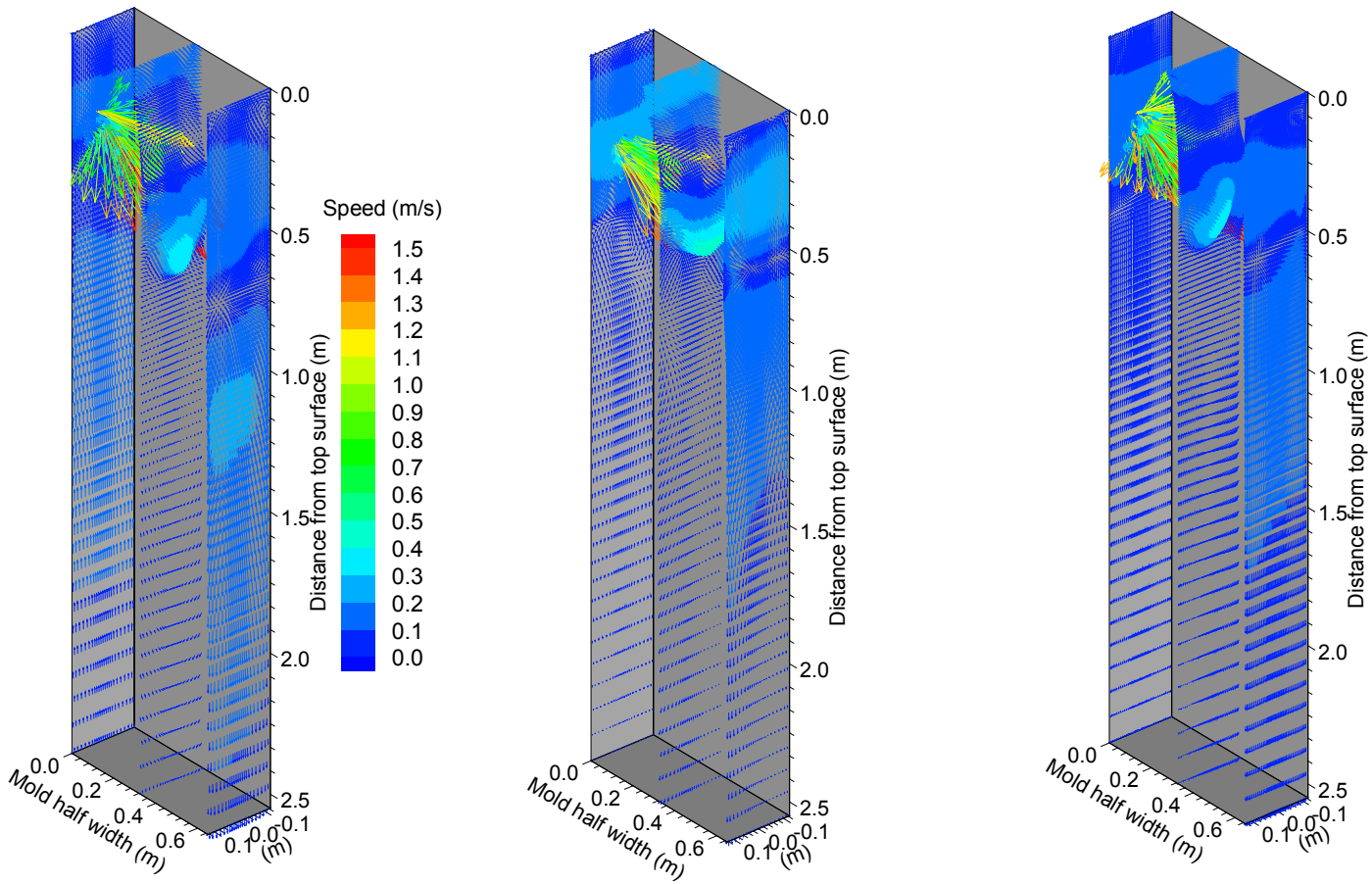

Down 15°,Non-Step Down 15°, Step Up 15°, Non-Step

Steps in the SEN decrease the jet impingement depth in the mold.

Functions of Steps in the SEN

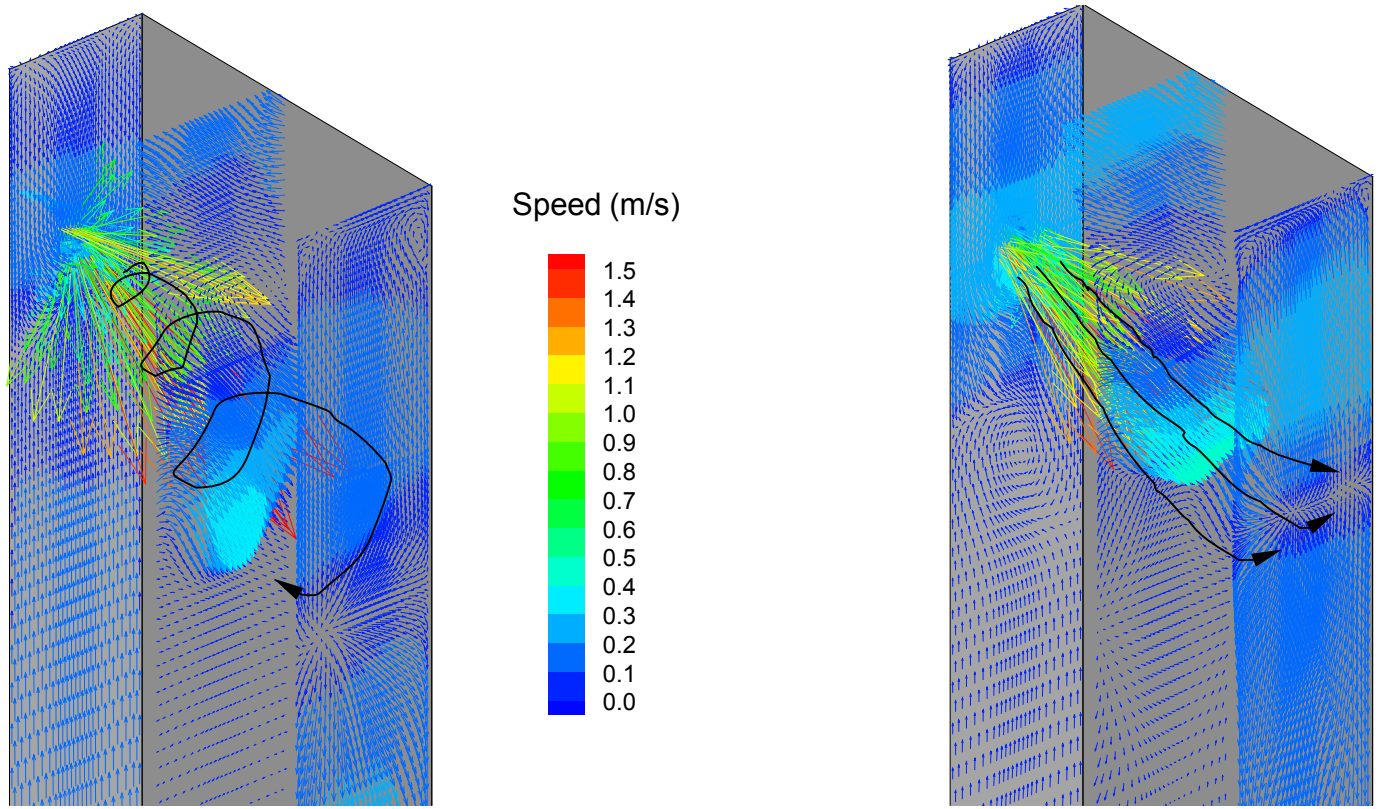

Down 15°,Non-Step

Down 15°, Step

— Eliminate the swirl flow at the SEN outport and the mold;

— Decease the jet impingement depth in the mold.

Inclusion Motion (50μm) and Removal in Caster (down 15° Non-Step SEN)

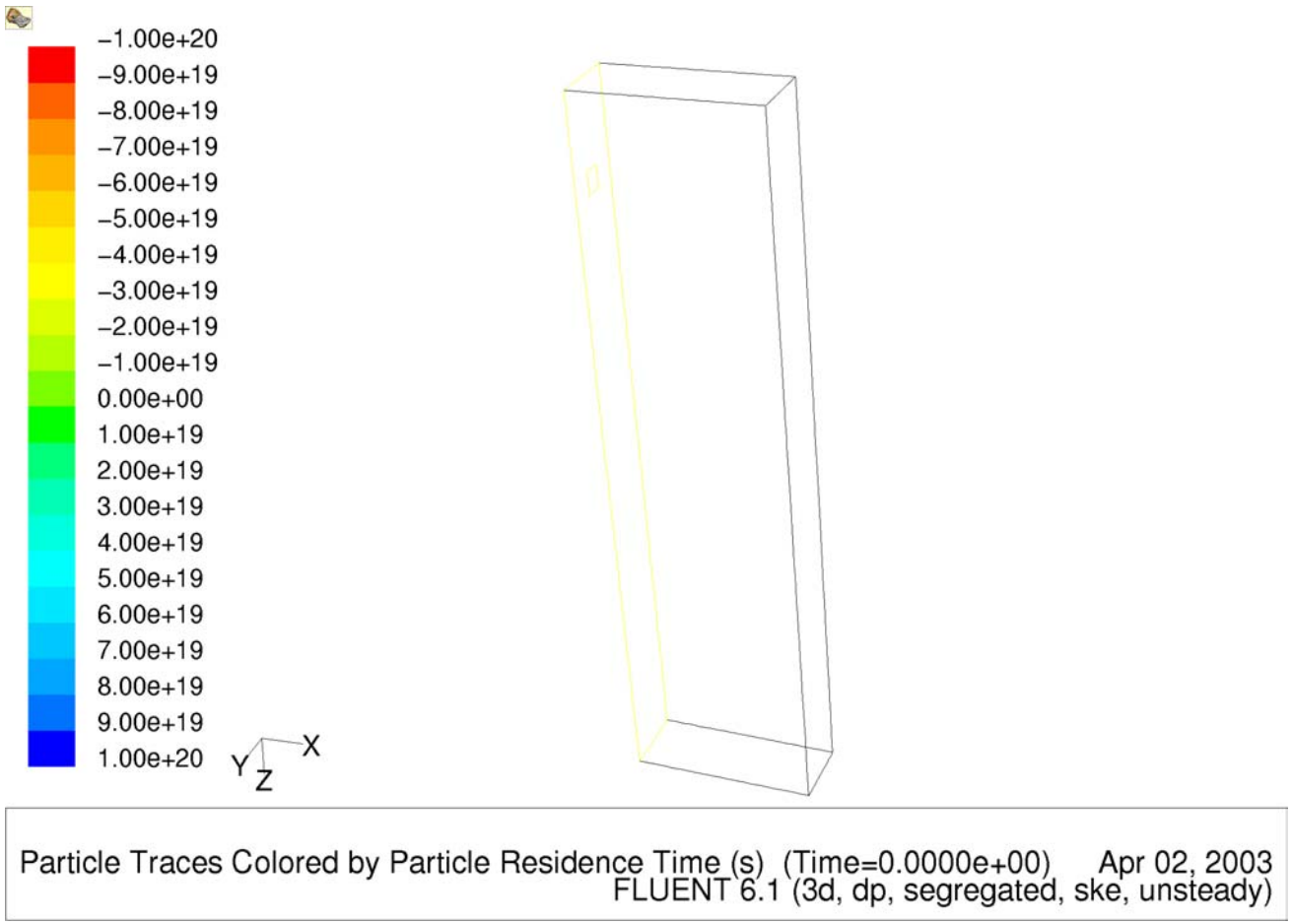

Inclusion Motion (50μm) and Removal in Caster (down 15° Step SEN)

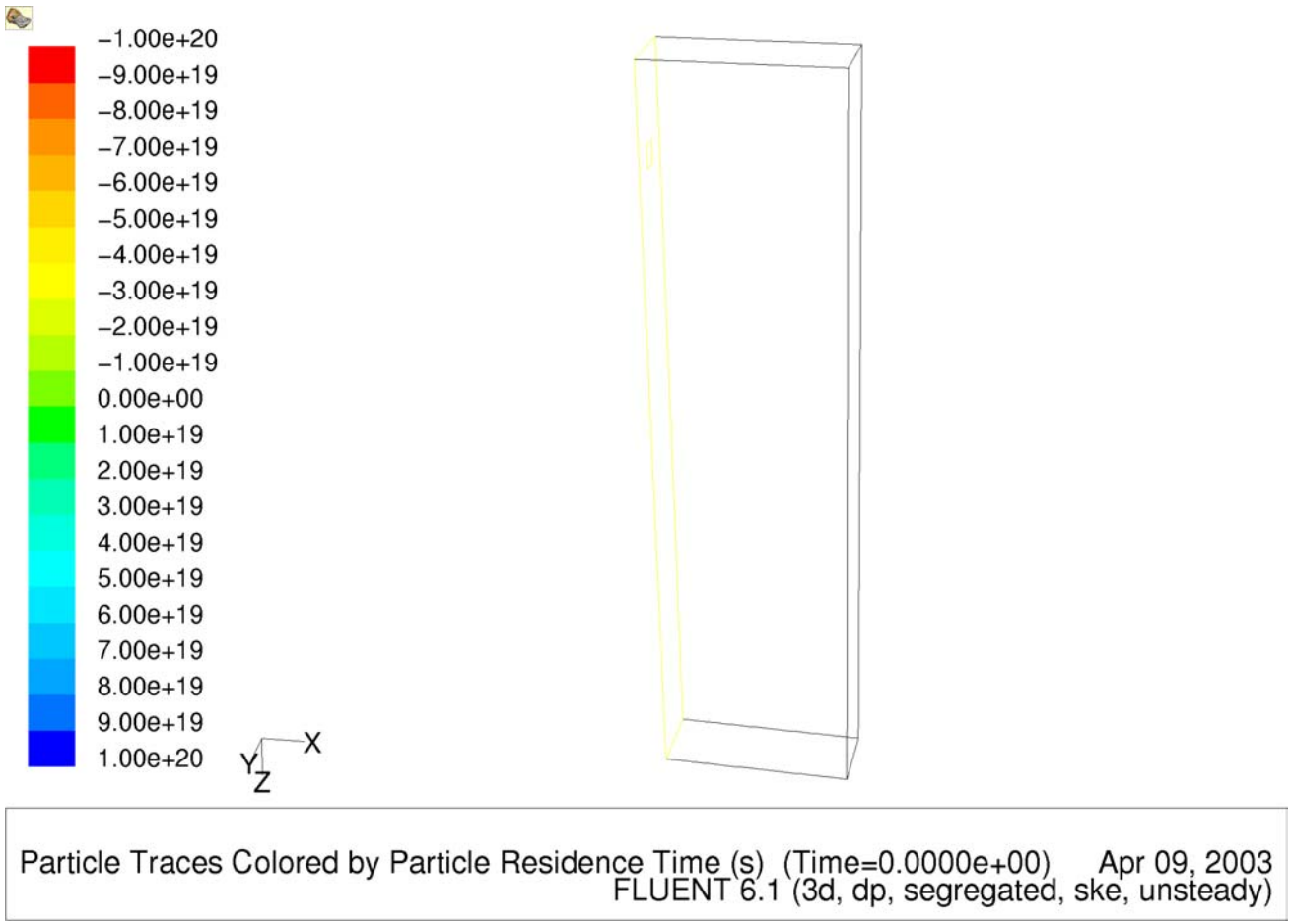

Inclusion (50μm) Motion and Removal in Caster (Up 15° Non-Step SEN)

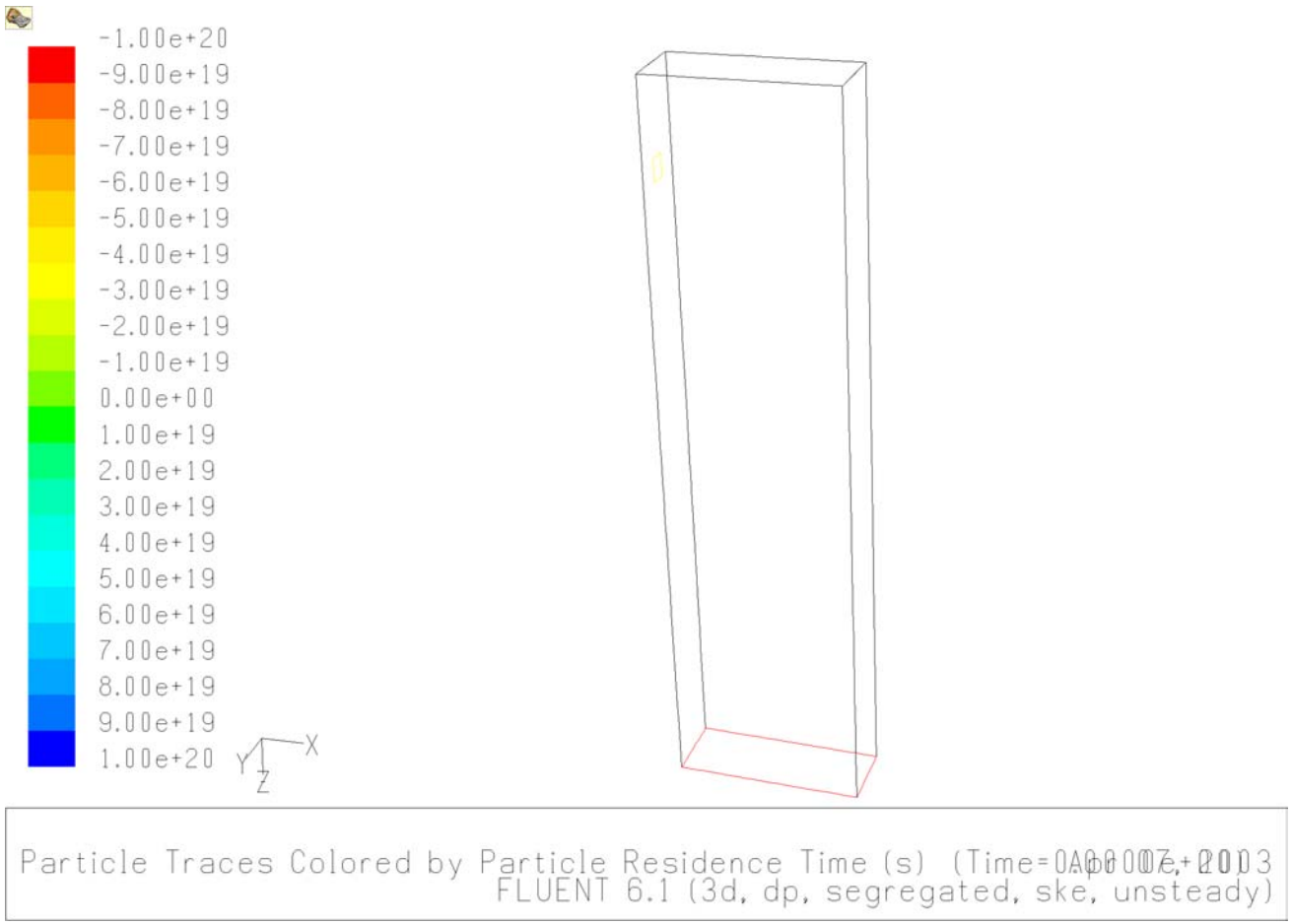

Inclusion Destinations in Caster (15000 50mm Inclusions Per Case)

SEN Outport angle	0-28mm		28-125mm	Top	Inlet
	Wide faces	Narrow faces			
Down15^o	24%	17%	55%	2%	1%
Down15^o Step	44%	24%	23%	8%	1%
Up15^o	41%	20%	32%	5%	2%

1. Step nozzle favors inclusion removal to the top surface of the mold;
2. 55% 50 mm inclusion will be entrapped in the slab thickness of 28-125mm by using non-step down 15° nozzle. This number decreases to 23% for step down 15° nozzle, and 32% for up 15° nozzle;
3. 1-2% 50mm inclusions backflow to SEN outport, and possible stay there as nozzle clogging.

Velocity and Particle Entrapment in Caster

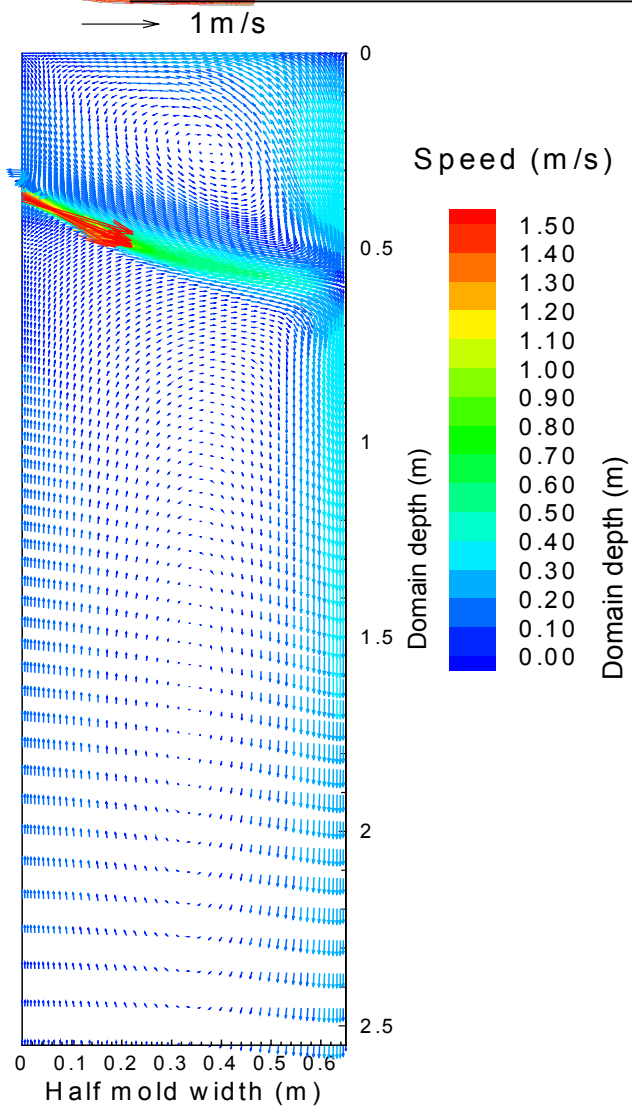

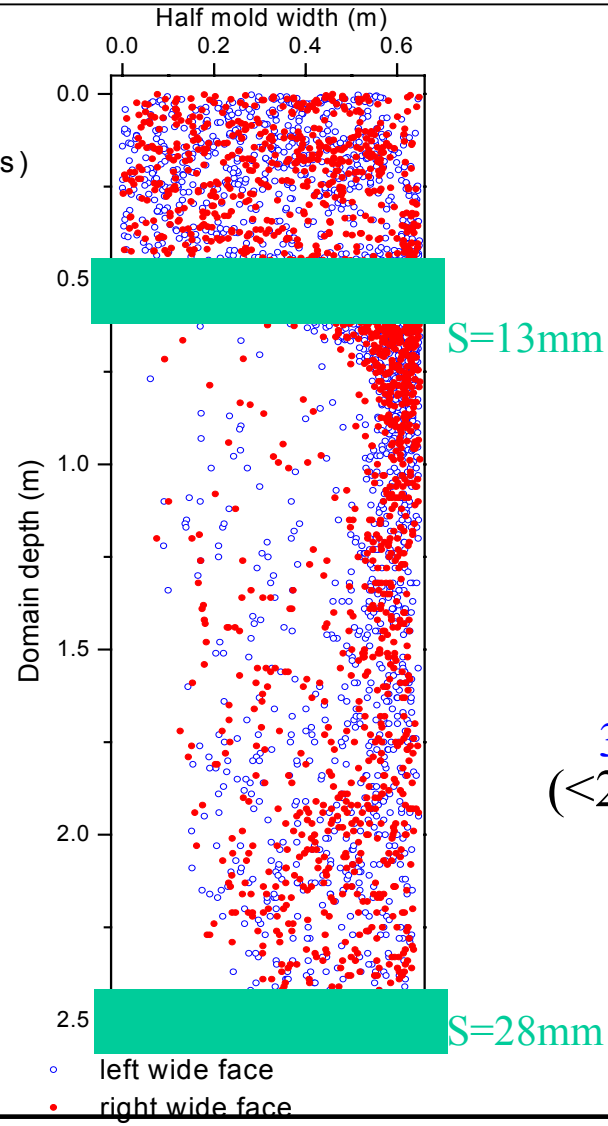

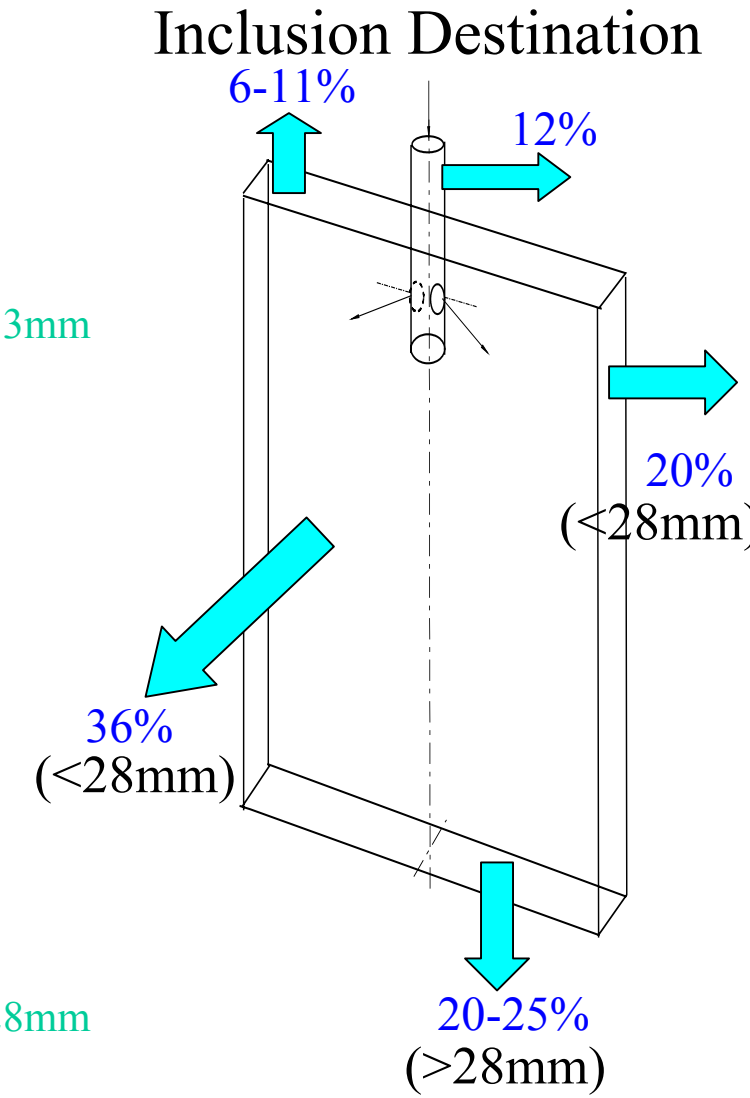

Inclusions Distribution along Slab Thickness (Measurement)

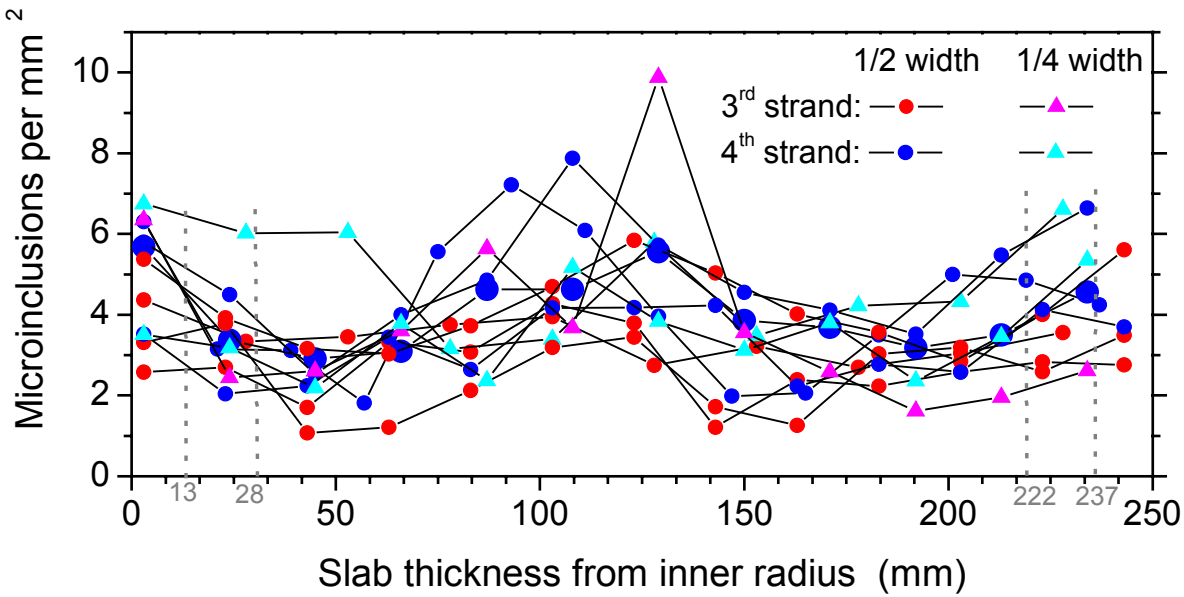

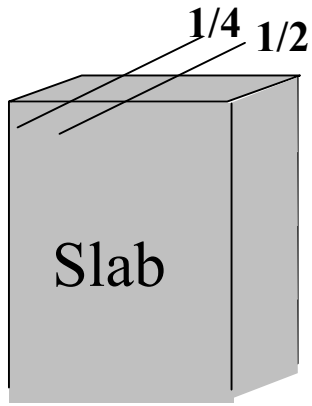

Sampling position

Inclusion Size Distribution Measurement

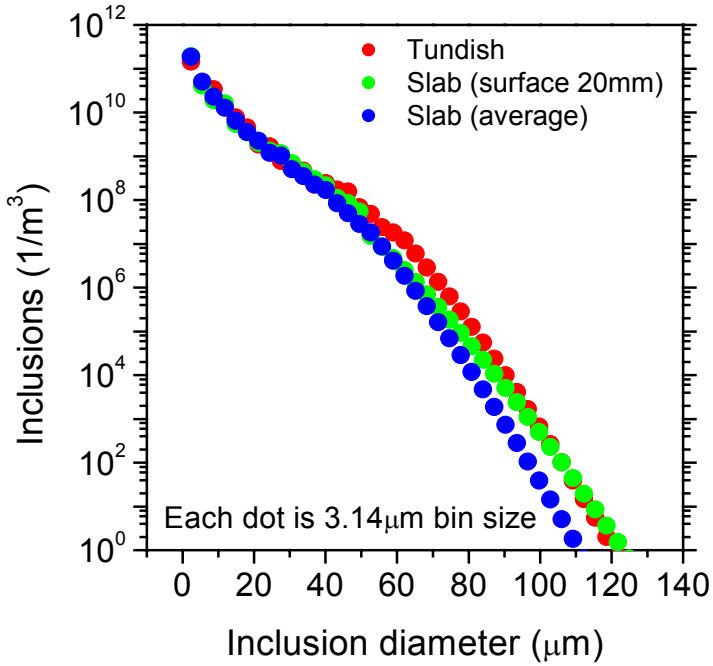

Number density distribution

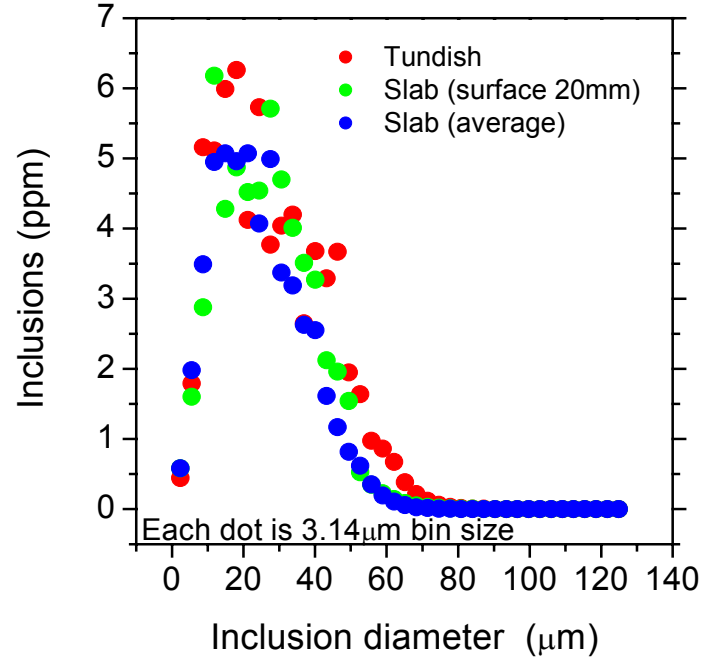

Mass fraction size distribution

Measurement: Al_2O_3 inclusion mass fraction

- In the tundish: 66.8ppm
- In the slab:51.9ppm
- Removal from tundish to slab: 22%.

Simulation:

- Removed from tundish to slab: 18-23%.

Fraction of Inclusion to Top Surface

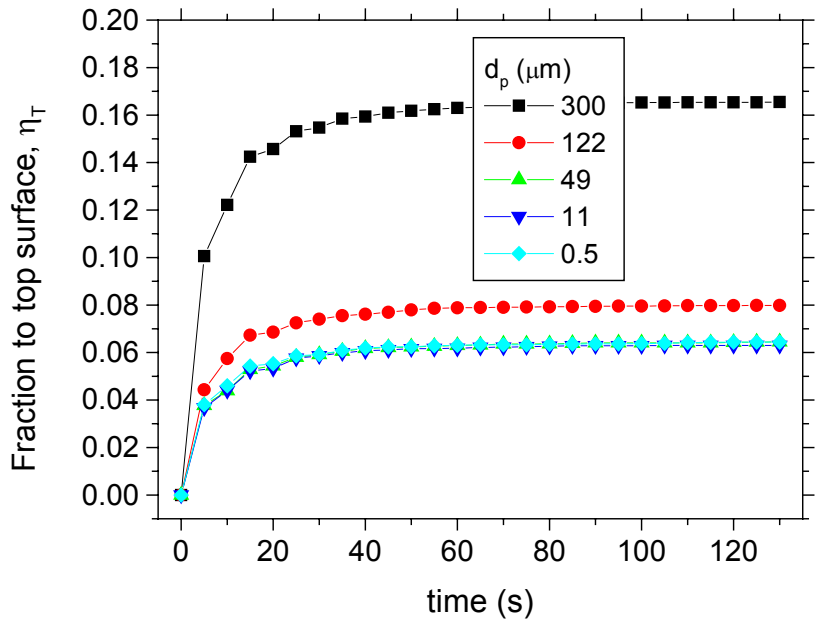

1) For the inclusions smaller than 50 μm, the fraction to the top surface is independent on inclusion size, and this fraction is around 6% after 40seconds.;
2) Beyond that, the removal to top surface increases with size increasing.

Fraction of Inclusion to Narrow Face and Wide Face

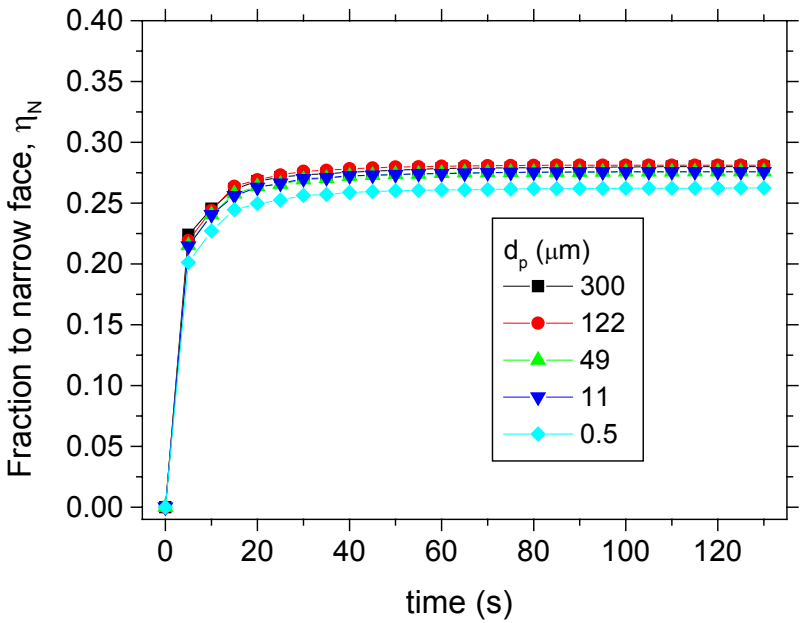

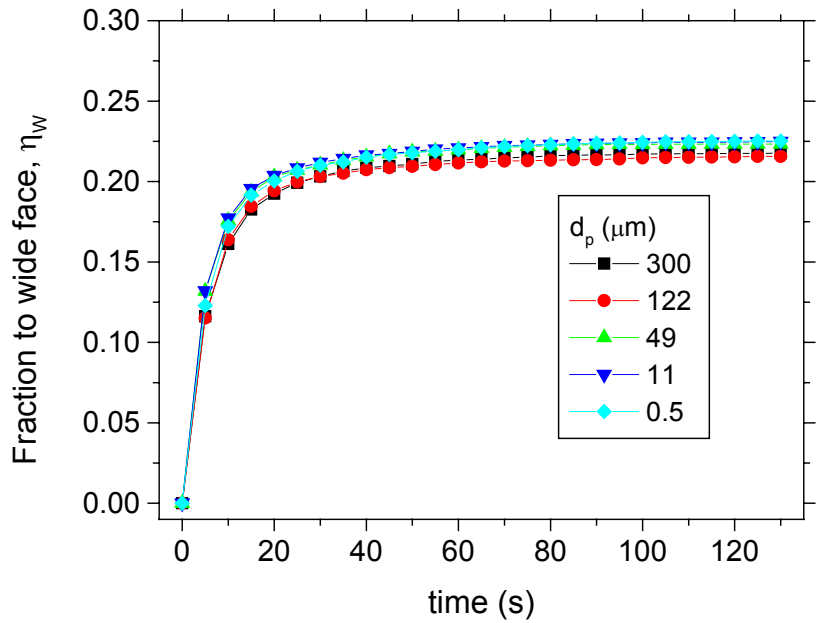

1) Inclusions captured by the wide face and narrow is independent on inclusion sizes.

2) 28% inclusions are captured by narrow face, and 22% are captured by wide face.

Conclusions

1. Step nozzle favors inclusion removal to the top surface of the mold by eliminating swirls at SEN outports and in the mold, and deceasing the impingement depth of the jet in the mold.

2. 55% 50 μm inclusion will be entrapped in the slab thickness of 28-125mm by using non-step down 15° nozzle. This number decreases to 23% for step down 15° nozzle, and 32% for up 15° nozzle;

3. 1-2% 50 μm inclusions backflow to SEN outport, and possible stay there as nozzle clogging.

3.5 Effect of Argon Gas Fluid Flow in the Mold

Objectives

- Develop multiphase model to simulate the 3-D flow pattern of molten steel in the continuous casting mold with multisize-argon gas injection
- Validate model using water model & steel caster comparisons
- Estimate flow pattern (single roll, double roll, etc.) and gas penetration (contours) obtained in steel caster as a function of casting conditions (gas flow rate, gas volume fraction, argon bubble size, steel throughput, mold width, and SEN submergence depth)
- Recommend practices related to argon gas injection optimization to improve the flow pattern in continuous casting mold

Bubble Size Distribution in Nozzle (Bai's Double-needle Water Experiment)

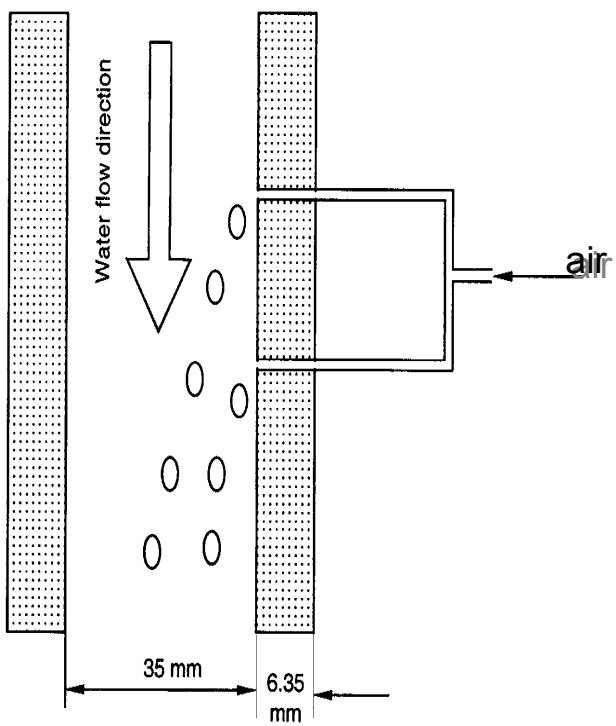

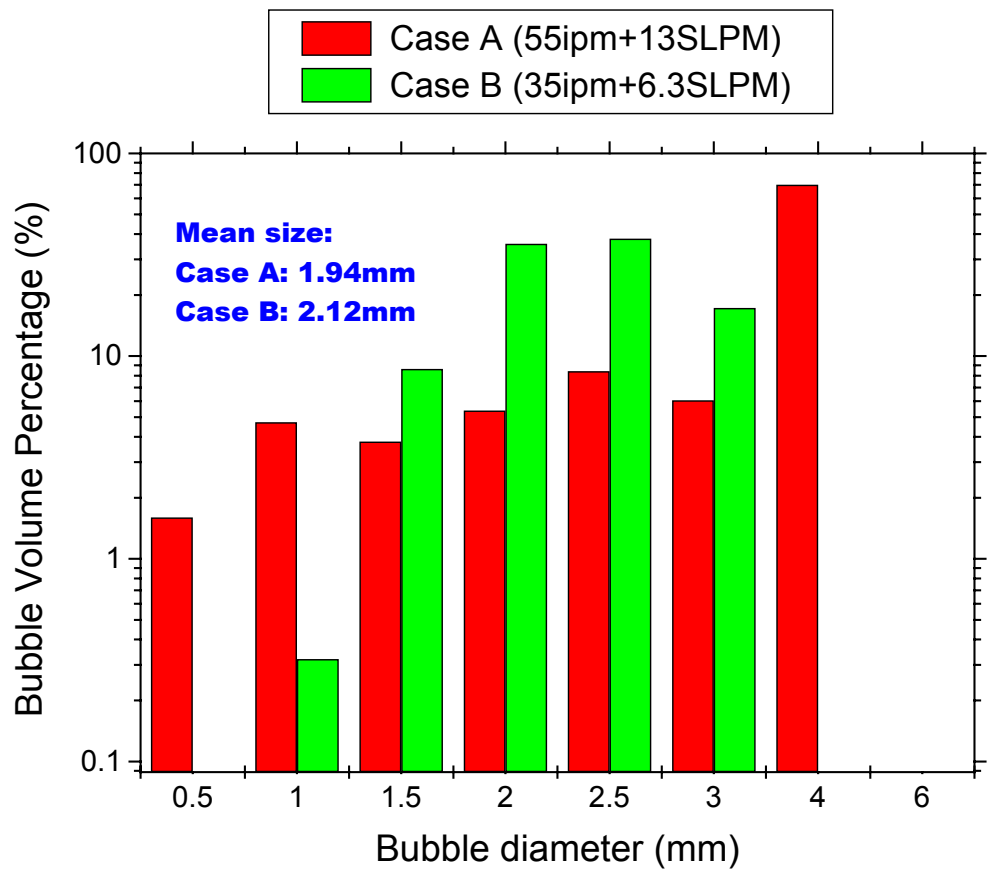

Bubble Size Distribution in Mold (0.4 Scale LTV Water Model)

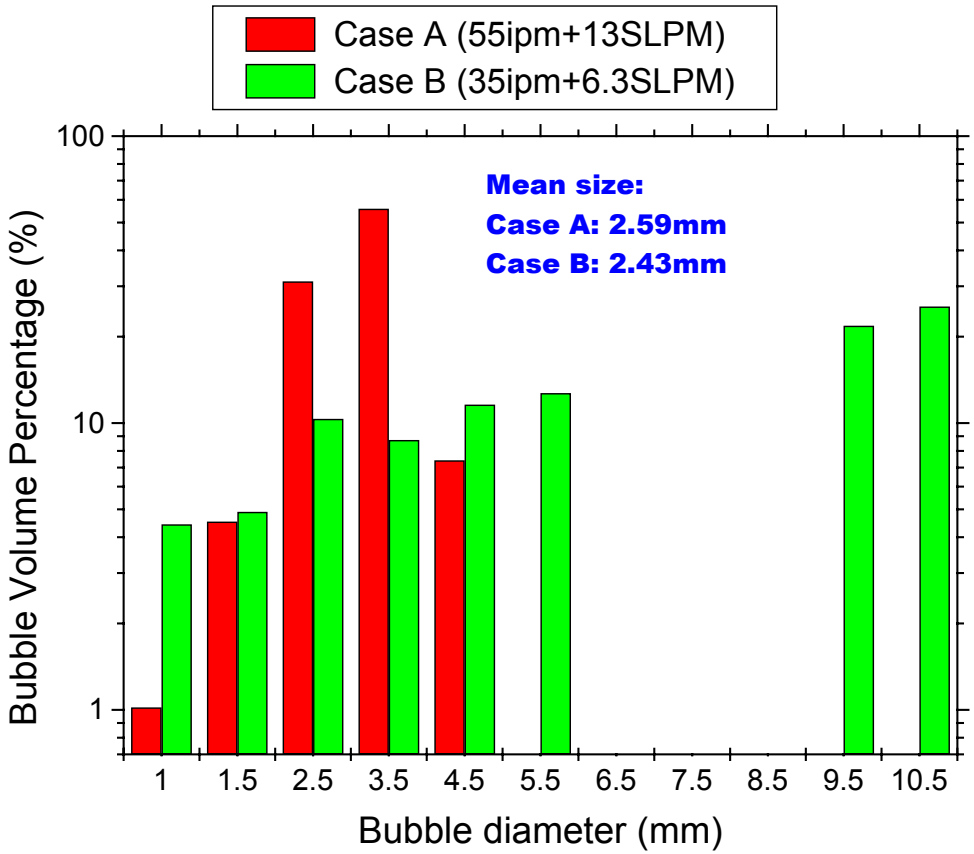

Bubble size distributions: estimated in steel caster

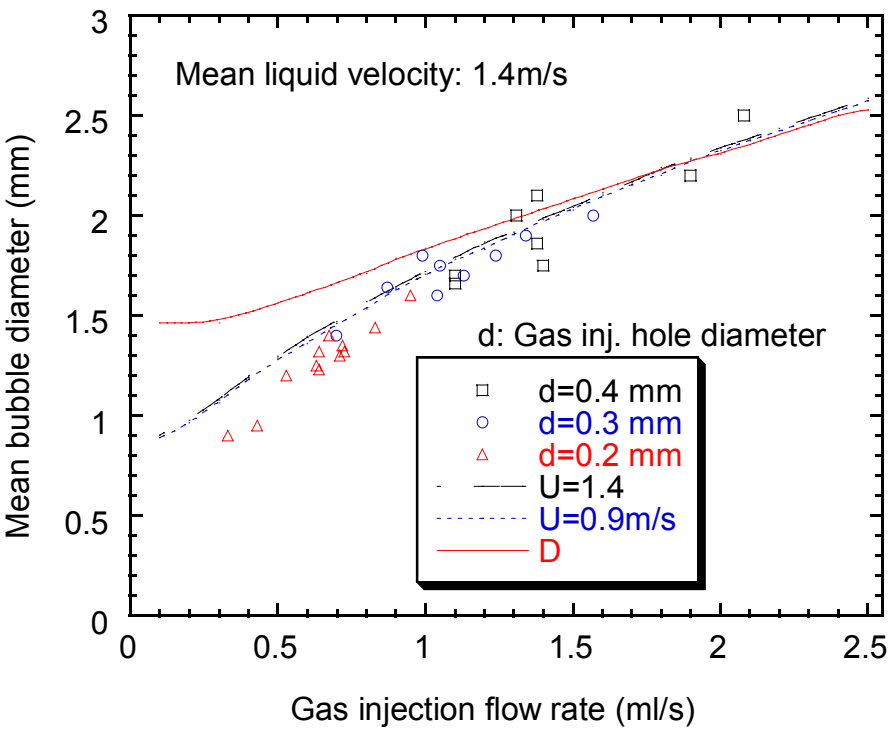

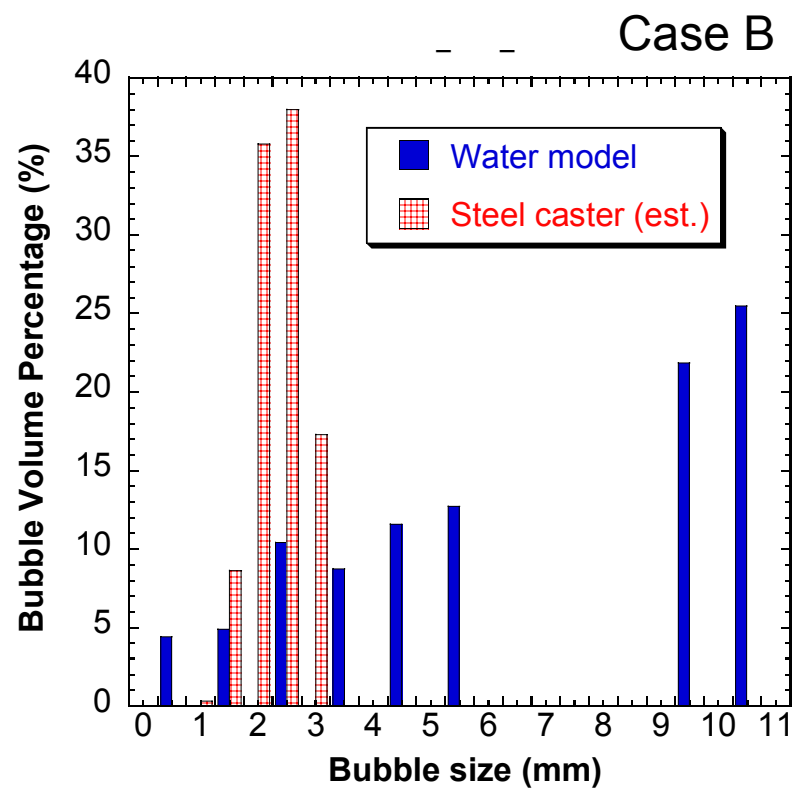

Bubble size prediction model:

$$5.2692\frac{\pi U}{Q_g D_N^{1/7}}\int_{r_e}^{r_d}\left(r^{15/7}(ar+b)^{3/2}+\frac{ar^{22/7}}{2}(ar+b)^{1/2}\right)dr$$

$$=2r_d e_d^{3/2}+\frac{d}{2}-r_e$$

Estimate for steel caster using Bubble model

Nozzle simulation: inlet BCs for mold

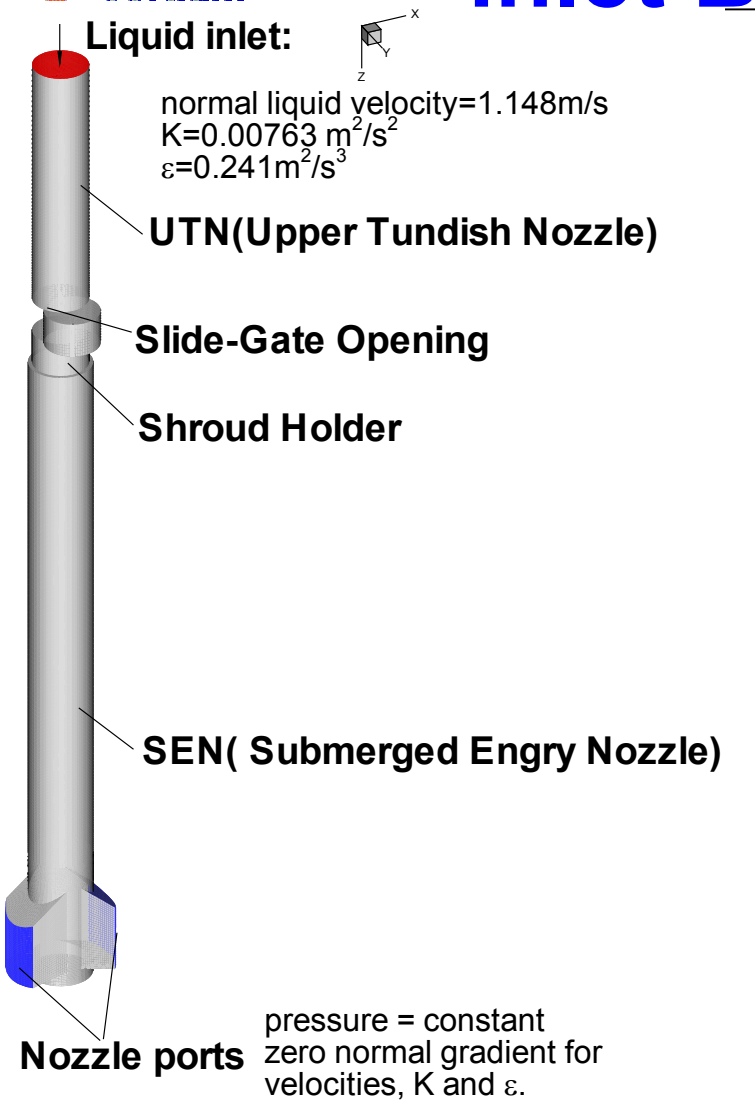

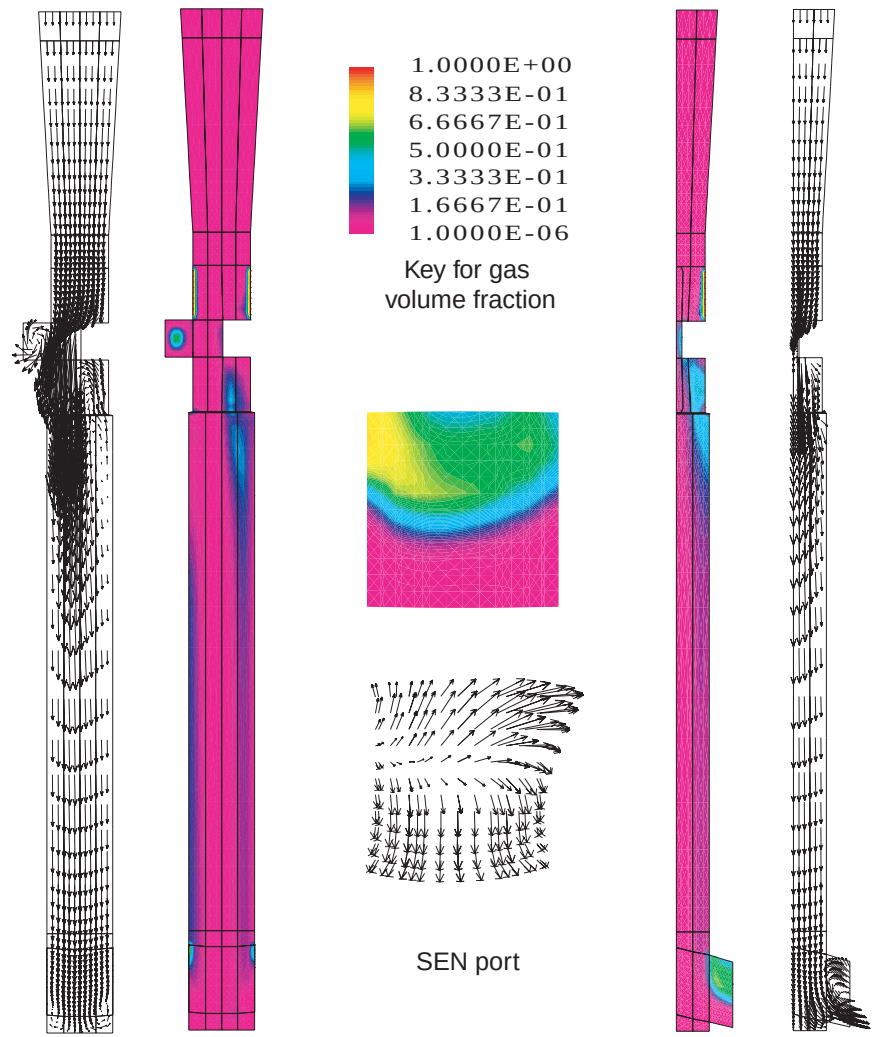

Model Validation Cases

	Cast A	Case B
Nozzle Submergence Depth *(mm)*	165	165
Vertical Velocity in Nozzle *(m/s)*	2.05	1.31
Casting Speed (*mm/s*)	23.2 (55 ipm)	14.8 (35 ipm)
Inlet Steel Flow Rate *(m^3/min)*	0.584	0.376
Throughput *(tonne/min)*	**4.10**	**2.64**
Inlet Gas Flow Rate *(SLPM)*	**13**	**6.3**
Inlet Gas Volume Fraction *(% hot)*	11	8.5
Avg. Gas Bubble Diameter *(mm)*	2.59	2.43
Quality (Defects)	**More Pencil pipe**	**More Sliver Defects**

Results Comparison: Case A

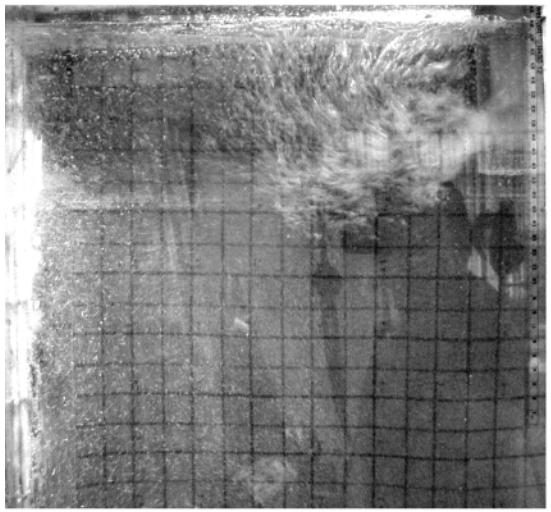

Photo of Water Model

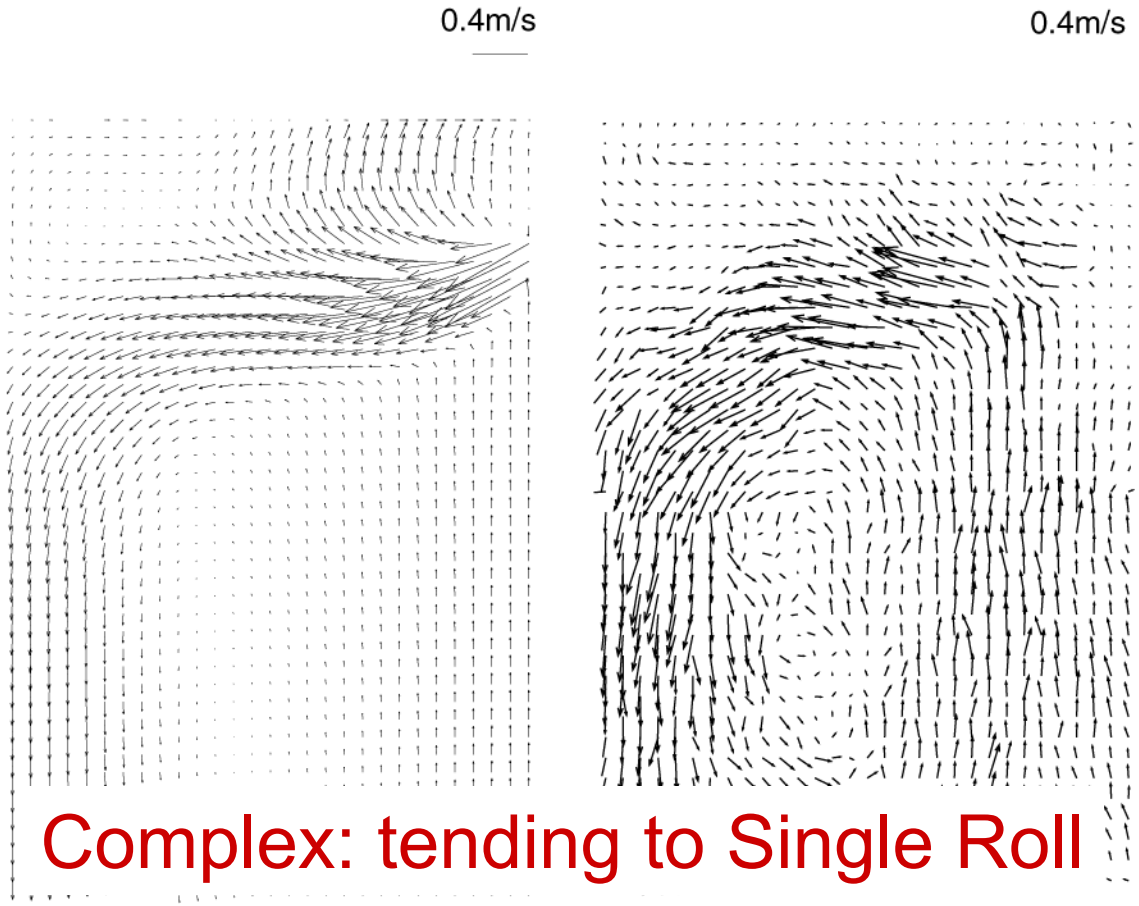

***K-ε* Simulation** **PIV Measurements**

Velocity at Centerplane

Case A
1.4 m/min
11% gas

Results Comparison: Case B

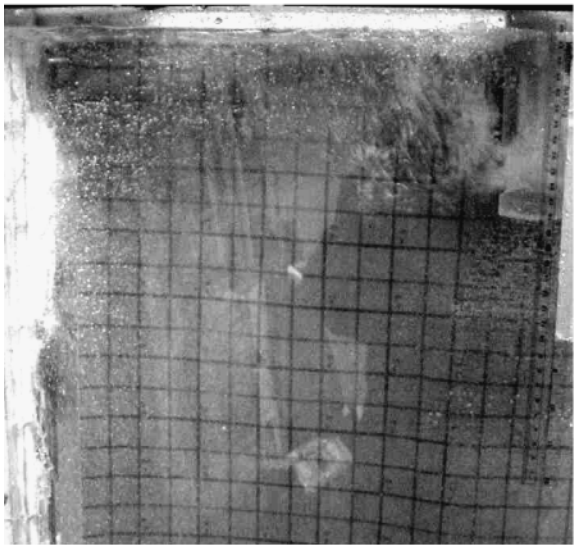

Photo of Water Model

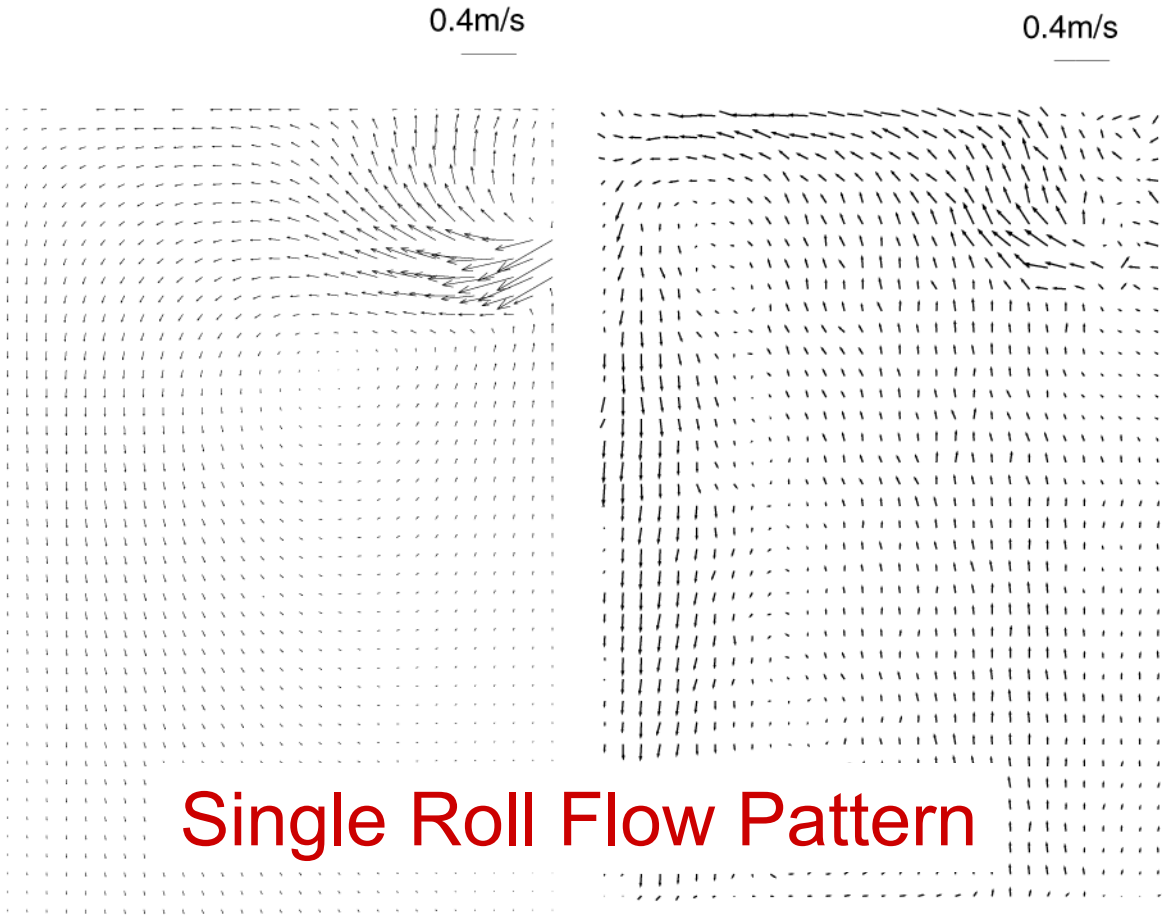

***K-ε* Simulation** **PIV Measurements**

Velocity at Centerplane

Case B
0.9 m/min
8.5% gas

Differences between Steel Caster and Water Model

1. Increasing the dimensions by a factor of 2.5 to simulate the full-scale geometry ;
2. Increasing the inlet velocity by a factor of $(2.5)^{1/2}$ (to simulate the actual casting speed rather than the velocities in the water model, which were scaled down according to the standard modified Froude criterion);
3. Replacing the domain bottom with a pressure boundary condition;
4. Changing the bubble distribution
5. Changing the liquid properties
6. Nozzle geometry slight change and simulated with 3D model

Simulated Flow in Steel Caster (Case A)

Continuous Casting Consortium

Bubble mean size: 2.59mm

Normal distribution

10 mm below Meniscus

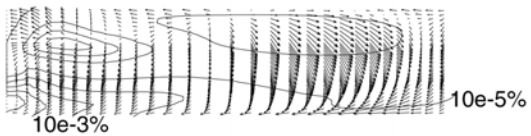

Casting conditions:

1.854 m slab
23.2 mm/s
13 SLPM
11% Gas (hot)

1m/s

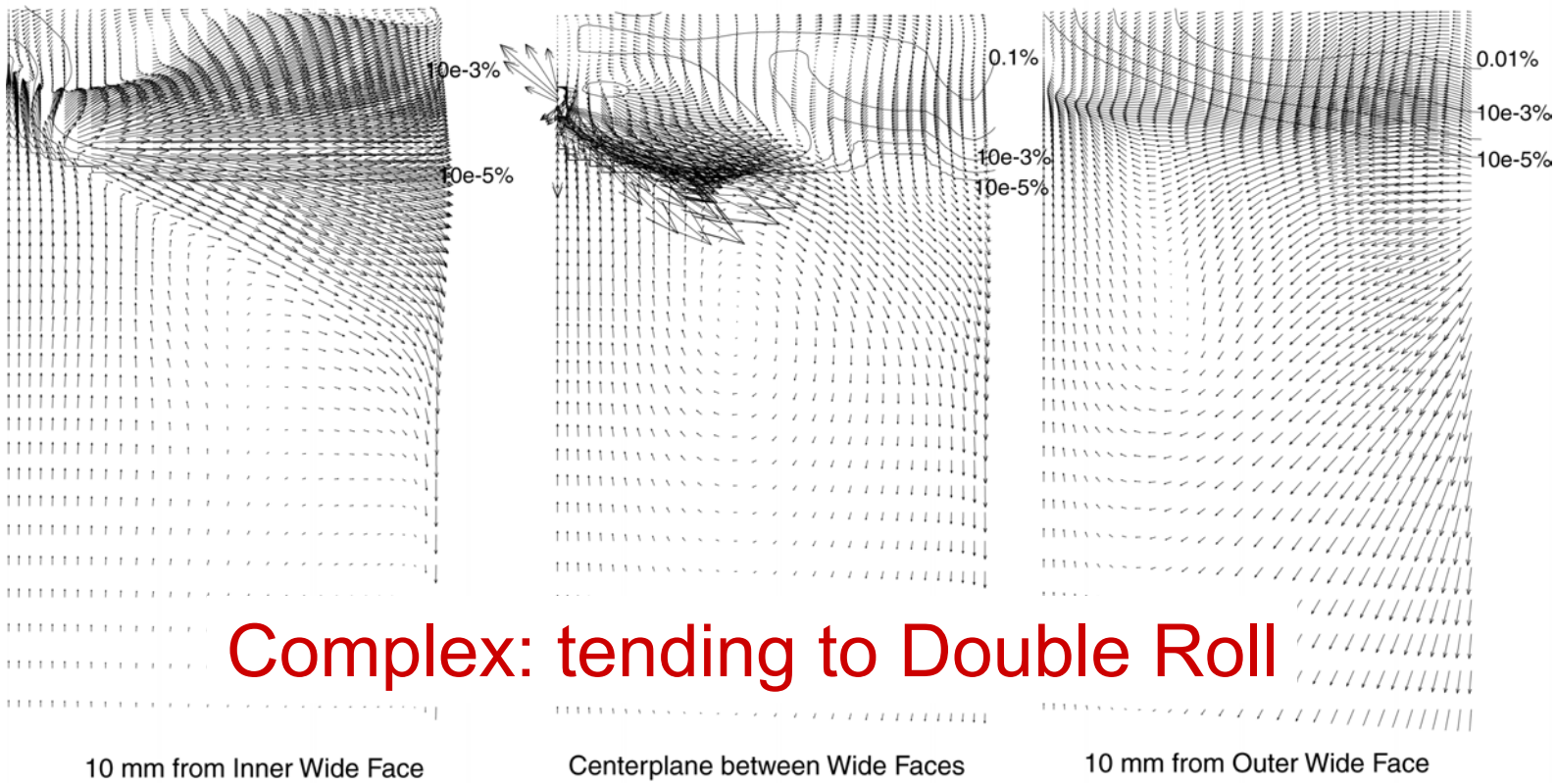

Complex: tending to Double Roll

Simulated Flow in Steel Caster (Case B)

Continuous Casting Consortium

Bubble mean size: 2.43mm

Bi modal distribution

Casting conditions:

1.854 m slab
14.8 mm/s
6.3 SLPM
8.5% Gas (hot)

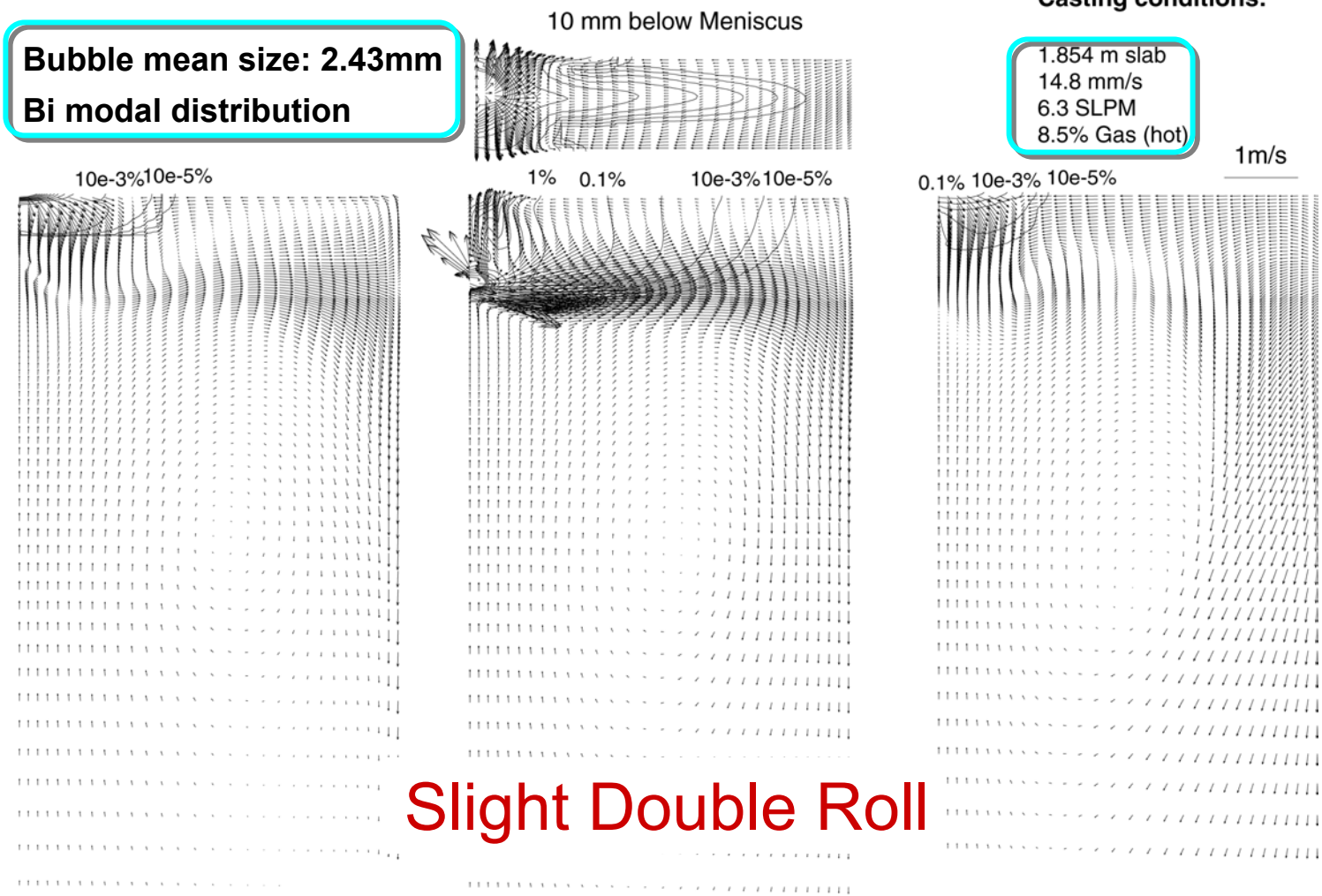

Slight Double Roll

10 mm from Inner Wide Face

Centerplane between Wide Faces

10 mm from Outer Wide Face

Measured Flow Pattern in Steel Caster

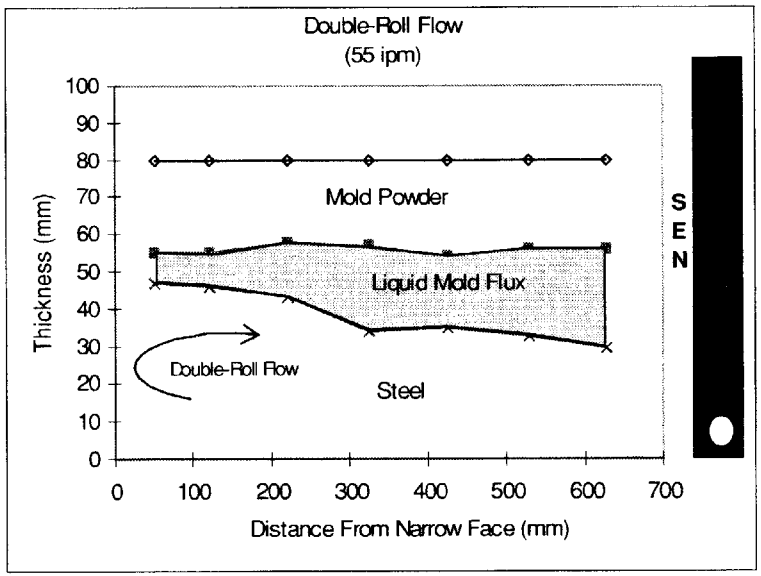

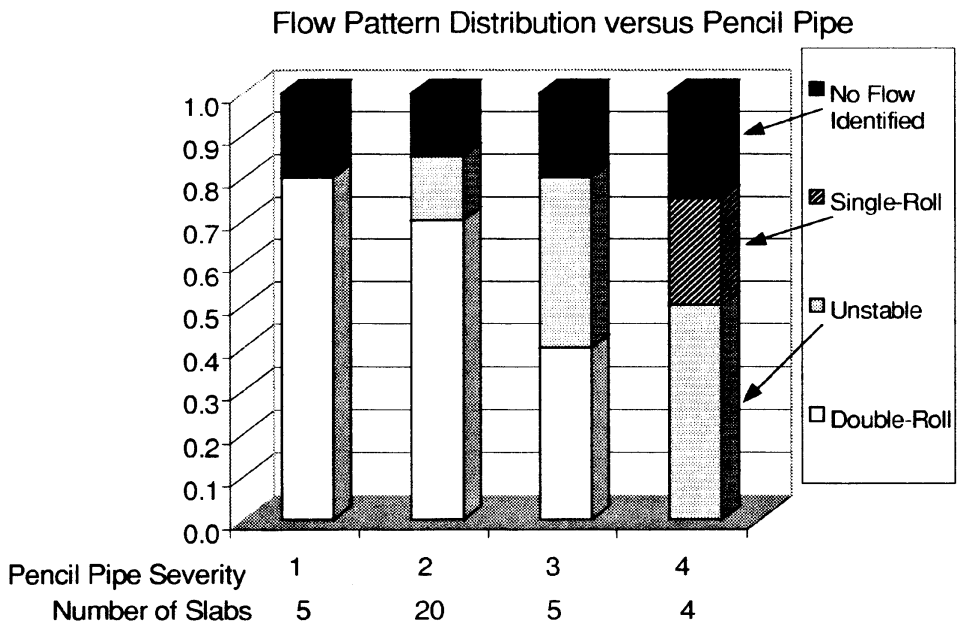

Case A, 11% gas:

Usually double roll.

Almost Case B:

Usually double roll but sometimes has flow pattern switching.

M. B. Assar, P. H. Dauby and G. D. Lawson. Opening then black box: PIV and MFC measurements in a continuous caster mold. 83rd Steelmaking Conference Proceedings, P397-411

Summary of Comparisons with Water Model and Steel Caster

Case A			
Water model		**Steel Caster**	
PIV measurement	Complex: tending to Single roll	Nailboard / MFC measurement	Usually double roll
k-ε calculation (CFX)	Complex: tending to Single roll	k-ε calculation (CFX)	Complex: tending to Double roll

Case B			
Water model		**Steel Caster**	
PIV measurement	Single roll	MFC measurement	Mostly double roll, but with some flow pattern switching
k-ε calculation (CFX)	Single roll	k-ε calculation (CFX)	Slight Double roll

Parametric Study

Effects of

- Steel throughput
- Gas volume fraction (gas flow rate)
- Bubble size and its distribution
- Slab width
- SEN submergence depth

Results of

- Flow pattern
- Gas Penetration

Lower Steel Throughput, More Single Roll and Less Gas Penetration.

Continuous Casting Consortium

Conditions:
1.854 m slab
23.2mm/s
(**4.1tonne/min**)
6.4 SLPM
5.7% Gas
2.59mm bubble(normal)

Conditions:
1.854 m slab
16.8mm/s
(**3.0tonne/min**)
4 SLPM
5% Gas
2.59mm bubble(normal)

Conditions:
1.854 m slab
14.8mm/s
(**2.64tonne/min**)
4 SLPM
5.7% Gas
2.59mm bubble(normal)

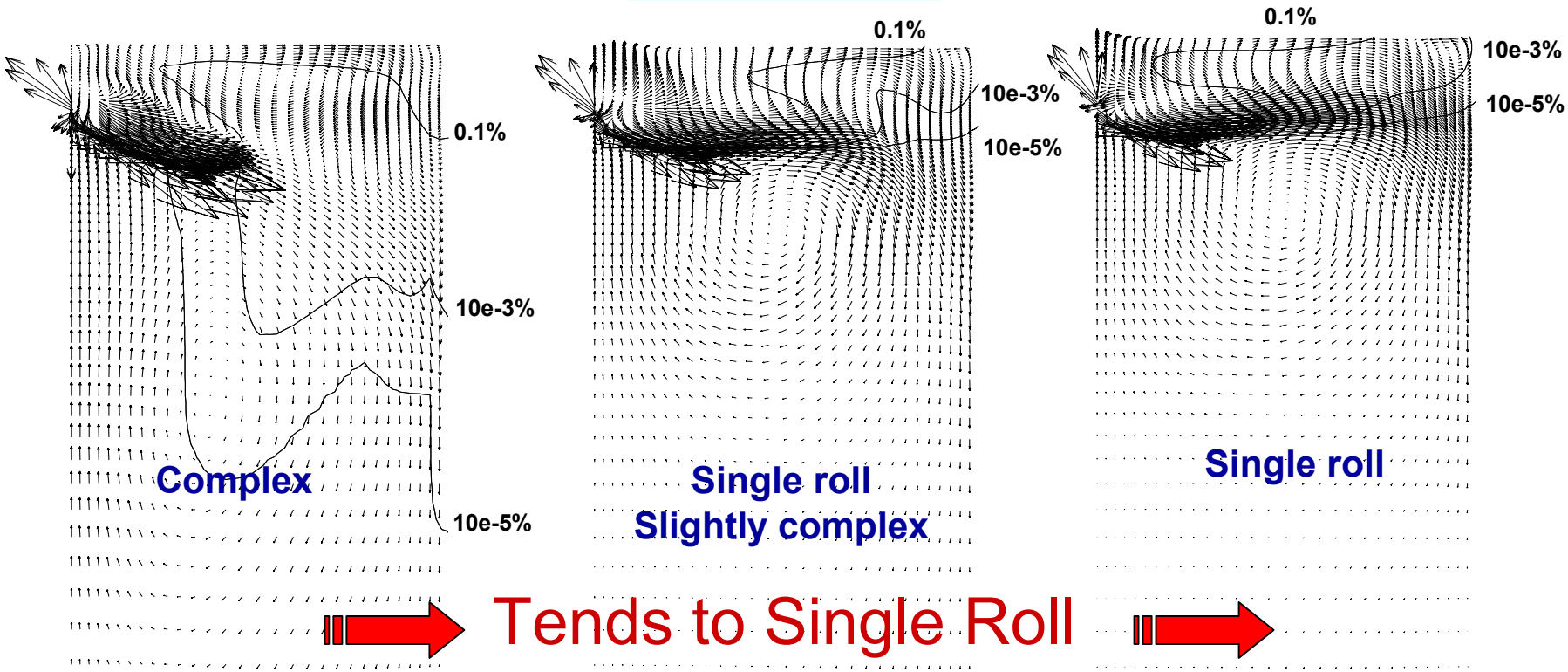

Tends to Single Roll

Effect of Gas Volume Fraction on Gas Penetration Depth

Continuous Casting Consortium

Conditions:
1.854 m slab
23.3mm/s
(4.1tonne/min)
4 SLPM
3.7% Gas
2.59mm bubble(normal)

Conditions:
1.854 m slab
23.2mm/s
(4.1tonne/min)
6.4 SLPM
5.7% Gas
2.59mm bubble(normal)

Conditions:
1.854 m slab
23.2mm/s
(4.1tonne/min)
13 SLPM
11% Gas
2.59mm bubble(normal)

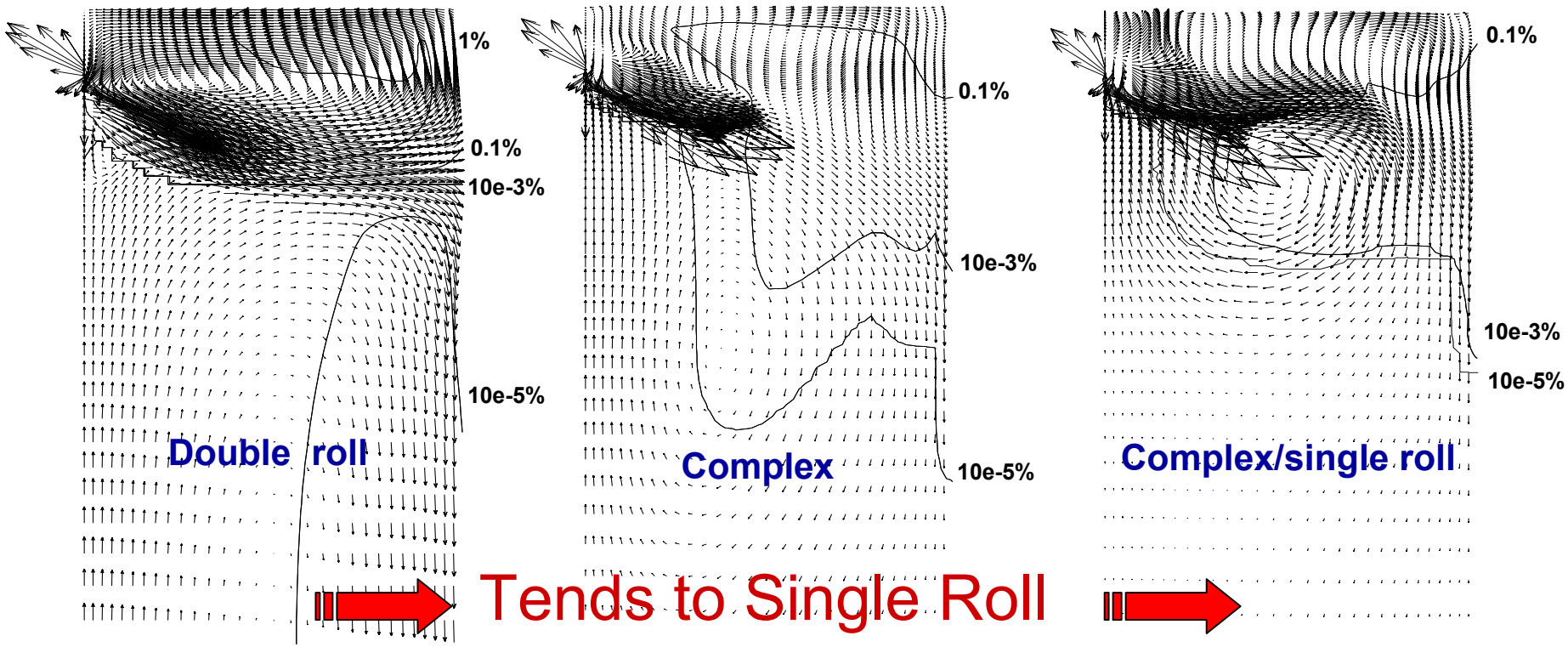

Decreasing Gas Volume Fraction , Single roll→Complex flow → Double roll

Conditions:
1.854 m slab
23.2mm/s
(4.1tonne/min)
13 SLPM
11% Gas
2.59mm bubble(normal)

Conditions:
1.854 m slab
23.2mm/s
(4.1tonne/min)
6.4 SLPM
5.7% Gas
2.59mm bubble(normal)

Conditions:
1.854 m slab
23.3mm/s
(4.1tonne/min)
4 SLPM
3.7% Gas
2.59mm bubble(normal)

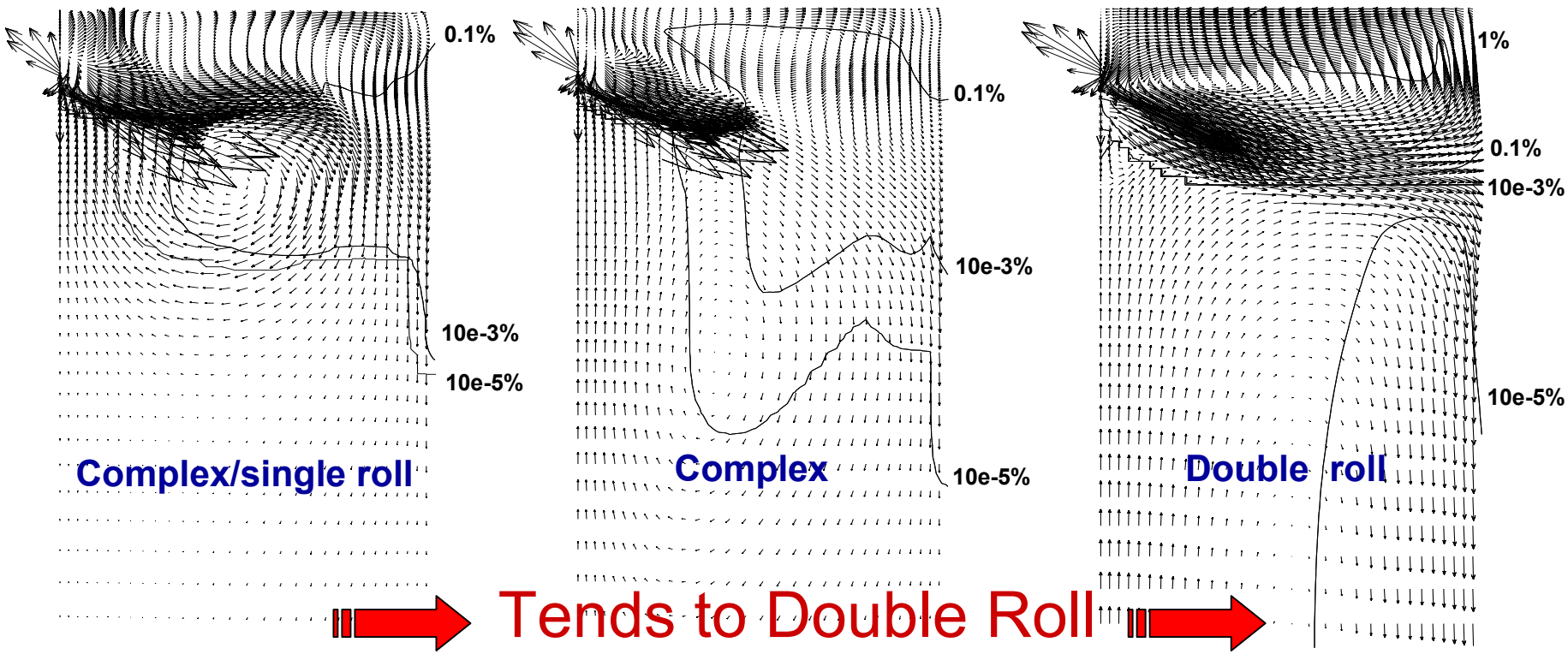

Tends to Double Roll

Lower Gas Volume Fraction Tends to Double Roll Flow Pattern

Conditions:
1.854 m slab
14.8mm/s
(2.64tonne/min)
13.4 SLPM
16.4% Gas
2.43mm bubble(Bi modal)

Conditions:
1.854 m slab
14.8mm/s
(2.64tonne/min)
6.3 SLPM
8.5% Gas
2.43mm bubble(Bi modal)

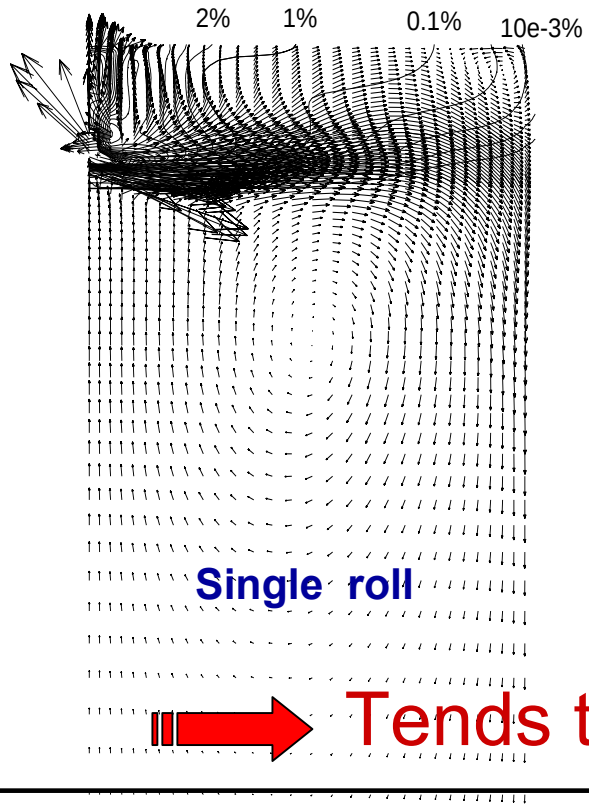

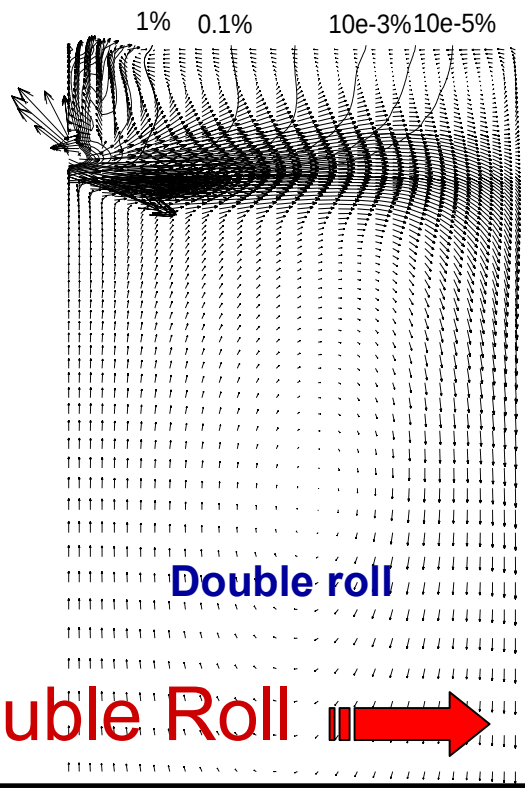

Tends to Double Roll

Best Case with the Lowest Gas Penetration Depth

Conditions:
1.854 m slab
14.8mm/s
(2.64tonne/min)
6.3 SLPM
8.5% Gas
2.43mm bubble(bi model)

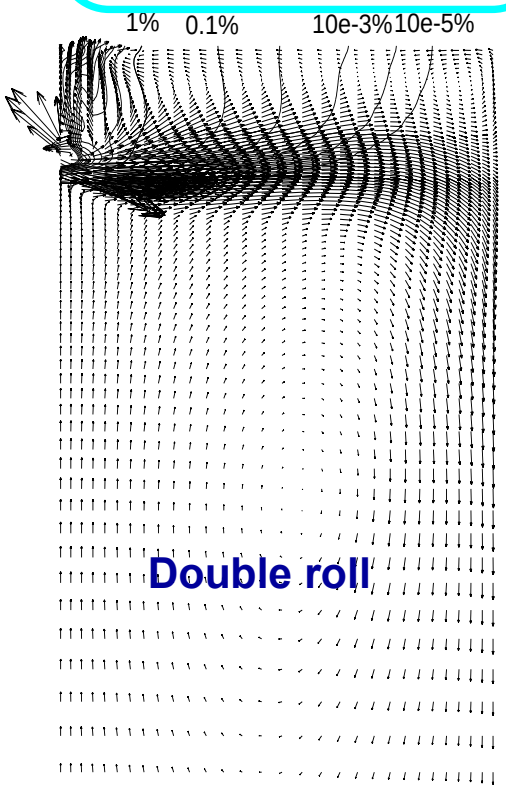

Conditions:
1.854 m slab
14.8mm/s
(2.64tonne/min)
4 SLPM
5.7% Gas
2.59mm bubble(normal)

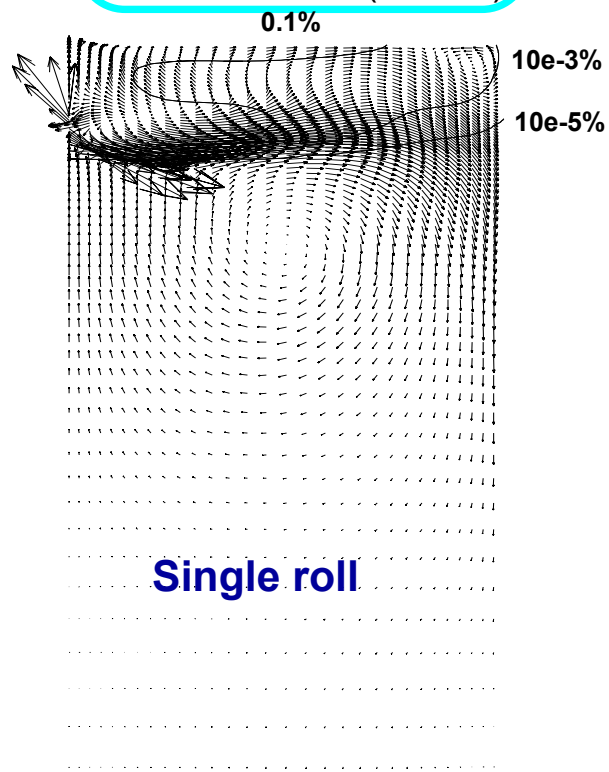

Conclusion:

Lower gas penetration depth for:

1. Double roll flow pattern

2. Lower steel throughput

Flow Pattern Identification (Water Model) (Modified from M. Assar et al)

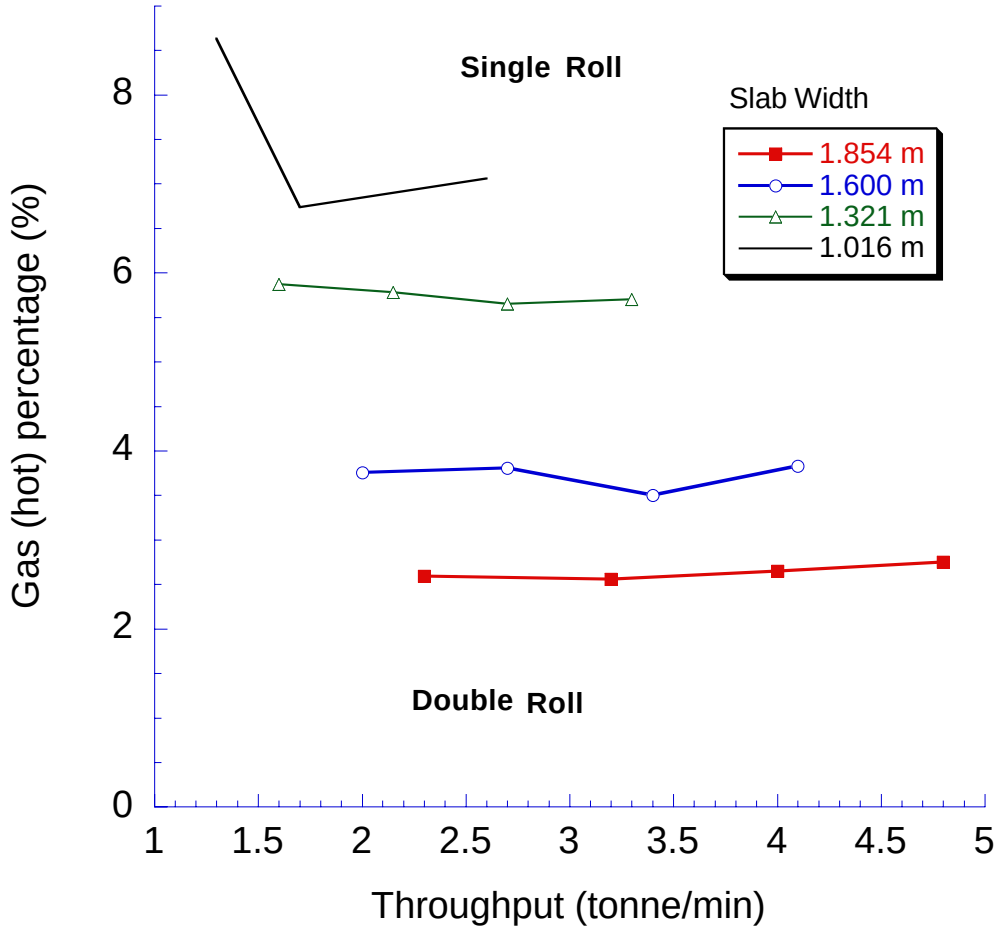

M. B. Assar, P. H. Dauby and G. D. Lawson. Opening then black box: PIV and MFC measurements in a continuous caster mold. 83rd Steelmaking Conference Proceedings, P397-411

Flow Pattern Identification (Real Caster) Gas (Hot) Volume Fraction and Steel Throughput

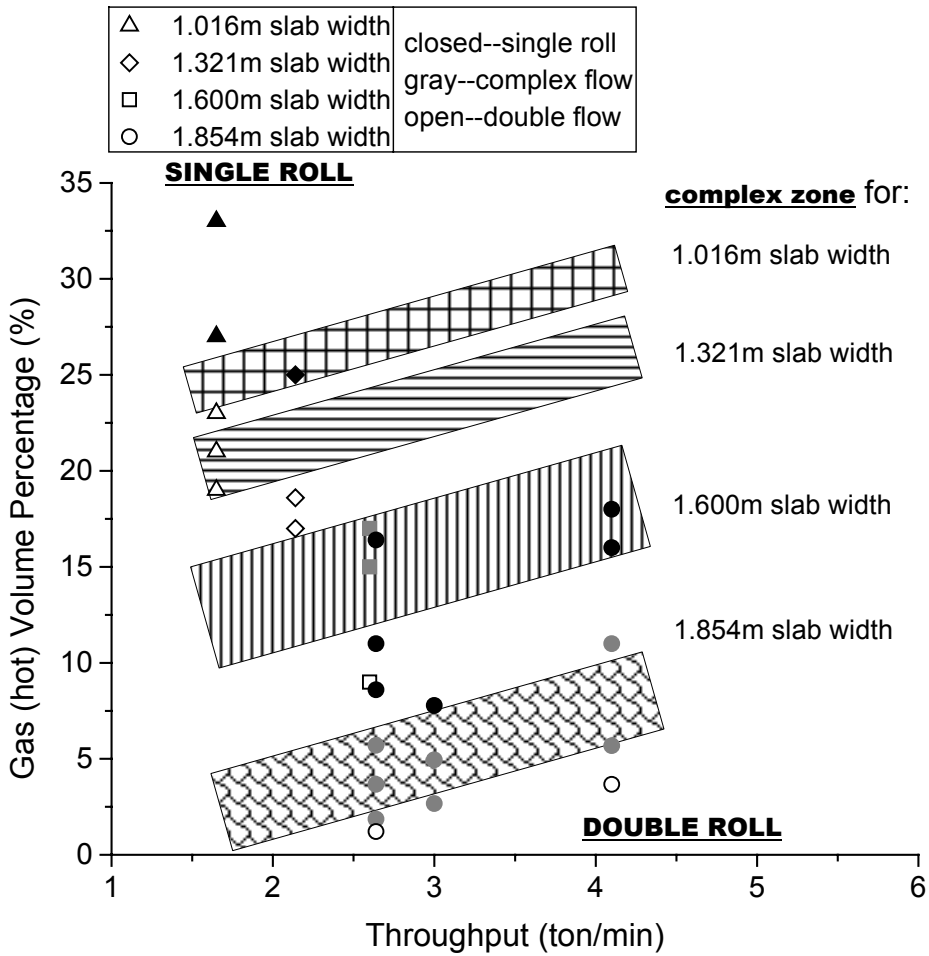

Note: The points for the cases with 2.43 mm mean size bi modal bubbles are deleted.

Flow Pattern Identification (Real Caster) Effect of Gas Flow Rate (Approx.)

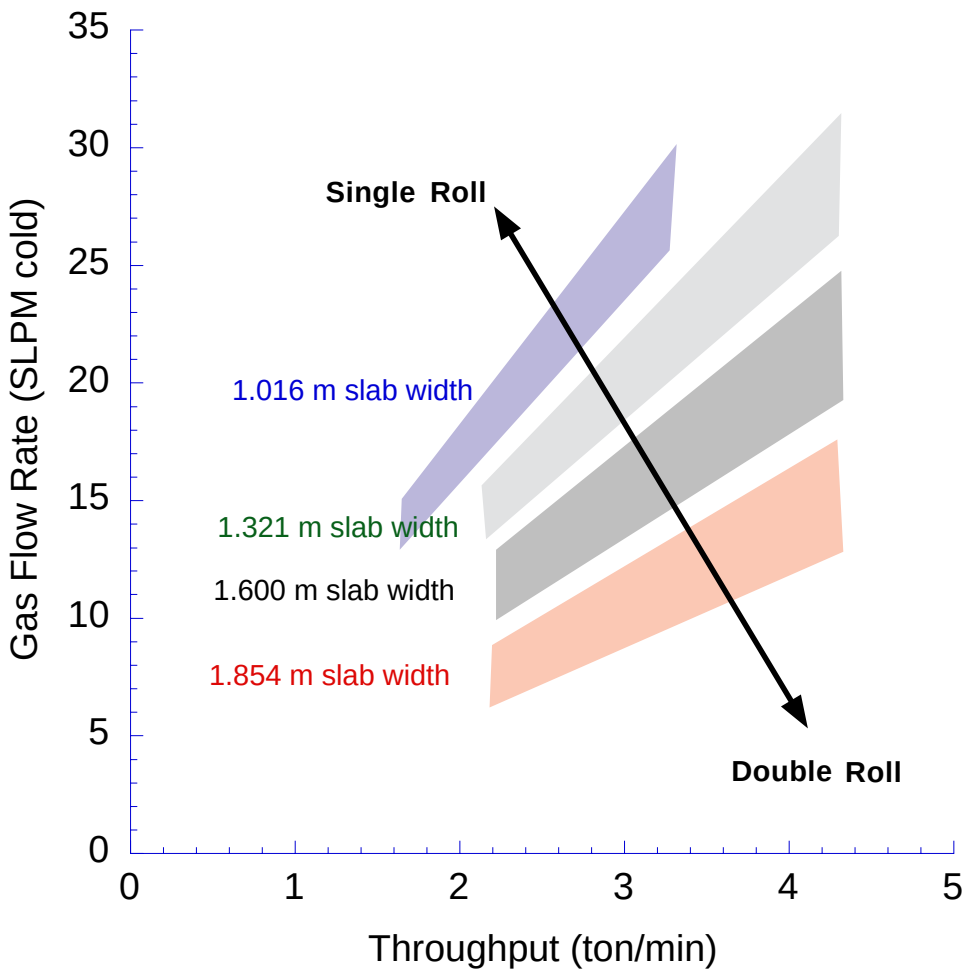

Flow Pattern Identification (Real Caster) Effect of SEN Submergence Depth

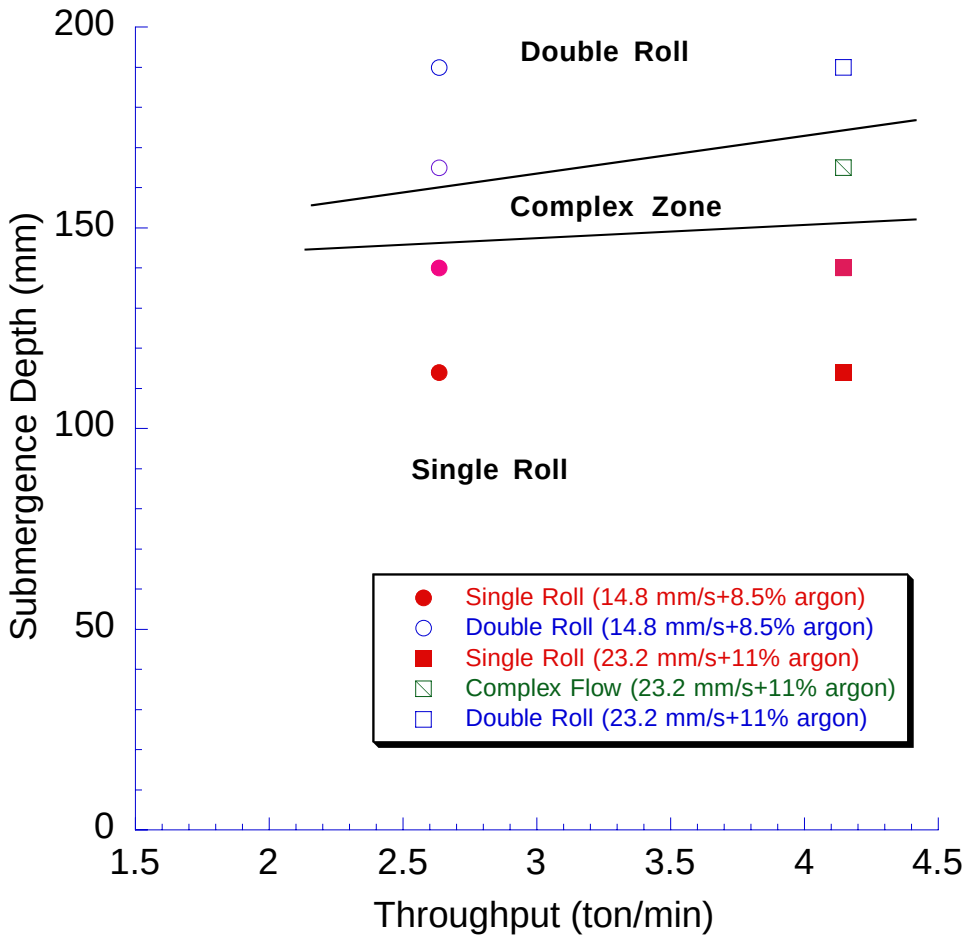

Computed Velocity at Centerplane with Different SEN Submergence

Conditions: 1854mm slab, 14.8mm/s, 8.5%gas (hot)

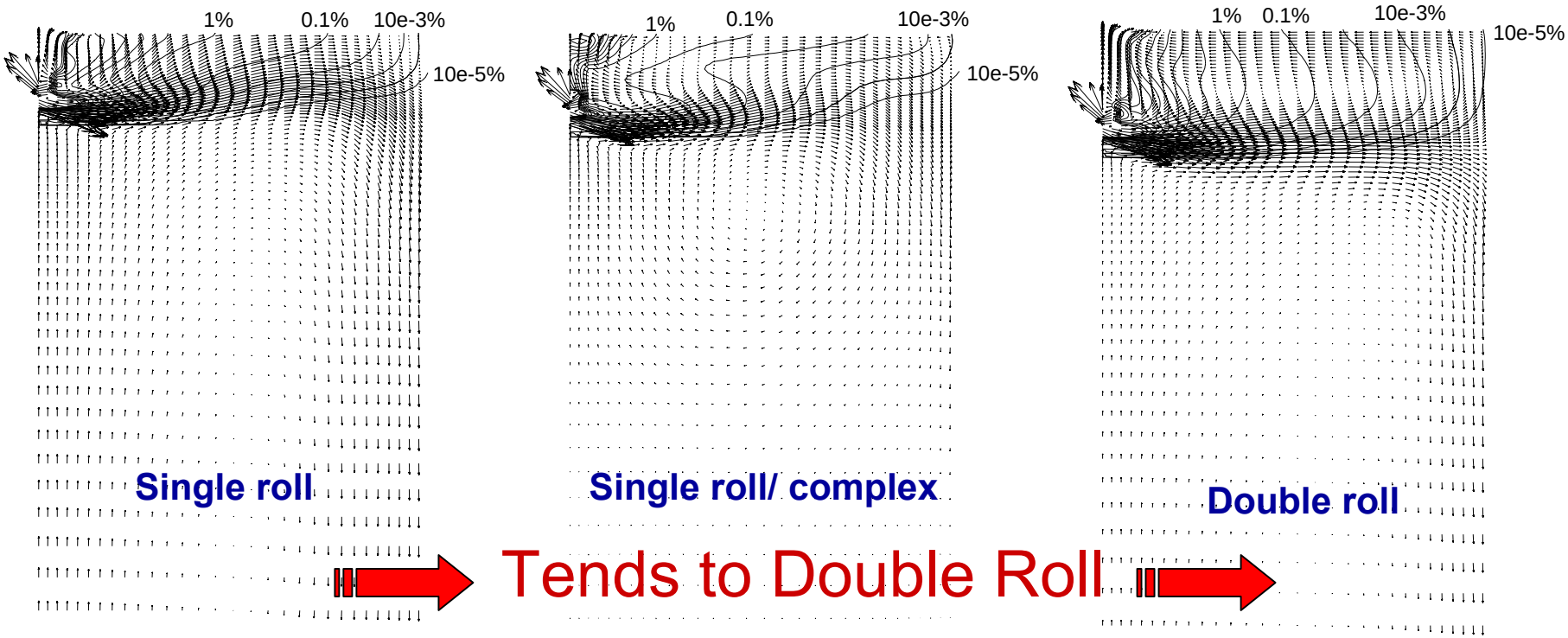

submergence depth 114 mm (4.5 inch)

submergence depth 140 mm (5.5 inch)

submergence depth 190mm (7.5 inch)

Conclusions

1. Computational simulation and measurements show that the flow pattern in the steel caster is sometimes very different from that in a scale water model and the steady, multiphase k-ε computation can match both. The main reason for this difference is the reduced scale of water model combined with the Froude-based velocity scaling criterion used to choose the water model flow rates.
2. Flow pattern changes during continuous casting, leads to surface contour changes and accompanying level fluctuations and defects, so should be avoided
3. Gas flow rate, casting speed, gas volume fraction, mold width, SEN submergence depth all change the fluid flow pattern. Optimal argon injection depends on all of these factors.
4. Lower steel throughput generates less gas penetration and tends to more single roll.

Conclusions

5. For the same flow pattern, increasing gas volume fraction causes deeper gas penetration. Double roll flow pattern generally has less penetration than single roll. When flow pattern changes, the effect of gas volume fraction on is unclear.

6. Decreasing gas volume fraction tends to change the flow pattern from single roll to complex flow pattern and then to double roll.

7. With other conditions constant, the bi modal bubble distribution tends to double roll and the normal bubble distribution tends to single roll.

8. The least gas penetration depth is found with double roll flow pattern and lower steel throughput.

9. For a given gas fraction and steel throughput, increasing submergence depth tends to generate double roll.